Predicting Fuel Characteristics of Black Spruce Stands Using Airborne Laser Scanning (ALS) in the Province of Alberta, Canada

by

Hilary Cameron

A thesis submitted in partial fulfillment of the requirements for the degree of

Master of Science

in
Forest Biology and Management

Department of Renewable Resources
University of Alberta

Abstract

Maps that describe the characteristics of live and dead biomass across large areas (i.e., fuel maps) are a critical input to a wide range of research models and decision support systems that aim to describe potential fire behaviour and inform fire management actions. As remote sensing technologies become more affordable, the ability to utilize these technologies to create comprehensive fuel maps on small and large scales is becoming increasingly pragmatic. Airborne Laser Scanning (ALS), a remote sensing technology that uses LiDAR, has already been used extensively to characterize forest attributes such as stand height, above ground biomass and stem density; however, few studies have used ALS within the boreal forest to describe forest structural attributes such as fuel loading at a fine resolution (i.e., <10 m grid cell resolution), which is particularly relevant to fire behaviour. This study investigates the viability of using ALS to predict forest attributes in black spruce (*Picea Mariana*) stands, located in Alberta, Canada. Five fuel attributes important to wildfire behaviour were investigated: canopy bulk density (CBD), canopy fuel load (CFL), stem density, canopy height and canopy base height (CBH). Predictive models for estimating fuel attributes from ALS data were developed and compared among ALS datasets with three different pulse point cloud densities (i.e., dense, intermediate and thin). Least absolute shrinkage and selection operator (lasso) regression was used to develop linear models with a training dataset (52 field plots) and evaluated on a testing dataset (28 field plots). Statistically significant relationships were found between all ALS datasets and the forestry metrics of interest. Predictive power decreased with decreasing ALS pulse density. Model accuracy was acceptable and consistent with similar prior studies. Results of this study suggest that ALS can be a useful tool for estimating black spruce canopy fuel attributes at a 40 m^2 resolution in Alberta, Canada. Maps of model outputs are a cost-effective alternative to field-

based sampling to predict potential wildfire behaviour and support with fire-management

decisions.

Table of Contents

List of Tables

List of Figures

List of Acronyms

ABA	Area Based Approach
ALS	Airborne Laser Scanning
AVI	Alberta Vegetation Inventory
AWFIP	Alberta Wildland Fuels Inventory Program
C-2	Boreal Spruce fuel type within the FBP system
CBD	Canopy Bulk Density
CBH	Canopy Base Height
CF_i	Canopy Fuel Load for an individual tree
CFL	Canopy Fuel Load
CSV	Comma Separated Value
DBH	Diameter at Breast Height (1.37 m)
DEM	Digital Elevation Model
FBP	Fire and Behaviour Prediction
FFE-FVS	Forest Vegetation Simulator with Fire and Fuels Extension
GLAS	Geoscience Laser Altimeter System
GPS	Global Positioning System
ICFME	International Crown Fire Modeling Experiment
IMU	Inertial Measurement Unit
ITD	Individual Tree Detection
k-NN	k-nearest neighbours
Lasso	Lease Absolute Shrinkage and Selection Operator
LiDAR	Light Detection and Ranging

LMS   LiDAR Mapping Suite

OLS   Ordinary Least-Squares

R^2 Coefficient of Determination

RMSE   Root Mean Square Error

SD   Standard Deviation

sqrt   Square Root Transformation

SUR   Seemingly Unrelated Regression

WUI   Wildland Urban Interface

Chapter 1 Introduction

1.1 Research Context

Wildfire is a dominant natural disturbance in Canada's boreal forest ecosystems (Rowe, 1983; Weber and Flannigan, 1997; McRae et al., 2001). Although wildfires play an important role in supporting healthy ecosystem functioning, they can have adverse effects on communities and other human values. Damages that accompany some of the most destructive wildfires in the Boreal Region have reached billions of dollars when factoring in insurable losses, wildfire-suppression costs and recovery costs. Examples of wildfires in Alberta that resulted in losses that exceeded one billion dollars include the Flat Top Complex wildfires that affected the town of Slave Lake in 2011 (Flat Top Complex Wildfire Review Committee, 2012) and the Horse River Wildfire that affected Fort McMurray in 2016 (Insurance Bureau of Canada, 2016).

To protect communities, infrastructure and other values at risk, wildfire behaviour models are used to predict the manner in which a given fire can be expected to spread (e.g., Van Wagner 1987; Finney, 1998; Andrews et al., 2005). In addition, these models aid in informing operational fire management decisions, such as fire suppression tactics and evacuation recommendations. Moreover, these models are also used extensively in a wide range of strategic planning assessments and as inputs to research models (e.g., Linn et al., 2002; Parisien 2005). Information about the characteristics of live and dead biomass in an area (i.e., fuels) is a critical input to all fire behaviour models. Accurate fuel maps are especially critical when assessing wildfire risk within the vicinity of a community. Wildfire fuel maps utilized in wildfire behaviour models and strategic fire risk management and planning tools typically summarize fuel attributes into broad categories called fuel types due to the difficulty associated with directly

measuring fuel characteristics in the field across a landscape (e.g., Wilson et al., 1994; Chuvieco et al., 2003; Nadeau et al., 2005). Advancements in remote sensing technologies provide a less expensive alternative to field sampling and are able to describe the characteristics of flammable vegetation in much more detail than categorical fuel types (e.g., Andersen et al., 2005; Erdody and Moskal, 2010; Skowronski et al., 2011; Hermosilla et al., 2014; Engelstad et al., 2019). Airborne Laser Scanning (ALS), a form of remote sensing that utilizes LiDAR (Light Detection and Ranging), is a promising new source of data for describing forest characteristics in dense stands, due to its ability to penetrate small openings in the canopy and describe the three-dimensional structure of a forest (Vastaranta et al., 2012; White et al., 2016; Wu et al., 2016). This thesis evaluates the viability of using ALS to derive fine-scale fuel attributes of black spruce (*picea mariana*) stands. It also assesses the effect of ALS data resolution on model predictive performance.

1.2 Fire Regime in the Canadian Boreal Forest

Fire processes in a given ecosystem are commonly referred to as the *fire regime*, which is typically described using a set of standard fire attributes characteristic of an area within a given period of time (Sugihara et al., 2006). Defining characteristics of a fire regime include the fire frequency, size, intensity, seasonality, type and severity (Merrill and Alexander, 1987). The boreal forest is a dominant fire regime in Canada that covers 270 million ha of land (NFI, 2013). Wildland fire is the most common form of natural disturbance within the Boreal Region and plays a critical role in healthy biotic and abiotic ecosystem functioning (Rowe, 1983).

In Canada between 2008 and 2018 there was an average of over 6000 wildland fires per year burning an average annual area of over 2.7 million ha (CIFFC, 2018). Most wildfires in boreal ecosystems are extinguished when they are relatively small with only 3% of fires growing larger than 200 ha; however, these large fires account for 97% of annual area burned within the Boreal Region (Stocks et al., 2002). On average, 0.7% of forested land in the Boreal Region burns annually (Stocks et al., 2002). As climate change continues to progress, the average annual area burned and number of large fires per year is expected to increase, particularly in the boreal (Hanes et al., 2018).

Lightning and human caused ignitions are the two main mechanisms for wildfires starting in the boreal forest. Although lightning is the ignition source for only 35% of Canada's fires, it is responsible for 85% of the area burned (Krezek-Hanes et al., 2011). This is likely because human caused ignitions tend to be closer to resources that can be used for fire suppression (Stocks et al., 2002). The Canadian forest fire season generally begins in April and continues to mid-October (Stocks et al., 2002). Human caused ignitions are most common in the spring and fall months where lightning caused ignitions dominate the summer months (Stocks et al., 2002).

There are three main classifications of wildfires: ground, surface and crown; and each type can contribute to different ecological functions (Stocks et al., 2002). Ground fires burn in the organic matter beneath the litter surface on the forest floor and are common in the boreal forest where there is abundant peat to keep the fire smoldering for lengthy periods of time. Dormant ground fires can smolder through the winter months and become active by igniting new surface fires in the spring. Surface fires consume low level vegetation, litter and duff at or above the forest floor.

Unlike ground fires, surface fires have a visible flame and are easier to extinguish. Ground and surface fires tend to spread relatively slowly, but can transition to a crown fire when surface combustion reaches critical intensities (Van Wagner, 1987). Involvement of crown fuels in combustion results in much higher intensities compared with surface fires and the intensities of crown fires exceed the capabilities of direct suppression along the fire front (Alexander, 1982; Hirsch et al., 1998). The boreal is characterized by crown or surface fires with a high enough intensity to kill entire stands, resulting in even-aged post-fire regeneration (Heinselman, 1981; Bonan and Shufart, 1989). These fires are necessary for healthy ecosystem functioning and play a critical role in regeneration (Zackrisson et al., 1996; Nguyen-Xuan et al., 2000; McRae et al., 2001). For example, some species, such as Jack Pine (*Pinus banksiana*) are dependent on high intensity, stand-replacing fires as they have evolved to have serotinous cones, which require the heat of a fire to release their seeds (Heinselman, 1981). Wildfires can also expose nutrients and mineral soil which helps with forest succession (Rowe. 1983).

Despite wildfires being recognized as a natural part of the boreal landscape, most provinces and territories in Canada aim to contain wildfires as soon as possible. This is because the risk of letting a wildfire burn unsuppressed is unacceptably high, due to the potential liability associated with adverse fire effects on public safety, property and other values (Martell, 2001). Wildfires can threaten human life, destroy infrastructure, increase soil erosion, decrease water quality and generate huge economic losses (Shakesby et al., 1993; Parise and Cannon, 2012; Moritz et al., 2014; Reid et al., 2016). As a result, the benefit of accommodating wildfires naturally on the landscape is widely recognized by fire management agencies across Canada as an important

goal, but remains elusive in practice (e.g., Martell, 2001; Flannigan et al., 2009; Alberta Wildfire, 2019).

1.3 Fire Environment and Behaviour

Wildfire behaviour is commonly defined as "the manner in which fuel ignites, flame develops and fire spreads" (CIFFC, 2017). Wildfire behaviour is determined by three interacting factors: topography, weather and fuel. Topography describes the shape of the land and includes attributes such as slope, elevation and aspect. Topography is the most stable component of the fire environment where weather is arguably the most variable over time. Weather attributes include temperature, humidity, precipitation and wind speed. Weather greatly influences the moisture content of fuels and their ability to ignite and propagate a wildfire (Van Wagner, 1987; Van Wagner, 1993; Beverly and Wotton, 2007). Wildland fuels consist of live and dead biomass that are available to combust and contribute to the spread, intensity and severity of a forest fire (Anderson, 1981; Andrews and Queen, 2001; Arroyo et al., 2008). The vegetation type, loading, structure and continuity of fuel will affect fuel receptivity to ignition and the ability for a wildfire to spread (Anderson, 1981).

Despite fuel being a main component of the fire environment, it can be quite difficult to describe and quantify (Keane et al., 2001; Arroyo, 2008). This is in part because there are so many physical characteristics that can be used to describe a given fuel complex (Keane et al., 2001). One way to describe fuel is to focus on size. Fine combustible materials, such as needles or dried dead leaves, respond faster to environmental conditions (Anderson et al., 1966; Fosberg, 1970) due to their higher surface-to-volume ratio. The higher surface-to-volume ratio enables quicker

endothermic preheating and speeds up the combustion process, making fine materials much easier to ignite than coarser materials such as tree boles or downed woody debris (Stocks et al., 2004). The moisture content of these fine fuels will modulate their flammability (Beverly and Wotton, 2007). Expansive quantities of fine crown fuels (i.e., needles) in coniferous forests are highly combustible and therefore enable extreme fire intensities, whereas leafy, green vegetation in deciduous or mixedwood stands are resistant to burning due to their moisture content and only contribute to fire spread when leaves accumulate as dead, dried fuel on the forest floor. Coarser materials > 1.0 cm in diameter are often not fully consumed in a wildfire and do not make a large contribution to wildfire intensity (Stocks et al., 2004).

Fuel can also be described by its vertical position above the ground and horizontal continuity across an area. Ground fuels consist of all combustible materials below the litter layer on the forest floor. Surface fuels, such as dead and downed woody debris, understory shrubs, mosses and litter, are combustible materials that are close to the forest floor. Canopy fuels consists of combustible materials over 2 m in height and are typically composed of a tree's foliage and branchwood, but can also include mosses, lichen or other dead material (Keane, 2013). Ladder fuels provide a connection between the surface fuels and crown fuels and consist of taller shrubs, small trees and lichen for example. The vertical continuity of the fuel strata will affect fire behaviour and the presence of ladder fuels provides a path for a surface fire to transition into a crown fire (Van Wagner, 1977; Anderson, 1981). Horizontal continuity of fuels is also important to fire behaviour and affects the rate of and potential for fire spread (Anderson, 1981; Stephens, 1998; Knapp & Keeley, 2006).

Another important characteristic of fuels that will affect wildfire behaviour is vegetation type. Some species have a chemical composition and structure that make them easier to ignite and spread fire. For example, black spruce trees have resinous needles and cones that contribute to flammability, as well as accumulations of dead branches that facilitates fire spread into the crown (Viereck and Little, 1972). The moisture content of fuel is also a key factor in fire behaviour. Depending on species type, time of year and age of the foliage, moisture content of fuel can vary significantly (Agee et al., 2002).

1.4 Fuel Models and Mapping

Fuel characteristics are a key determinant of fire behaviour and are therefore a required input to any fire behaviour model. Typical modelling parameters to describe canopy fuels include canopy height, canopy base height (CBH), canopy fuel load (CFL) and canopy bulk density (CBD) (Keane et al., 2001; Cruz et al., 2003). Canopy height affects wind trajectory and speed (Finney, 1998) which will influence observed fire behaviour and affect the distance embers travel aloft (Chuvieco et al., 2003). Canopy base height is a measurement of the vertical separation between the ground and the live canopy fuel layers and is important for determining whether a surface fire will progress into a crown fire (Van Wagner, 1977). Canopy fuel load is a determinant of fire intensity and refers to the amount of fuel in the canopy that is available for combustion and often includes foliage and small branches (Stocks et al., 2004). Canopy bulk density describes the available canopy fuel per unit volume which will affect the rate of fire spread (Chuvieco et al., 2003). These varied stand attributes have an important influence on wildfire behaviour but would be prohibitively costly and time consuming to measure in the field. Measuring fuel characteristics manually also results in a limited inventory of stand attributes across a landscape

(Andersen et al., 2005; Hermosilla et al., 2014). Due to their limited extent, field measurements are ineffective for capturing fine scale variability of fuels across large areas. Consequently, simplified representations of fuels are widely relied on in fire research studies and fire management applications.

In the United States, fuel models are used to provide a generalized description of fuel properties that are important to wildfire behaviour (Keane et al., 2001). Fuel models can also be used to define categorical fuel types. Within a given fuel type, species type(s) and the form, size, arrangement and continuity of fuels is assumed to be relatively static (Anderson, 1981; Arroyo, 2008). Fuel types are used as inputs into wildfire behaviour models. For example, in Canada and parts of the United States, the Canadian Forest Fire and Behaviour Prediction (FBP) System is used to generate quantitative estimates of the rate of fire spread, fire intensity and other fire behavior attributes specific to one of 18 possible fuel types (Forestry Fire Danger Group, 1992). This is one of several fire prediction modelling systems that uses inputs describing topography, weather and fuel moisture to predict how a wildfire will behave in a specific fuel type.

The FBP System is used by Canadian fire managers to assess initial conditions at the site of a newly reported fire and estimate the potential for a fire to escape, given the predicted fire behaviour. Within the FBP System, fuel types are used to describe dominant vegetation types in Canada **(**Forestry Fire Danger Group, 1992). Although the FBP System has proven valuable for informing fire management decisions, it cannot be used with high precision to determine exactly how and where a wildfire will burn (Taylor & Alexander, 2016). This is in part because the model assumes uniform and continuous fuels and that the fuels of interest fit into one of the 18

benchmark fuel types. Studies show that even within the same FBP fuel type, the variability in stand structure can significantly affect crown fire intensity and the chances of a fire escaping containment (Lavoie, 2004; Johnston et al., 2015; Beverly, 2017). As a result, inaccurate predictions of wildfire behaviour may occur by not accounting for the structural variability of stand characteristics (Keane et al., 2012).

Mapping fuel attributes over space provides fire researchers and resource managers forest structure information to support wildfire behaviour models (Keane et al., 2001; Andersen et al., 2005; Hermosilla et al., 2014). In Canada, satellite image-based land cover classification, ecozone and ecoregion boundaries, and National Forest Inventory data are used to create FBP fuel type maps (Nadeau et al., 2005). Limited or outdated data for any of these sources could affect the reliability of the produced fuel grids (Nadeau et al., 2005). The operational FBP System fuel type grid resolution for Canada is 250 m although provinces may develop their own finer resolution grids. For example, Alberta uses a 1-ha fuel type grid for operations (Stockdale et al., 2018). This coarse classification and often outdated inventory information, can lead to incorrect fuel typing and therefore inaccurate fire behaviour predictions.

The FBP System fuel types have been deeply integrated into fire management decision processes across Canada since 1984 (Stocks et al., 1989). There is no doubt that fuel typing has made an invaluable contribution to helping fire managers better understand how wildfire may behave (Stocks et al., 1989). That said, technology is improving and studies show that remote sensing technologies are now able to accurately measure and map over space fuels at high resolutions (e.g. Andersen et al., 2005; Erdody and Moskal, 2010; Hermosilla et al., 2014; Bright et al.,

2017; Engelstad et al., 2019). The limitations of relying on simplified fuel types and ignoring variability in fuel structure within these broad categories, will eventually be overcome with advances in fuel mapping methods. Availability of better fuel data will enable development of new and improved fire behavior models and more realistic fire behaviour predictions.

1.5 Introduction to Airborne Laser Scanning

Airborne laser scanning (ALS) is a form of remote sensing that uses a laser mounted on an aircraft to map the surface of the earth. Airborne laser scanning has been used operationally in forestry since the early 2000s (White et al., 2016). It has the unique ability to capture more accurate 3D forest characteristics compared with other forms of remote sensing, making it an ideal technology for enhanced forest inventories and mapping forest characteristics across small and large scales (Dubayah and Drake, 2000; Lim et al., 2003; White et al., 2016; White et al., 2017). Airborne laser scanning has been used extensively to summarize forest attributes such as stand canopy height, basal area and stem volume and is a well-established technology in forestry applications (Wulder et al, 2013; Næsset, 2014; White et al., 2016). In contrast, the use of ALS for wildfire management research, applications and planning remains relatively unexplored within the Canadian boreal forest context.

An ALS system is composed of a Light Detection and Ranging (LiDAR) sensor, a GPS receiver, an inertial measurement unit (IMU), an onboard computer and data storage devices (Wulder et al., 2013). The ALS system works by emitting a laser pulse from the airborne platform and measuring the time it takes for the energy of that pulse to be returned after hitting a reflective surface. In a forestry context this could be the ground, a branch, a shrub or other land-based

feature (White et al., 2013). The laser travels at the speed of light, such that accurate distance measurements can be obtained between the sensor and the reflected surface using the travel time of the laser to the ground and back. With the GPS receiver and inertial measurement unit, very accurate X, Y and Z locations can be defined for whatever surface receives and reflects the laser (White, et al., 2013). ALS systems are capable of transmitting and receiving up to 500 000 laser pulses per second which generates dense point clouds representing the forest beneath the ALS system (White, et al., 2013). In discrete-return systems, one laser pulse can also have multiple returns. This is when some of the energy is reflected back to the sensor, but some of the energy from the emitted laser continues to penetrate the canopy and is able to detect more objects on the way. The point clouds generated with an ALS system can be compared with field data to generate a model that predicts forest characteristics of interest. A robust model can then be applied to map these forest characteristics across a given area without requiring time- and resource-intensive ground-based field sampling campaigns.

Andersen et al. (2005) was one of the first research groups to successfully relate ALS metrics to field-measured fuel data with the purpose of developing fuel maps that could be direct inputs into fire behaviour models. They used stepwise regression followed by cross-validation to create and test their models which were designed to make fuel maps of critical canopy fuel parameters over Pacific Northwest conifer forests. Numerous studies have since followed this approach for describing the variability of fuel characteristics over space (e.g., Skowronski et al., 2011; Hermosilla et al., 2014; Zhang et al., 2017). Many statisticians argue that stepwise regression tends to overfit models and should be used with extreme caution (Thompson, 1995; Babyak, 2004;); however, other studies used alternative variable selection methods to relate ALS data to

field-measured fuel data and continue to find promising results (e.g., Hall et al., 2005; Skowronski, et al., 2007; Erdody and Moskal, 2010; González-Ferreiro et al., 2014; Botequim, et al. 2019). As technology and computer processing advances, machine learning is becoming a popular method for predicting forest canopy fuel attributes from ALS data (e.g., Jakubowski et al., 2013a; Bright et al., 2017).

As ALS data becomes less expensive and easier to obtain, higher quality datasets are being produced. Interestingly, many studies show that even low point cloud resolutions (<1 first returns per m^2) can have good relationships with forestry metrics important to wildfire behaviour (Botequim et al., 2019) or forestry metrics in general (Treitz et al., 2012; Jakubowski et al., 2013b). The point resolutions required to generate reliable models ultimately depends on the forest structure and scale represented by the models.

1.6 Black Spruce Stand Management

One of the recommendations made by the Flat Top Complex Wildfire Review Committee after the devastation caused by the Flat Top Complex Wildfire on the town of Slave Lake, Alberta was to increase our understanding of "the contribution of black spruce as a source of extreme wildfire behaviour and spotting" (2012). Black spruce stands within the boreal forest are a highly combustible and structurally diverse fuel. Crown fires or surface fires with enough intensity to kill overstory trees are the most common types of fire for black spruce stands (Viereck, 1983). Black spruce stands are typically represented by the Boreal Spruce (C-2) fuel type within the FBP System. These fuels are characterized by canopies that extend to the forest floor and contain accumulations of dead branches and lichen (Forestry Fire Danger Group, 1992), adaptations that

allow for efficient transition of a surface fire into a crown fire (Viereck, 1983). Due to the high intensity crown fires characteristic of these stands, black spruce fuels are a significant challenge for fire suppression within much of Canada (Viereck, 1983).

Evidence shows that the FBP System does not provide enough structural information to predict fire behaviour in black spruces stands with a high degree of precision. For example, Beverly (2017) used an indirect method to infer stand structure in black spruce based on the time elapsed since the last fire and showed this variable was a significant determinant of whether or not a fire in C-2 fuel will escape and become large, likely due to natural changes in fuel loads as the stand develops and ages. Johnston et al. (2015) analyzed black spruce stands in boreal bogs and measured canopy fine fuels in a chronosequence of stands consistent with the C-2 Boreal Spruce fuel type. The large variability in canopy bulk density measurements led Johnston et al. (2015) to conclude that stand structure would result in different fire behaviours in C-2 stands with different ages. Finally, Taylor et al. (2004) found that while fire spread in black spruce stands is highly dependent on wind conditions, it is also influenced by fuel characteristics.

Managed stands introduce another source of variability in fuel structures that deviate from the standard natural forest types represented in the FBP System. Stand management through mechanical alteration (i.e., thinning, limbing) is increasingly used as a proactive method to reduce potential fire behaviour in the vicinity of high valued areas like communities. Mechanical thinning treatments typically involve reductions in stand density and limbing the bole of the tree to separate crown fuels vertically and horizontally in an effort to inhibit movement of a surface fire upwards into the canopy. Since 2012, when the Flat Top Complex Wildfire Review

Committee recommended increasing fuel management practices across the province of Alberta (particularly in black spruce stands), communities have increasingly applied for funding to conduct vegetation management treatments. Between 2011 and 2017 almost $43 million in funding was distributed to over 50 communities in Alberta for vegetation management projects or related wildfire community safety initiatives (Alberta Agriculture and Forestry, 2017). Unfortunately, managed stands are not represented by any FBP System fuel types, such that expected fire behaviour in these stands is largely unknown. Anecdotal evidence from wildfires (Saperstien et al., 2014; Government of Saskatchewan, 2015; Perrine 2016) and prescribed fires (Butler et al., 2013; Miller 2016) suggest that thinning treatments in black spruce stands reduces observed fire behaviour, an outcome that is also supported by modelling studies (Little et al., 2019). Unfortunately, there are no existing models for predicting how fires will behave in mechanically altered Canadian fuel types.

Airborne Laser Scanning offers an opportunity to describe black spruce forest characteristics important to wildfire behaviour at a high resolution. This may help fire management personnel better understand what structural attributes cause black spruce stands to show extreme fire behaviour. Airborne Laser Scanning has been used for documenting conditions in other stand types with notable success; however, when building models, it is common practice to account for species type (White et al., 2017) and to date, no prior studies have investigated the viability of using ALS to derive fuel attributes in black spruce stands. Treitz et al. (2012) and Luther et al. (2013) showed that ALS data could successfully predict wood quality and quantity attributes of black spruce stands, but did not measure characteristics important to wildfire behaviour. By addressing this research gap, high-precision and high-resolution maps that reflect the spatial

heterogeneity of a forest could allow land managers to better model fire behaviour, smoke emissions and prioritize hazardous fuel reduction treatments (Andersen et al., 2005; Erdody and Moskal, 2010; Skowronski et al., 2011) and efficiently monitor changes in stand conditions over time.

1.7 Research Objectives

This thesis explores the use of ALS for mapping the structural attributes of black spruce stands that are relevant to wildland fire behavior. The following specific research questions are addressed: (1) Are ALS data suitable for estimating forest stand metrics relevant to wildland fire behaviour in black spruce stands? and (2) What is the influence of ALS pulse density on model performance? To achieve these objectives, field plots were established in two study areas in the province of Alberta in both natural and hand-thinned black spruce stands. Airborne laser scanning data was collected over these study sites and split into three different pulse density resolution datasets. Predictive models were developed and evaluated for each forestry metric of interest (CBD, CFL, stem density, height and CBH) and for each of the three-pulse density resolution point clouds.

Chapter 2 Data and Methods

The methods for this study were developed to evaluate the suitability of using ALS data to predict forest stand metrics related to fuel flammability and to assess importance of ALS pulse density in deriving fuel measures for properties of black spruce (*Picea mariana*) stands. Field measurements were related to ALS data using lasso regression and models were evaluated on a testing dataset. A schematic overview of the methods used in this study is shown in Figure 2.1 summarizing the step-by-step sequence of the analysis detailed in the remainder of this chapter. In total, 15 models were created for this study, three for each of five canopy fuel metrics of interest.

2.1 Study Area

Two study sites were selected to represent the structural variability of black spruce stands within Alberta's boreal forest: one site was established at the Pelican Mountain Research Site (hereafter referred to as Pelican Mountain) and a second site was established within the community of Conklin (Figure 2.2). Locations were selected based on three criteria: presence of abundant black spruce stands; representation of a range of stand structures (e.g., unmanaged versus thinned and pruned states); and logistical ease of accessing the site and establishing field sampling plots. Both sites were located in the Boreal Natural Region, which covers 58% of the province and contains a variety of deciduous, mixedwood and coniferous forest ecosystems characterized by short summers and long and cold winters (Natural Regions Committee, 2006).

The Pelican Mountain Research Site spans 150 ha and was established by the agency responsible for fire management in the province, the Alberta Wildfire Management Branch, to evaluate the

effectiveness of fuel reduction treatments in black spruce stands (Figure 2.3). The site is composed almost entirely of black spruce trees, with pockets of aspen (*Populus tremuloides*), balsam poplar (*Populus balsamifera*), tamarack (*Larix laricina*), paper birch *(Betula papyrifera)* and willow (*Salix spp.*). Pelican Mountain has predominantly flat terrain, with elevations ranging from 590 m to 657 m above sea level.

Conklin is a hamlet in northern Alberta (Figure 2.4) with a land area of 16.3 km^2 (Statistics Canada, 2016) that contains and is surrounded by forest cover that includes mixedwood, deciduous, black spruce and other conifer stands, as well as some grassland areas. Elevations range from 530 m to 624 m above sea level. Due to the high fire risk associated with the black spruce stands surrounding the community, many stands were thinned and pruned in fuel reduction treatments between 2001 and 2011 with the intention to decrease the potential for extreme wildfire behaviour. Stands thinned and pruned at Conklin are representative of a range of older managed forest stands that can be found throughout Alberta. These managed stands also approximate the structure of black spruce stands that are naturally open.

This study focused on stands within the Pelican Mountain and Conklin research sites that fit the descriptions of the C-2 Boreal-Spruce fuel type of the Canadian Forest Fire Behaviour Prediction System (Forestry Canada Fire Danger Group, 1992). Canopies were almost purely composed of black spruce trees. Dead branches were often draped with bearded lichens and tree crowns in unmanaged stands extended to or near the ground. The forest floor was often a nearly continuous cover of feather mosses, dominated by big red stem moss (*Pleurozium schreberi*) with occasional small hummocks of sphagnum moss, primarily common brown sphagnum (*Sphagnum fuscum*).

Surface vegetation was dominated by Labrador tea (*Ledum groenlandicum*), lowbush cranberry (*Vaccinium vitis-idaea*), blueberry (*Vaccinium myrtilloides*) and bog cranberry (*Vaccinium oxycoccos*). Downed woody debris was largely absent in the natural stands, with a moderate presence in treated stands. Most sites had a thick organic layer, often > 40 cm in depth.
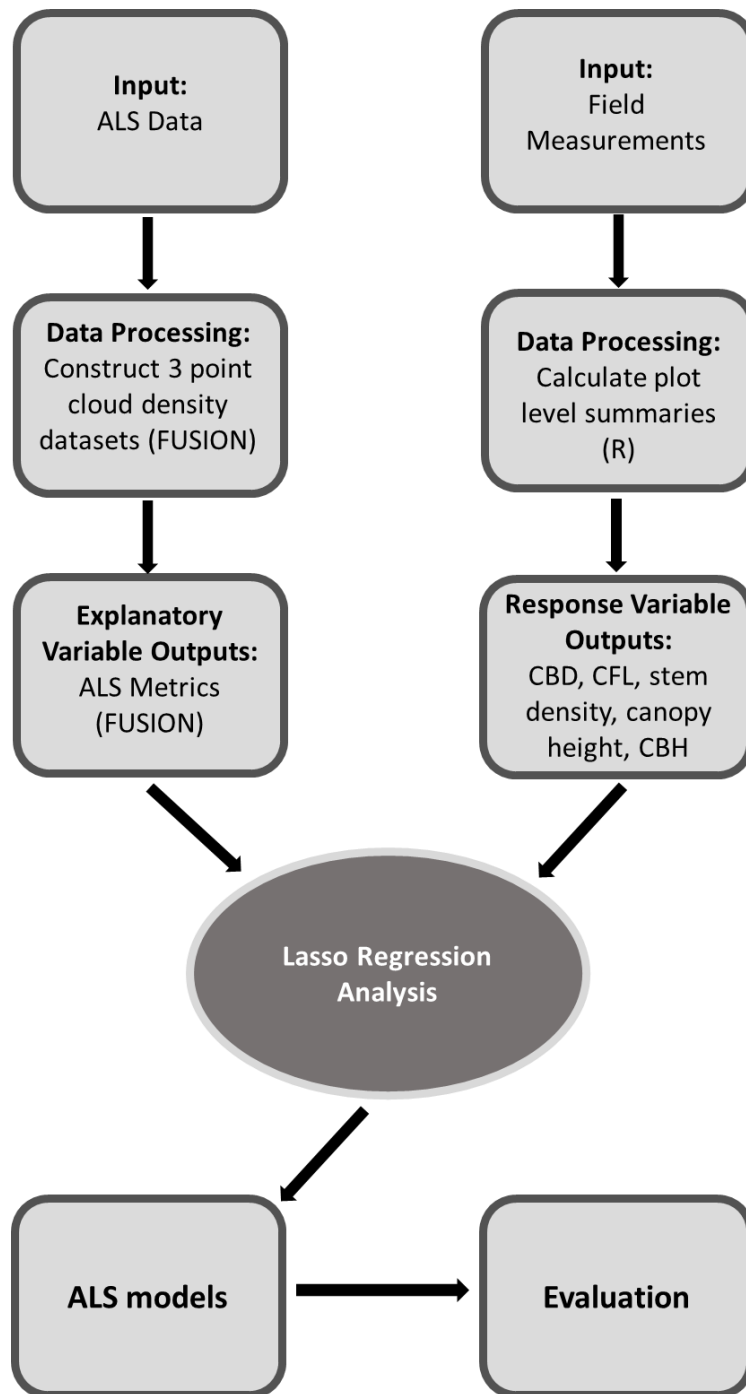
Figure 2.1 Schematic diagram of the data processing and modeling methods used to compare airborne laser scanning (ALS) data to field measurements.
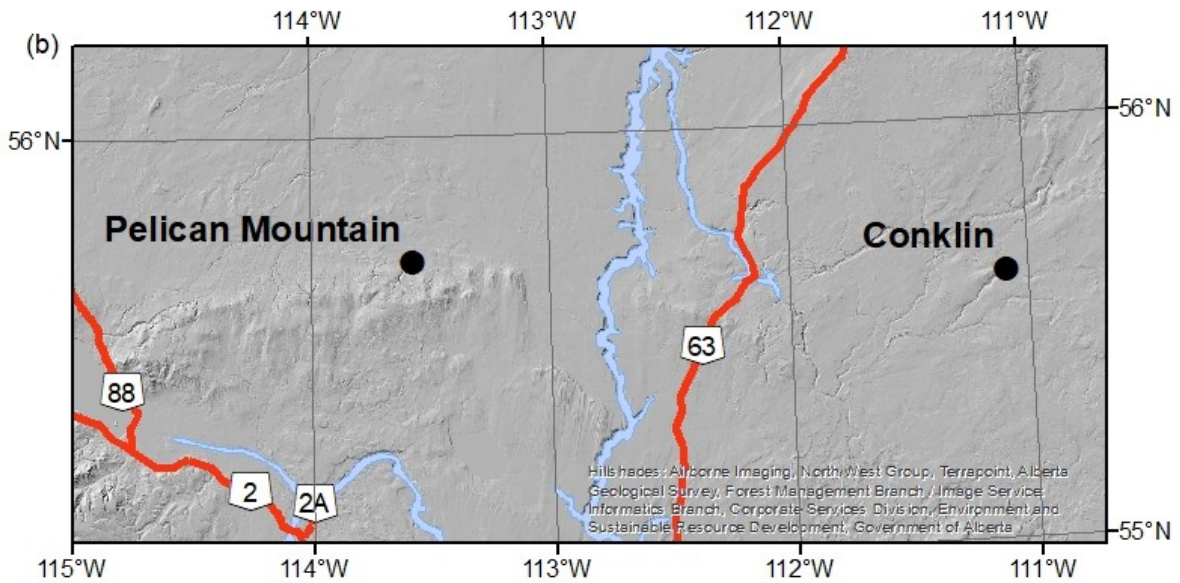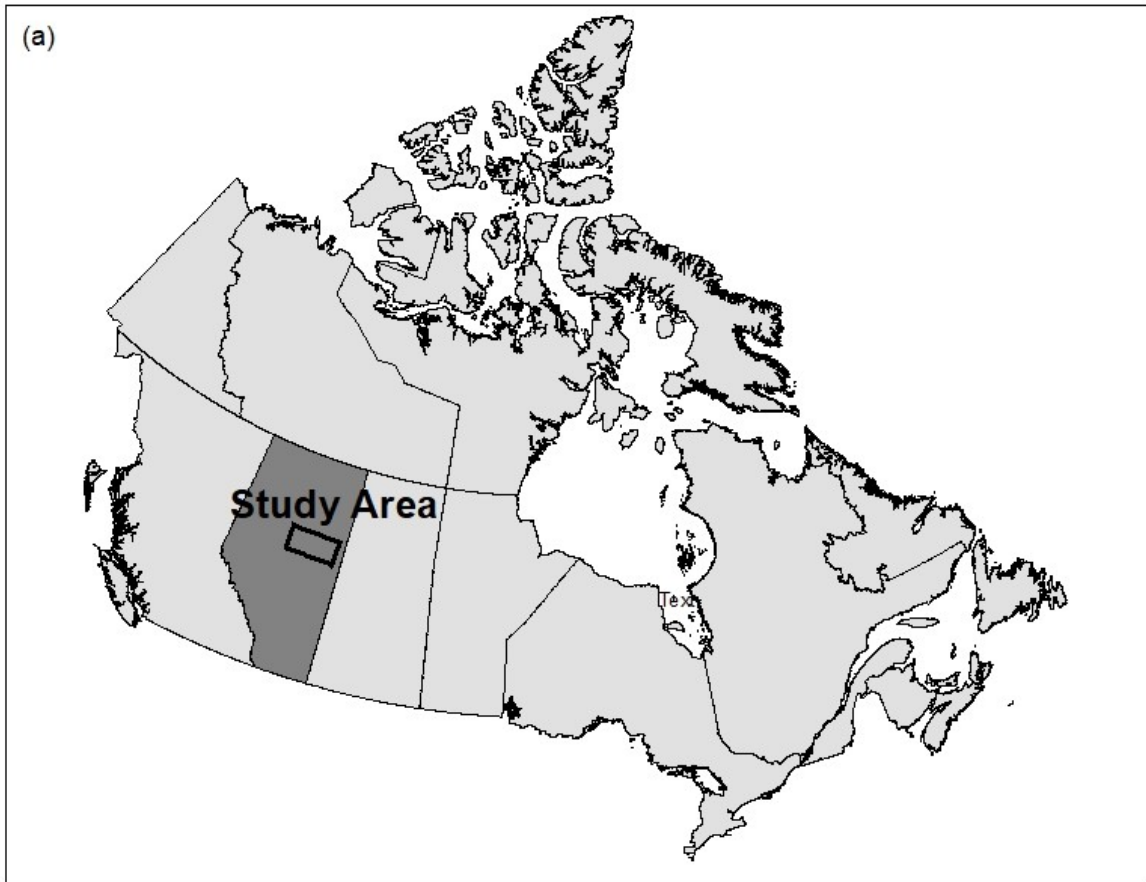
Figure 2.2 (a) Location of the study area within Alberta, Canada and (b) location of the Pelican Mountain Research Site and community of Conklin within the study area.
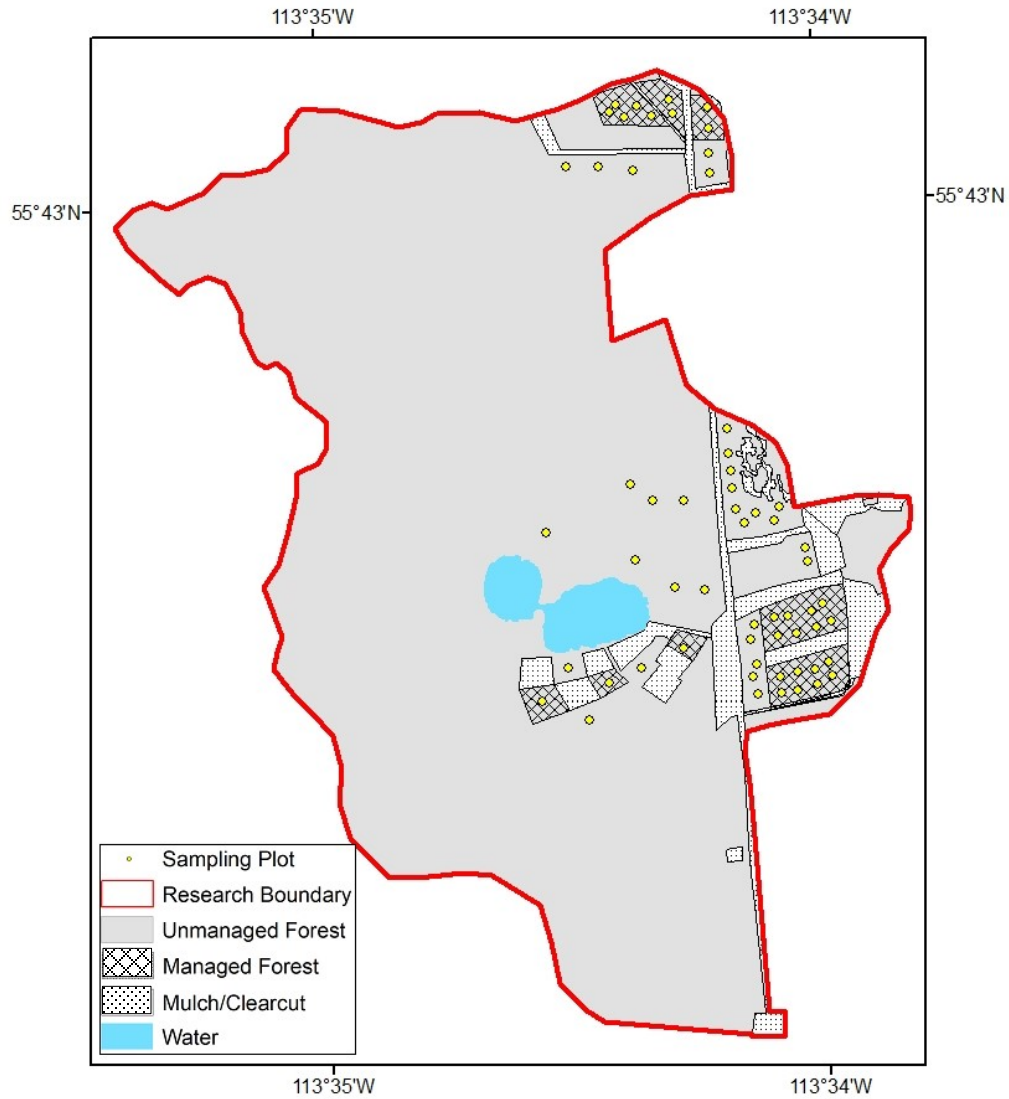
Figure 2.3 The Pelican Mountain Research Site is composed of unmanaged and managed black spruce forest. Managed forest stands have undergone stem thinning and have had the lower branches removed on remaining trees. Sampling plots were established to capture the full structure variability of black spruce stands across the research site.
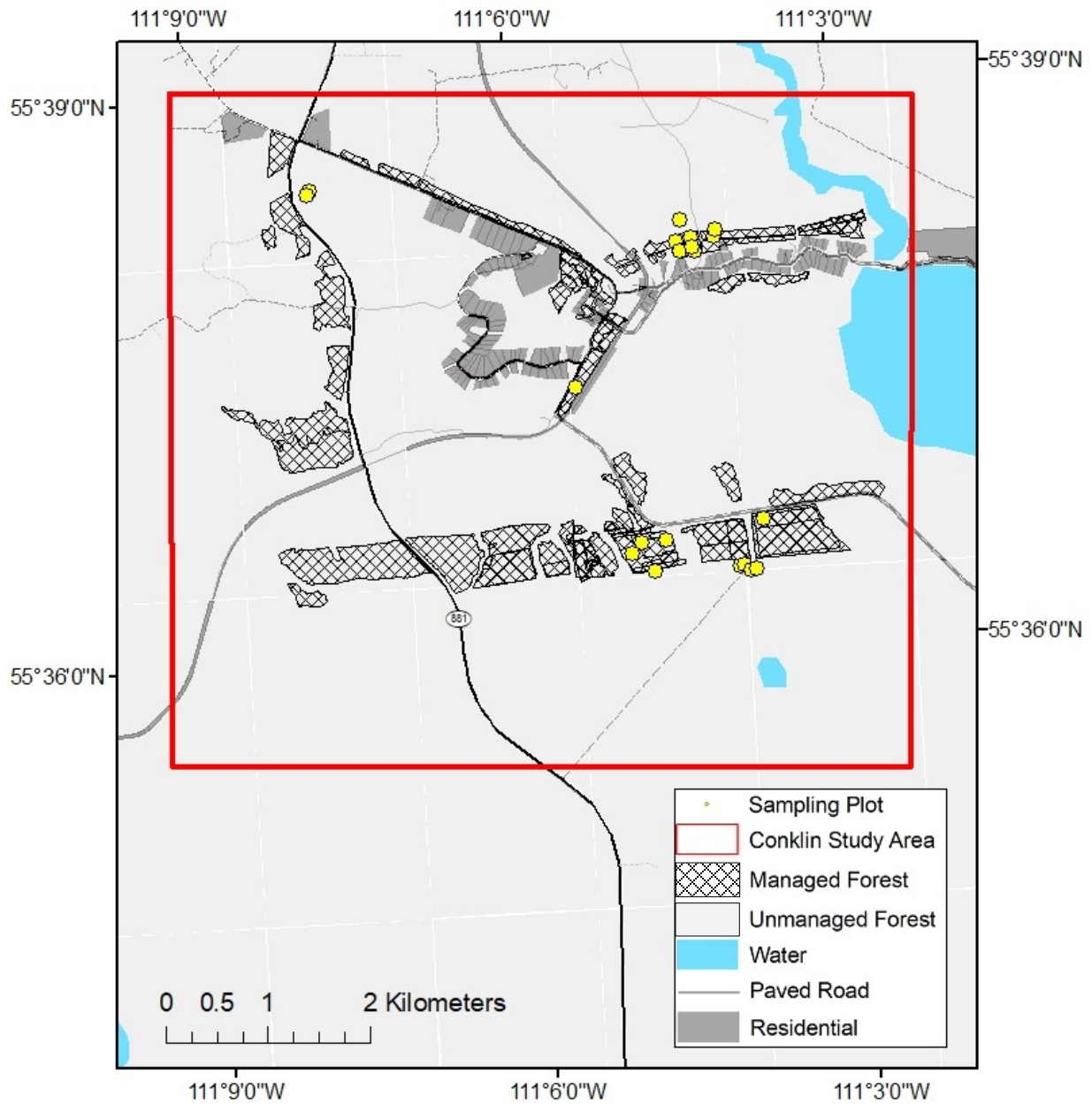
Figure 2.4 The Conklin community study area is surrounded by managed and unmanaged forest. Managed forest stands have undergone stem thinning and have had the lower branches removed on remaining trees. Sampling plots were established to capture the full structure variability of black spruce stands across the research site.

2.2 Field-based Fuel Estimates

A total of 59 plots were established at Pelican Mountain including 31 in natural stands and 28 in managed stands that were thinned and pruned to reduce fuel loads prior to sampling. Tree core samples at 0.25 m in height were taken at each plot indicating that tree age varied from 40 to 100 years. Tree ages were not adjusted for height above ground in age. Ground observations of stand structure provided further evidence that multiple historical fires affected the research site. Sampling took place over three years between April and August of 2017 and May and August of 2018 and 2019. Measurements in managed stands occurred 0-2 years post-treatment.

Twenty sampling plots were established throughout the Conklin community in August 2018 and August 2019. Eight were located in natural black spruce stands and 12 were located in managed black spruce stands. Based on tree core samples taken at each plot location, stand age varied from 40 to 110 years.

Development of effective models with ALS data, is dependent on field plots that capture the full range of variability of stand characteristics being analyzed (White et al., 2017). Plot locations were selected using imagery and knowledge gathered through site visits in an effort to represent a wide variety of stand structures associated with natural and managed black spruce stands. Although other boreal stand types were present at both study sites, field measurements were limited to black spruce stands. Detailed descriptions and assumptions pertaining to calculations used to derive canopy characteristics are outlined below.

A total of 79 circular fixed inventory plots were established across the two study areas in natural and managed black spruce stands between April 2017 and August 2019. Circular plots are recommended when relating ground measured data to ALS data as edge effects are minimized (Frazer et al., 2011). Plot positions were determined to a horizontal accuracy of less than 0.6 m using a Trimble® Geo7X global navigation satellite system device with a Trimble® Tempest Antenna (Sunnyvale, CA). Trimble Pathfinder Office software was used for differential post-processing. Either Slave Lake or Fort McMurray base stations were used for correcting the coordinates, depending on which base station yielded higher horizontal accuracy. Average horizontal accuracy for the plot center coordinates was 0.39 m.

Plot size is an important parameter when developing ALS models (Frazer et al., 2011). Large plot sizes tend to minimize edge effects and decrease co-registration error (Frazer et al., 2011); however, when using the area-based approach, it is also critical to maintain consistency between the ground plot size and the grid resolution of the desired raster output of the modelled forest attributes (White et al., 2017). Consequently, to generate high-resolution spatial estimates of fuel characteristics, a small ground plot size was required. Although smaller plot sizes introduce potential error within the model, a number of studies have used very small ground plot sizes to generate wall-to-wall metrics across their study area with ALS data. Greaves et al. (2016) used circular ground plots with only a 0.45 m radius to capture shrub biomass estimates. Estornell et al. (2011) used plots with a minimum radius of 0.5 m to map shrubs in small forest stands. A study by Popescu et al. (2011) mapped more complicated forest structure using small ground plot sizes. In that study, Geoscience Laser Altimeter System (GLAS) data and ALS data with 5.64 m radius ground plots were used to calculate wall-to-wall above ground biomass estimates for

young pine stands. Zhao et al. (2009) also mapped forest biomass using an individual tree-delineation approach with 5.64 m radius plots. The sampling radius for ground plots in this study was either 3.57 m (76 plots) or 5.64 m (3 plots). The 5.64 m sampling radius was used when fewer than 20 trees occurred within the 3.57 m sampling radius area. Reliance on a variable radius plot when using the ABA to relate ground data to ALS data is usually not recommended (White et al., 2017), but was necessary in this study to efficiently capture canopy characteristics in low density stands.

Field crews from the Alberta Wildland Fuels Inventory Program (AWFIP) assisted with data collection. The AWFIP is run by the Alberta Wildfire Management Branch, the agency responsible for fire management in Alberta. Ground measurements were collected following the standard AWFIP sampling protocol. For each sampling area, all trees greater than 1.37 m in height were measured to record species, status (live or dead), height, live crown base height and diameter at 1.37 m (DBH). For trees with a DBH of 9.0 cm or greater, dead crown base height was also measured. Canopy height, canopy fuel load (CFL), canopy bulk density (CBD), canopy base height (CBH) and stem density were calculated using field measurements for each plot in the statistical software package R (R Core Team, 2018).

Canopy Height

Canopy height (m) was defined as the tallest tree within the sampling area and was measured using a Haglöf Sweden® Vertex instrument.

Canopy Fuel Load

Canopy fuel load (CFL, kg m^{-2}) was defined as crown biomass available to be consumed in the flaming stage of a passing crown fire per unit area. There is no consensus within the scientific community as to what components of the canopy should contribute towards the CFL measurement (Arroyo et al., 2008). Some researchers suggest that live crown foliage is the main source of fuel for a crown fire (e.g., Van Wagner, 1977), while others argue that lichen, moss and branch wood should also be considered (e.g., Alexander et al., 2004; Stocks et al., 2004). Based on documented fuel consumption for crown fires in stand types similar to black spruce, I opted to include foliage and fine branchwood less than 1.0 cm in diameter in my CFL calculations. This assumption follows Stocks et al. (2004) which reports fuel consumption for different fuel size classes at the International Crown Fire Modeling Experiment (ICFME), located in the Northwest Territories, Canada. They found that on average, 95% of the mass consumed in the overstory canopy during a crown fire was from foliage and woody material less than 1.0 cm in diameter (Stocks et al. 2004). Linn et al. (2012) modeled the ICFME fires with FIRETEC (Linn, 1997), a physics-based, 3-D stand-level wildfire behaviour model, using CFL values from total loads of needles and roundwood up to 1 cm in diameter. This assumption was also used by Johnston et al. (2015) to calculate CFL values in black spruce forested bogs. The purpose of this study was to evaluate the effectiveness of using ALS data to describe forest characteristics important to flammability and potential wildfire behaviour. Assumptions about CFL composition used in this study differ from those used in the FBP system, where only foliage mass counts towards canopy fuel load values. Consequently, direct comparisons of fire behaviour modelled using the CFL values produced in this study with fire behaviour predicted using the FBP system are not possible.

Published allometric equations based on DBH and species type were used to calculate the mass

of available canopy fuel for each tree over 1.37 m in height (Table 2.1). Canopy fuel load

(kg m^{-2}) for the plot was then calculated as follows (Eq. 1):

$$CFL = \frac{\sum CF_i}{a}, \qquad \text{[Eq. 1]}$$

where CFi is the mass of canopy fuel contributed by an individual tree in kg and a is the

sampling area of the plot (m^2). For dead trees it was assumed that no foliage was present;

however, dead, fine branchwood less than 1.0 cm was included. Although plots used in this study

were almost entirely composed of black spruce, occasionally other species were found within the

plot. Observed species considered to contribute to canopy fuel load are listed in Table 2.1 along

with the allometric equations used to estimate their contribution to the plot level fuel load. Paper

birch, trembling aspen, balsam poplar, tamarack and willow species were also found within some

plots, but it was assumed that these hardwood trees and shrubs were insignificant contributors to

available canopy fuel load and were omitted from analysis. This assumption is consistent with

other widely used models including the Fire and Fuels Extension (FFE; Reinhardt and Crookston

2003, Rebain et al., 2010) contained within the Forest Vegetation Simulator (FVS; Wykoff et al.,

1982). The FFE-FVS is used to simulate fuel dynamics and potential fire behaviour for different

vegetation types in the United States and parts of Canada. It is one of the most commonly used

models to simulate wildfire effects and has proven to be a valuable tool for informing fire

management and response decisions (Barker et al., 2019).

Table 2.1 Allometric equations used to calculate an individual tree's canopy fuel load (CFi) based on tree diameter at breast height

Species	Source for Calculating Canopy Fuel Load	Equation
Black spruce (*picea mariana*)	Alexander, 2004	$CF_i = 0.23317(DBH)^{1.25384} + 0.13267(DBH)^{1.11546} + 0.05553(DBH)^{1.12281} + 0.04995(DBH)^{1.29626} + 0.000167(DBH)^{3.81224}$
Jack pine (*pinus banksiana*)	Alexander, 2004	$CF_i = 0.00672(DBH)^{2.25699} + 0.00478(DBH)2.08881 + 0.00824(DBH)^{1.88877} + 0.00105(DBH)^{2.43234} + 0.00161(DBH)^{2.30592}$
Lodgepole pine (*pinus contorta*)	Johnson et al., 1990	$CF_i = 0.0525(DBH)^{1.6057} + 0.0533(DBH)^{1.8052} + 0.1369(DBH)^{1.3553}$
White spruce (*picea glauca*)	Johnson et al., 1990	$CF_i = 0.6373(DBH)^{1.1457} + 0.0869(DBH)^{1.8938} + 0.0304(DBH)^{1.7481}$

Canopy fuel loads predicted from allometric equations based on DBH had to be adjusted for 42 plots in managed stands where the trees had been pruned during fuel reduction treatments. There are no strict recommendations for how fuel reduction treatments are carried out across Canadian boreal forests (Butler et al., 2013), but typically the guidelines set out by FireSmart Canada are followed. FireSmart Canada recommends thinning trees to a minimum 3 m spacing between crowns and pruning remaining trees by removing all live and dead branches at least two meters from the ground (Vicars and Luckhurst, 1999). The purpose of these treatments is to remove the amount of fuel available to burn in a crown fire and to separate ground and canopy fuels making it more difficult for a surface fire to transition into a crown fire (Vicars and Luckhurst, 1999). These guidelines were followed during fuel treatments of the managed stands included in this study. In both study areas, any biomass mechanically removed during the treatment was piled and burned on site. As a result, the fuel load for each pruned tree was less than what would be

predicted using allometric equations. To account for this, a regression comparing tree height and

live crown base height was made for all live natural black spruce trees measured in this study

(Figure 2.5). Live crown base height was measured to the average height above the ground

where live foliage began. The relationship between field-measured tree height and live crown

base height was used to estimate the pre-treatment crown base height for each tree in managed

stands using the following equation (Eq. 2):

$$CBH_1 = 0.53 \times h + 0.15, \quad \text{[Eq. 2]}$$

where h is the height of the tree (m) and CBH_1 is the predicted crown base height for the tree

before pruning took place. The predicted crown fuel load from all trees in managed stands based

on DBH was then adjusted by the percent of canopy removed using the following equation

(Eq. 3):

$$CF_i = CF_{pi} \times [(h - CBH_2) \div (h - CBH_1)], \quad \text{[Eq. 3]}$$

where CF_{pi} is the mass (kg) of canopy fuel predicted using the allometric equations from Table

2.1 and CBH_2 is the recorded crown base height for the tree post-pruning (m). If a post-treatment

tree had a CBH_1 greater than CBH_2, then no adjustment was used and CF_i was calculated solely

on the allometric equations from Table 2.1. It should be noted that CBH_1 values for dead trees

were calculated using the same method as for live trees. This was because the sampling protocol

did not involve collecting crown base height information for dead trees with a DBH below

9.0 cm and therefore a reliable regression could not be created. Given that only 32 trees out of

the 546 trees measured in managed sites were classified as dead, the effects of this assumption

would be minimal. An important assumption is associated with Equation 3, where it is assumed

that no fuel would contribute to the canopy fuel load under the predicted crown base height. For

live trees, this means that if there were dead branches beneath the live crown base height, it was

assumed they did not contribute to the available canopy fuel load. This assumption could result in overestimates of canopy fuel loads in managed stands.
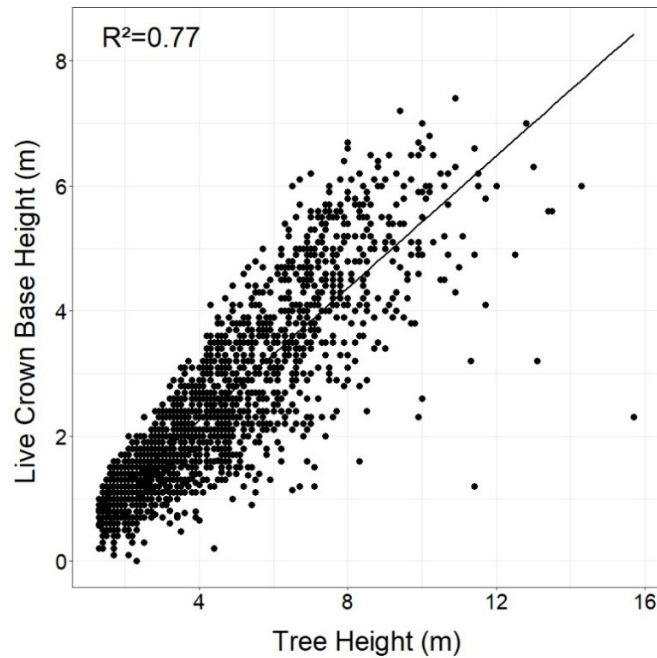
Figure 2.5 Relationship between tree height and live crown base height for all black spruce trees from unmanaged stands used in this study.

Canopy Bulk Density

Canopy bulk density (CBD, kg m^{-3}) was defined as the amount of fuel available to burn per unit volume and was calculated following the same methodology as the FFE-FVS (Reinhardt and Crookston, 2003; Rebain et al., 2010). For each individual tree, a uniform distribution of fuels was assumed between the crown base height and height of the tree. The crown base height was defined as the live crown base height for live trees and dead crown base height for dead trees. Since only dead trees with a DBH of 9.0 cm or greater had the dead crown base height recorded, dead crown base height was estimated using Equation 2 for dead trees with a DBH less than 9.0 cm. Using the crown position above the ground, the fuel density for all trees within the plot was summed in 0.3 m horizontal increments from the ground to the top of the canopy (Figure

2.6). Canopy bulk density was defined as the maximum 4.6 m running mean of crown fuel density for the plot. It should be noted that the FFE-FVS only counts conifer trees over 1.8 m tall towards canopy fuels (Rebain et al., 2010). In this study a slightly shorter threshold of 1.37 m is used because black spruce stands are typically stunted due to poor growing conditions, yet smaller trees still contribute significantly to the canopy (Johnston et al., 2015). A number of assumptions were made that may affect CBD values. Firstly, CBD was calculated based on the canopy fuel load values. The canopy fuel load values were derived from allometric equations and further assumptions as to what components of a forest should actually contribute to the canopy fuel load. Any errors or false assumptions would be propagated in calculated CBD values. Secondly, by evenly distributing canopy fuel load throughout the "depth" of a tree's canopy, CBD could be overestimated at the top of the tree and underestimated near the base. A study by Ex et al. (2016) found that the FFE-FVS underestimated CBD values by about 10-30% for even-aged interior western conifer stands in the United States when using uniform canopy fuel load distributions compared to nonuniform distributions. Finally, CBD could also be overestimated because the crown base height values used for live trees assumes that there are no dead branches that could contribute to the available canopy fuel load beneath this height. If this assumption is false, then the "depth" of the canopy would be too short resulting in a larger calculated CBD value. To mitigate these assumptions in the future, destructive samples could be collected to create a vertical fuel density profile, such as in Linn et al.'s study (2012) for the ICMFE site. Although Alexander et al. (2004) did create vertical fuel load and density profiles for jack pine and black spruce stands for at ICMFE, there was significant variation in the amount of fuel contributed by black spruce trees across their plots. Because of this, their vertical fuel profiles for black spruce stands were not deemed suitable for this study. Regardless of the assumptions used

for estimates, CBD values should always be used with caution as there is no published theory, model or empirical data that provides a critical CBD value that is necessary to propagate a fire vertically through the crown (Alexander et al., 2004; Werth et al., 2016).

Canopy Base Height

Crown base height (CBH, m) is easy to measure for an individual tree, but it is much more difficult to quantify canopy base height (CBH) for an entire stand (Scott and Reinhardt, 2001). In a wildfire context, CBH represents the height at which there is sufficient canopy fuel for a surface fire to transition into a crown fire. In the FFE-FVS model, CBH is identified using the vertical fuel density profile for calculating CBD (Figure 2.6). After applying a 0.9 m running mean, CBH is identified as the lowest height that the 0.011 kg m^{-3} threshold value is passed (Reinhardt and Crookston, 2003; Rebain et al., 2010). This value was chosen rather arbitrarily by Scott and Reinhardt (2001) and has been repeatedly used despite the lack of evidence to show it is an appropriate threshold (Cruz and Alexander, 2010). Reinhardt et al. (2006) acknowledge that the 0.011 kg m^{-3} threshold was "not based on any kind of combustion physics", but continued to use it because "it seems to perform well." Due to the lack of empirical information to support this approach, Van Wagner's (1977) simpler approach to defining CBH was used instead based on the average height from the ground surface to the live crown base height. Given that the live crown base height was measured for every live tree in the sampling area, minimal assumptions were needed when defining this parameter. To further support this method, Cruz and Alexander (2010) found that using Scott and Reinhardt's (2001) CBH definition over Van Wagner's (1977) led to an underprediction of potential crown fire behaviour in conifer forests of western North America. Canopy base height values calculated for this study should be used with caution as the

influence of ladder fuels which can help propagate a surface fire into a crown fire was not

accounted for.
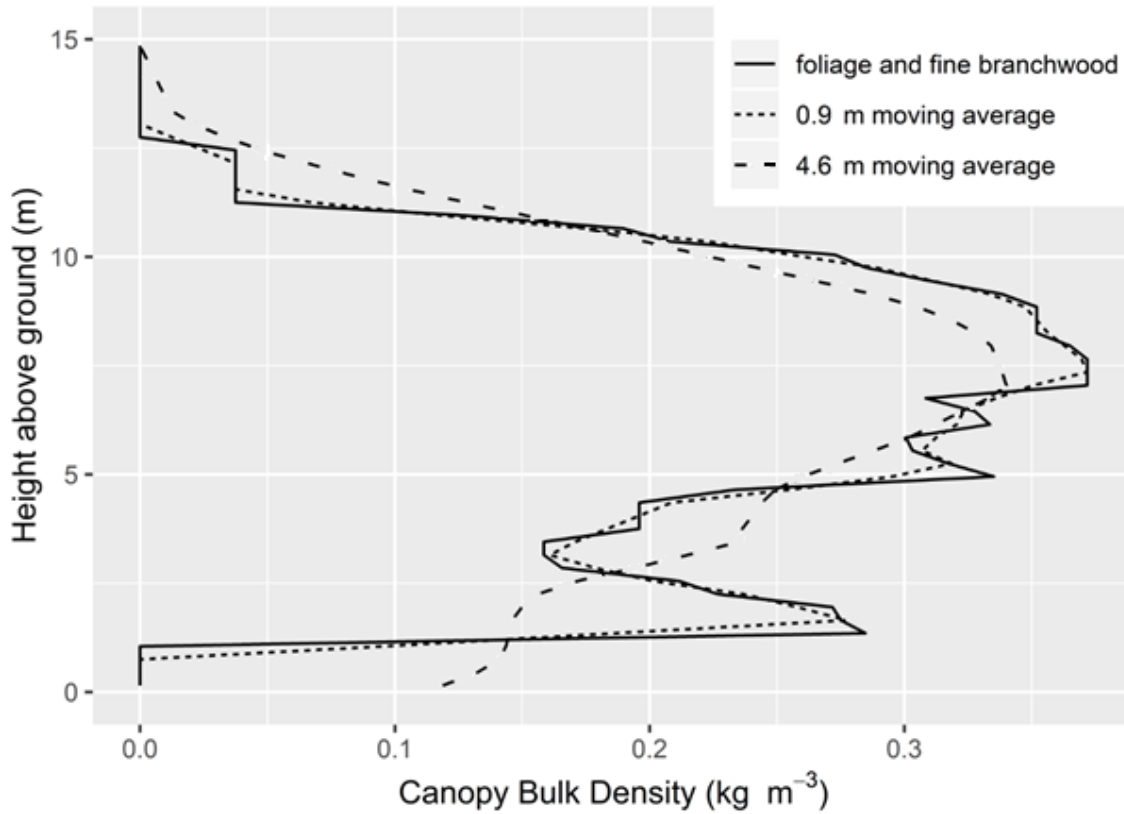
Figure 2.6 The vertical distribution of canopy fuel calculated using FFE_FVS methods. Canopy bulk density is defined as the maximum of the 4.6 m running mean and canopy base height is defined as the height where the 0.9 m running mean exceeds the 0.011 kg m^{-3} threshold.

Stem Density

Finally, stem density (stems ha^{-1}) was calculated using all trees over 1.37 m tall within the

sampling area. All field measurements for this study were conducted within at least 15 months of

ALS data acquisition. Given that black spruce stands grow quite slowly it was assumed that no

significant changes took place in the study area and the ALS data represents the stand at the time

of measurement.

2.3 Airborne Laser Scanning (ALS) Data

Airborne Laser Scanning data for forest inventory is often analyzed using one of two techniques: the area-based approach (ABA) or the individual tree detection (ITD) approach (Lim et al., 2003; Reutebuch et al., 2005; Wulder et al., 2008; Vauhkonen et al., 2011; Vastaranta et al., 2012). The ABA is the most common manner of utilizing ALS data to describe forestry metrics (Vastaranta et al., 2012). The ABA entails developing a predictive model that relates statistical ALS metrics to field based measurements (White et al., 2017). Once a relationship is estimated, the model can be used to map predicted forestry attributes over the entire area where ALS data were collected using some form of tessellation, often a raster. This is one of the key advantages of using remote sensing data in comparison with classic field-based measurements (Wulder et al., 2013). The ABA allows detection of detailed, within-stand variability for the entire area, rather than relying on a single field plot to represent stand-scale characteristics (White et al., 2017). In addition, the ABA is functional across a variety of scales, including plot, stand or regional extents (Wulder et al., 2013). The ABA approach has become the standard operational method to process and analyze ALS data (White et al., 2017).

As ALS technology improves, the ITD approach has gained more attention as a viable method for describing forest characteristics (Kaartinen et al., 2012; Zhen et al., 2016). The ITD approach attempts to identify and distinguish individual trees within a forest stand, usually above some height threshold (e.g. 5- 10 m). Most ITD approaches find a maximum in the canopy height model derived from the ALS point cloud to identify individual trees and then segment the trees based on the predicted crown edge (Hyyppä et al., 2008; Vauhkonen et al., 2011; Vastaranta et al., 2012). Multiple ITD approaches have been used, but comparisons of derived algorithms are

complicated by the lack of standards for assessing accuracy; further, algorithms effective in one

stand type may not be equally effective in others (Ke and Quackenbush, 2011; Kaartinen et al.,

2012; Zhen et al., 2016). Research to date into ITD using ALS data has produced encouraging

results (e.g., Breidenbach et al. 2010; Vauhkonen et al., 2011; Mohan et al., 2017), but evidence

suggests performance is sensitive to stand density, configuration and structure (Breidenbach et

al., 2010; Vauhkonen et al., 2011; White et al., 2017). Compared with ABA methods, ITD

typically requires a higher density point cloud, which was cost prohibitive in the early years of

ALS (Vastaranta et al., 2012). Although point densities can now be collected in much higher

resolution, the ITD is still considered a developing research approach in comparison with the

operationally-established ABA method (White et al., 2017). In addition, the raster-based output

of ABA is intuitive and easily integrated with other spatial data. In this study, the ABA was

utilized to describe forest metrics due to its status as an established operational tool.

Discrete return multi-spectral, ALS data were acquired in 2018 for Conklin and Pelican

Mountain on August 18th and 19th, respectively, using a Teledyne Optech Titan multispectral

sensor mounted on a Piper Navajo aircraft. This system emits three independent laser pulses in

the 1550 nm (short wave infrared), 1064 nm (near infrared) and 531 nm (green) wavelengths.

Metadata for the LiDAR system settings, flight parameters and data are shown in Table 2.2. The

University of Lethbridge ARTEMis lab collected and preprocessed the data using the LiDAR

Mapping Suite (LMS, proprietary software from Teledyne Optech) to generate a point cloud for

each channel. After block adjustment, point cloud height accuracy had a delta height RMSE of

3.5 cm and 3.1 cm for Pelican Mountain and Conklin, respectively. To create a bare-earth digital

elevation model (DEM), returns presumed to be measurements of the terrain surface were

classified as ground points for the 1064 nm channel only. Point cloud data were delivered in LAZ file format. The LASzip application (Version 3.2.9; Isenburg, 2018) was used to convert the LAZ data into LAS files for further processing. FUSION (Version 3.80, McGaughey 2018a), an open source software specialized for LiDAR data processing, was used as the main software for manipulating LiDAR data in this study.

Three different point cloud datasets were utilized in this study to evaluate how point cloud density can affect the predictive power of ALS models. The first point cloud represents a high-resolution dataset with a mean density of 10.5 pulses per m^2 and 11.3 pulses per m^2 for Pelican and Conklin, respectively. This point cloud was created by merging the point clouds from all three of the multispectral channels using the MergeData tool within FUSION. The second point cloud represents an intermediate point cloud resolution with a mean point density of 4.4 pulses per m^2 and 4.7 pulses per m^2 for Pelican and Conklin, respectively. It consists of only returns from the 1064 nm channel, which is the wavelength typically used in single-channel LiDAR systems (Okhrimenko et al., 2019). The third point cloud represents a low resolution dataset and one that equals the lowest sampling intensity of ALS data collected by the Government of Alberta for the province between 2003 and 2014. To obtain the desired resolution, the point cloud from the 1064 nm channel was thinned to 1 pulse m^{-2} using the ThinData tool within FUSION. Only the 1064 nm channel was used, rather than all three multispectral channels, to align with the ALS data collected by the Government of Alberta.

Table 2.2 Summary table of Airborne Laser Scanning flight parameters and system settings

Parameter	Value	
Study Area	Pelican Mountain	Conklin
Area, km^2	1.5	16.5
Date of Survey	19-August-2018	18-August-2018
LiDAR Sensor Channels (C1, C2, C3)	Teledyne Optech Titan 1550 nm, 1064 nm, 532 nm	Teledyne Optech Titan 1550 nm, 1064 nm, 532 nm
Camera Sensor	CM-6500 (35 mm)	CM-6500 (35 mm)
Survey Altitude, AGL	1000 m	1000 m
PRF (total/per channel)	300 000/100 000	300 000/100 000
Scan Frequency	32	32
Scan Angle (full), degrees	50	50
Side Overlap (planned)	50%	50%
Camera Overlap (along, across)	30%, 50%	30%, 50%
Aircraft Speed, m/s	68	70
Point Density, Planned Single Returns (total/per channel), points/m^2	9/3	9/3
Point Density, Multiple Returns (all, C1, C2, C3)	10.5, 4.8, 4.4, 1.3	11.3, 5.1, 4.7, 1.5
Datum	NAD83 CSRS (Epoch 2002), UTM zone 12, ellipsoidal heights	NAD83 CSRS (Epoch 2002), UTM zone 12, ellipsoidal heights

The GridSurfaceCreate tool within FUSION was used to generate a 1-m resolution digital elevation model (DEM) for each ALS point cloud. This tool works within a specified grid system by averaging the elevation associated with each LiDAR point in the cell. Parameters were set so that only classified "ground" points were used for this calculation. If no ground points were within the designated cell boundary, the elevation value was interpolated using the distance-weighted average of the eight surrounding cells.

Processing and analysis of ALS data largely followed the work and recommendations of White et al. (2013, 2017). In order to compare ALS point cloud metrics to field sampling measurements, each point cloud was clipped to the sampling boundary of the field plots. This process involved transforming the plot coordinate information from the WGS84 geographic coordinate system to the NAD83 CSRS (epoch 2002), UTM zone 12 datum and projection, which matches the ALS data format. This transformation was performed in R using the "rgdal" package and spTransform function (Bivand, 2019). Within ArcGIS Desktop v.10.7.1 (ESRI, 2019), plot coordinates were buffered by their sampling plot radius and exported as a shapefile. Using the PolyClipData tool within FUSION, each of the three density ALS point clouds were cut to the boundary of every sampling plot area. Each return within the point clouds had an elevation above sea level recorded. To make plot-to-plot comparisons, the data were normalized so point elevations were in height above the ground. This was completed using the associated point cloud's DEM and the ClipData tool with the height switch in FUSION. Finally, ALS plot metrics were calculated using the CloudMetrics tool in FUSION. Returns of LiDAR pulses that were less than 1.37 m from the ground were excluded to ensure only data points related to the canopy were used to describe canopy characteristics following White et al. (2017). Strata subset

parameters were also calculated between default strata heights of 0.15, 1.37, 5, 10 and 20 m. Any

points with a height higher than 50 m above the ground were considered errors and were

excluded from analysis. The resulting output from the CloudMetrics tool was a comma separated

value (CSV) file that contained a variety of ALS statistical parameters associated with each field

plot.

2.4 Model Development

Modeling efforts should be guided by the principle of parsimony; however, when hundreds of

possible explanatory variables are available, models can quickly become overly complicated.

White et al. (2017) outline some of the common techniques used to develop a predictive model

using the area-based approach (ABA). They summarize two main approaches: parametric and

non-parametric. The two most commonly used forms of parametric methods are ordinary least-

squares (OLS) regression and Seemingly Unrelated Regression (SUR). In contrast, the most

commonly used non-parametric methods include k-nearest neighbours (k-NN) and random

forest. When comparing OLS and SUR, Næsset et al. (2005) recommended OLS as it performed

comparably to SUR, but is simpler and easier to implement. While non-parametric methods have

proven successful for modelling forest attributes, they are considered a "black box" approach

where the inputs and outputs of the model are known, but the internal workings are not. In

addition, non-parametric methods tend to require larger datasets to produce accurate results and

cannot be extrapolated past field measured values (Penner et al., 2013; White et al., 2017). Due

to the limited number of sampling plots in this study and the objective of developing a simple

model for operational use, a linear parametric method was deemed the most suitable.

With parametric regression, too many explanatory variables can result in unstable predictions due to multicollinearity (White et al., 2013). In addition, the more predictor variables used in the model the more complicated it gets, violating the goal of parsimony. The CloudMetrics tool in FUSION calculated 115 metrics for each plot, many of which are related to each other. This is clearly too many variables to include in a simple linear regression. Li et al. (2008) found that strong regression models to predict aboveground biomass can be largely explained with only the mean height, coefficient variation of height and canopy LiDAR point density metrics. Often, researchers manually subset these large datasets by variables they think may be important in predicting the response variables (e.g., Andersen et al., 2005; Erdody and Moskal, 2010; Skowronski et al., 2011). A selection method is then used to choose the best variables to predict the response variables. Stepwise regression is a common method to choose significant ALS predictor variables for parametric regression (e.g., Andersen et al., 2005; Skowronski et al., 2011; Hermosilla et al., 2014; Zhang et al., 2017); however, most statisticians agree that stepwise regression is outdated and tends to overfit models (Thompson, 1995; Babyak, 2004).

The lasso method (i.e., *least absolute shrinkage and selection operator*) performs shrinkage and variable selection to produce a linear regression model that can be used for predictions (Tibshirani, 1996). Lasso has been used with ALS data for variable selection (Domingo et al., 2018) and as a regression method for predicting forestry parameters (Vastaranta et al., 2011). The approach generates a linear regression equation with a penalty term that discourages reliance on excessive numbers of variables (Tibshirani, 1996). The penalty term reduces or "*shrinks*" coefficient values to zero for parameters that are not important for explaining variability within the model. The term λ is used as a tuning parameter that determines the amount of shrinkage.

Selecting a good value for λ is critical for the performance of the model. Lasso tends to create simple models that account for collinearity between predictor variables and is considered a superior alternative to stepwise regression (Babyak, 2004). Given that the dataset for this study has numerous predictor variables with unknown importance and the goal is to produce a simple, easy to implement model, lasso regression was chosen as the ideal method for both variable selection and model building for this study.

Prior to performing lasso, 15 candidate ALS variables were selected from the full set of 119 variables calculated with FUSION and output in the plot-level ALS metrics dataset (Table 2.3). Selected ALS-based predictor variables consisted of a variety of height and strata metrics. Although lasso is able to handle large datasets for variable selection, variables known to have little or no predictive power were removed to create a dataset composed of variables that have biological relevance and have been shown to have valuable predictive power for canopy fuel attributes in other studies (e.g., Andersen et al., 2005; Skowronski et al., 2011; Bright et al., 2017).

Lasso was performed in R using the "glmnet" package (Friedman et al., 2010). The plot-level ALS metrics and plot-level field-based canopy fuel estimates were merged by plot ID into a single dataframe. In order to satisfy the assumptions of linearity between the dependent and independent variables in linear regression, a square root transformation was used for CFL, CBD and stem density and CBH values. The 79 plots used in this analysis were divided into training data (52 plots) and validation data (27 plots). Note that data were combined for analysis irrespective of stand condition (i.e., managed versus natural) as it was assumed that the managed

stands would be representative of naturally thin black spruce stands. With the training data set, a linear regression model was fitted to each response variable (stand height, sqrtCFL, sqrtCBD, sqrtDensity and CBH) using the cv.glmnet function. To enable reproducible results, the set.seed value was set to "123". 10-fold cross validation with mean squared error was the evaluation statistic used to obtain the optimal value for λ.

Table 2.3 Plot metrics produced in FUSION (McGaughey, 2018b) and used for lasso regression.

Source	Predictor Name	Metric Description
First returns above 1.37 m height threshold	h_{Max}	Maximum height
	h_{Mean}	Mean height
	h_{CV}	Coefficient of variation for heights
	h_{25}	Height of 25th percentile
	h_{50}	Height of 50th percentile
	h_{75}	Height of 75th percentile
	h_{90}	Height of 90th percentile
	h_{99}	Height of 99th percentile
	$Pc_{1.37}$	Percentage first returns above 1.37 m
	Pc_{mean}	Percentage first returns above mean height
All returns, including ground and nonground	$Prop_{<0.15}$	Percentage of first returns <0.15 m
	$Prop_{0.15to1.37}$	Percentage of first returns >0.15 m and ≤1.37 m
	$Prop_{1.37to5.00}$	Percentage of first returns >1.37 m and ≤5.00 m
	$Prop_{5.00to10.00}$	Percentage of first returns >5.00 m and ≤10.00 m
	$Prop_{10.00to20.00}$	Percentage of first returns >10.00 m and ≤ 20.00 m

2.5 Model Performance and Evaluation

The estimated linear regression model with a λ value that resulted in the simplest model was then used to predict the response variable values of the testing data. Performance of each model was

evaluated on the training data using the coefficient of determination (R^2) and root mean squared error (RMSE). The coefficient of determination and RMSE of the testing data (R^2_{test} and $RMSE_{test}$ respectively) were also calculated and compared to the training R^2 and RMSE to evaluate the predictive power and goodness of fit of the models. The coefficient of determination is the proportion of variance that is explained by the model. The RMSE is the square root of the variance of the residuals. Both measurements indicate how close the observed values (field-measured metrics) are to the model's predicted values. These statistical parameters are a common way to evaluate the performance of ALS models (e.g., Andersen et al., 2005; González-Olabarria et al., 2012; Bouvier et al., 2015; Greaves et al., 2016; Engelstad et al., 2019).

The derived predictive models were used to map the Pelican Mountain study area to visually assess and compare model performance. The Pelican Mountain site was selected for visualizing predicted stand densities due to the largely homogenous C-2 fuel type across the site, and the researcher's personal knowledge of the pattern of natural and managed stand densities within the study area. Mapping was completed with the "GridMetrics" function in FUSION which calculates ALS metrics for each cell of a defined grid size over the area of interest. To maintain consistency, the same parameters were set as when the point cloud metrics were calculated for each plot location. A grid with a 6.3 m x 6.3 m cell size was used as this equals the 40 m^2 area of the circular ground plots. A CSV for each of the three LiDAR point clouds used in this study was generated with the GridMetrics tool and imported into R. The lasso regression model for each fuel characteristic of interest was then applied to the datasets to generate predictive values for each cell within the grid. For ease of interpretation, any variables transformed during the analysis process were transformed back to their original units for mapping. Finally, the files were

converted into ASC file format and imported into ArcGIS. The models were applied only to black spruce stands identified by the Alberta Vegetation Inventory (AVI) data and field-verified with site visits. Raw differences in predicted values between models was also mapped across Pelican Mountain using the Raster Calculator tool in ArcGIS. Scales used for mapping were based on maximum and minimum values.

Chapter 3 Results

This chapter presents the linear models developed using lasso regression that compare Airborne Laser Scanning (ALS) metrics to field-based measurements. This chapter also evaluates the predictive ability of each model by applying it to independent testing data and comparing the field-measured values to predicted model values. To demonstrate practical applications, the models were used to map forest attributes continuously across a broad area within the Pelican Mountain Research Site. A model was developed for each of five forest characteristics of interest (canopy bulk density (CBD), canopy fuel load (CFL), stem density, canopy height and canopy base height (CBH)) and for each ALS point cloud dataset using different resolutions (hereafter referred to as "dense" for the dataset consisting of all three multispectral ALS point clouds merged into one; "intermediate" for the ALS dataset consisting of returns only from the 1064 nm laser; and "thin" for the dataset consisting of the 1064 nm point cloud that had been thinned to approximately 1 pulse m^{-2}). Stand and canopy characteristics of field-measured stands are summarized in Table 3.1. Airborne Laser Scanning metrics selected for each of the models are shown in Table 3.2.

3.1 Canopy Bulk Density

Diagnostic plots indicated that the square root transformation of field measured CBD was appropriate for linear regression for all three ALS pulse density models. The linear models that were developed to predict the square root of CBD (sqrtCBD) using lasso regression for each ALS point cloud datasets are presented in Table 3.3. The lasso method generated relatively simple models with only four ALS metrics selected for the dense model ($Pc_{1.37}$, Pc_{mean}, $Prop_{<0.15}$

and Prop$_{1.37to5.00}$), three ALS metrics for the intermediate model (Pc$_{1.37}$, Pc$_{mean}$ and Prop$_{1.37to5.00}$)

and one ALS metric for the thin model (Pc$_{1.37}$).

Table 3.1 Stand and canopy characteristics of field-measured black spruce stands by status (a) natural/unmanaged, (b) managed and (c) combined and study area (Pelican Mountain, Conklin). Descriptive statistics of range, mean and standard deviation (SD) are shown by stand status to document variation in data sources. All data were combined irrespective of stand status for analysis and model building

(a) Unmanaged stands						
	Pelican (31 plots)			Conklin (8 plots)		
	Range	Mean	SD	Range	Mean	SD
Tallest Tree Height (m)	5.5-13.1	8.7	2.2	9.9-15.7	11.5	2.3
Stem Density (tree/ha)	3996-35 989	14 711	6577	5320-33 967	14 536	9413
Canopy Fuel Load (kg/m^2)	1.10-6.57	3.31	1.22	1.54-6.63	3.72	1.48
Canopy Bulk Density (kg/m^3)	0.17-1.06	0.57	0.19	0.24-1.07	0.55	0.24
Canopy Base Height (m)	1.17-3.83	2.19	0.75	1.25-3.95	2.64	0.79
(b) Managed stands						
	Pelican (28 plots)			Conklin (12 plots)		
	Range	Mean	SD	Range	Mean	SD
Tallest Tree Height (m)	4.5-11.3	8.7	1.8	2.6-17.2	10.6	4.3
Stem Density (tree/ha)	250-3497	1629	877	749-4995	2529	1339
Canopy Fuel Load (kg/m^2)	0.08-2.12	1.02	0.51	0.07-4.59	1.69	1.43
Canopy Bulk Density (kg/m^3)	0.02-0.34	0.19	0.09	0.03-0.62	0.24	0.19
Canopy Base Height (m)	1.56-5.48	3.45	0.91	0.32-5.13	2.44	1.53
(c) All data combined (79 plots)						
	Range	Mean	SD			
Tallest Tree Height (m)	2.6-17.2	9.3	2.6			
Stem Density (tree/ha)	250-35 989	8206	8156			
Canopy Fuel Load (kg/m^2)	0.072-6.63	2.30	1.55			
Canopy Bulk Density (kg/m^3)	0.02-1.07	0.38	2.72			
Canopy Base Height (m)	0.32-5.48	2.72	1.10			

Table 3.2 Predictor variables selected using lasso regression for each ALS pulse density dataset (i.e., dense (den), intermediate (int) and thin) and five canopy fuel attributes. Selected predictor variables chosen in the final models for square root transformed canopy bulk density ($\sqrt{CBD}$), square root transformed canopy fuel load ($\sqrt{CFL}$), square root transformed stem density ($\sqrt{stem\ density}$), canopy height (height) and square root transformed canopy base height ($\sqrt{CBH}$) and for each ALS dataset are indicated with an 'X'. All height measurements in meters.

Predictor Name	$\sqrt{CBD}$			$\sqrt{CFL}$			$\sqrt{stem\ density}$			Height			$\sqrt{CBH}$		
	Den.	Int.	Thin	Den.	Int.	Thin.	Den.	Int.	Thin.	Den.	Int.	Thin.	Den.	Int.	Thin.
h_{Max}										X	X	X			
h_{Mean}							X		X						X
h_{CV}												X			
h_{25}							X						X	X	
h_{50}															
h_{75}															
h_{90}												X			
h_{99}											X				
$Pc_{1.37}$	X	X	X	X	X	X	X	X	X		X				X
Pc_{mean}	X				X	X									X
$Prop_{<0.15}$	X	X		X			X	X	X						X
$Prop_{0.15to1.37}$															
$Prop_{1.37to5.00}$	X	X					X	X	X						
$Prop_{5to10}$															
$Prop_{10to20}$															X

Note: Predictor name and ALS metric descriptions are as follows: Maximum height, h_{Max}; Mean height, h_{Mean}; Coefficient of variation for heights, h_{CV}; Height of 25th percentile, h_{25}; Height of 50th percentile, h_{50}; Height of 75th percentile, h_{75}; Height of 90th percentile, h_{90}; Height of 99th percentile, h_{99}; Percentage of first returns above 1.37, $Pc_{1.37}$; Percentage of first returns above mean height, Pc_{mean}; Percentage of first returns <0.15 m, $Prop_{<0.15}$; Percentage of first returns >0.15 m and ≤1.37 m, $Prop_{0.15to1.37}$; Percentage of first returns >1.37 m and ≤5.00 m, $Prop_{1.37to5.00}$; Percentage of first returns >5.00 m and ≤10.00 m, $Prop_{5to10}$; Percentage of first returns >10.00 m and ≤20.00 m, $Prop_{10to20}$

The coefficient of determination (R^2) and root mean square error (RMSE) were used to evaluate model performance. The R^2 values for the sqrt(CBD) models fitted to the dense, intermediate and thin pulse density training datasets were 0.84, 0.84 and 0.75, respectively. When the model was applied to independent data (testing data), R^2_{test} values were 0.78 (dense), 0.78 (intermediate) and 0.69 (thin). It is important to keep in mind that R^2 values represent the linear relationship resulting from the square root transformation. Results should be interpreted with caution as they are not in the original units of the CBD field measurements.

The RMSE and RMSE$_{test}$ values for the dense, intermediate and thin pulse density ALS models to predict the sqrt(CBD) values were 0.087 and 0.098, 0.100 and 0.102 and 0.106 and 0.126, respectively. The RMSE and RMSE$_{test}$ values for each model are close enough to conclude that the models are suitable for generalized use (i.e., they are suitable for generating predictions with new data that was not used in the modeling process).

Goodness of fit of the ALS models for predicting the testing dataset sqrt(CBD) values was assessed visually with scatterplots of observed versus predicted values (Figure 3.1). The 1:1 diagonal line in these plots is a visual representation of perfect fit. Data points below the 1:1 line indicate the model has underpredicted the field-measured value. Data points above the 1:1 line indicate the model overpredicted the field-measured value. If the data points are not scattered symmetrically around the 1:1 line, it indicates that the model may have some bias. Shading of Figure 3.1 symbols denotes the origin of the data (i.e., managed or natural stands). Data origin was inspected visually to assess whether or not the relationship between ALS data and field measured sqrt(CBD) varied between managed and natural stand conditions. For all three

datasets, data points for natural and managed stands exhibited a consistent trend and were therefore grouped for analysis. Data points for the dense and intermediate models were scattered symmetrically around the perfect 1:1 line; however, the model showed apparent bias towards underpredicting at the highest values of square root CBD. This bias was exacerbated when the lowest density ALS data (i.e., the thin dataset) was used to fit the model.

Maps displaying predicted CBD in black spruce stands within the Pelican Mountain Research Site were created for each ALS pulse density model (Figure 3.2). In all cases, CBD is shown in true units, rather than the square root transformation used in model building. All maps are rasters with a 6.3 m x 6.3 m cell size that matches the extent of the majority of field sampling plots used in this study (i.e. 40 m^2). The model was only applied to areas identified as black spruce using the Alberta Vegetation Inventory (AVI) dataset and to cells that had at least one canopy return recorded (defined in this study as a lidar return at least 1.37 m above the ground). Differences in CBD values predicted by the dense model compared to the intermediate and thin models can be seen in Figure 3.3. The mean and standard deviation of CBD differences predicted by the intermediate and dense models across the Pelican Mountain Research Site was -0.039 and 0.053 kg m^{-3}, respectively. The mean and standard deviation of CBD differences predicted by the thin and dense models across the Pelican Mountain Research Site was -0.059 and 0.066 kg m^{-3}, respectively.

Figure 3.4 compares the FBP Fuel Type grid currently used by Alberta Wildfire to predict wildfire behaviour to the CBD map created using the dense ALS model. The FBP fuel grid currently maps stand structure across the Pelican Mountain Research Site uniformly for any cells

identified as C-2 Boreal Spruce (Figure 3.4a). Maps produced with ALS data were able to

describe stand structure in much more detail (Figure 3.4b). Photos of crown structure taken at

sampling plots throughout the Pelican Mountain Research Site suggest that the models were

doing a good job at capturing the natural variability of canopy bulk density values (Figure 3.4c).

Figure 3.1 Plot-level (square root transformed) canopy bulk density estimated from ALS data for the testing dataset (predicted) versus field-measured values (observed): (a) dense ALS pulse density model, (b) intermediate ALS pulse density model, (c) thin ALS pulse density model. Solid line shows 1:1 relationship denoting perfect model fit.

Table 3.3 Lasso linear regression models and performance metrics predicting the square root of canopy bulk density (CBD) by ALS point cloud density

ALS Dataset	Equation	R^2	R^2_{test}	RMSE	$RMSE_{test}$
Dense	$\sqrt{CBD}= 0.63 + (0.0032)Pc_{1.37} + (0.0000075)Pc_{mean} + (-0.40)Prop_{<0.15} + (0.013)Prop_{1.37to5.00}$	0.84	0.78	0.087	0.098
Intermediate	$\sqrt{CBD}= 0.25 + (0.0035)Pc_{1.37} + (0.0031)Pc_{mean} + (0.18)Prop_{1.37to5.00}$	0.84	0.78	0.100	0.102
Thin	$\sqrt{CBD}= 0.30 + (0.0052)Pc_{1.37}$	0.75	0.69	0.106	0.126
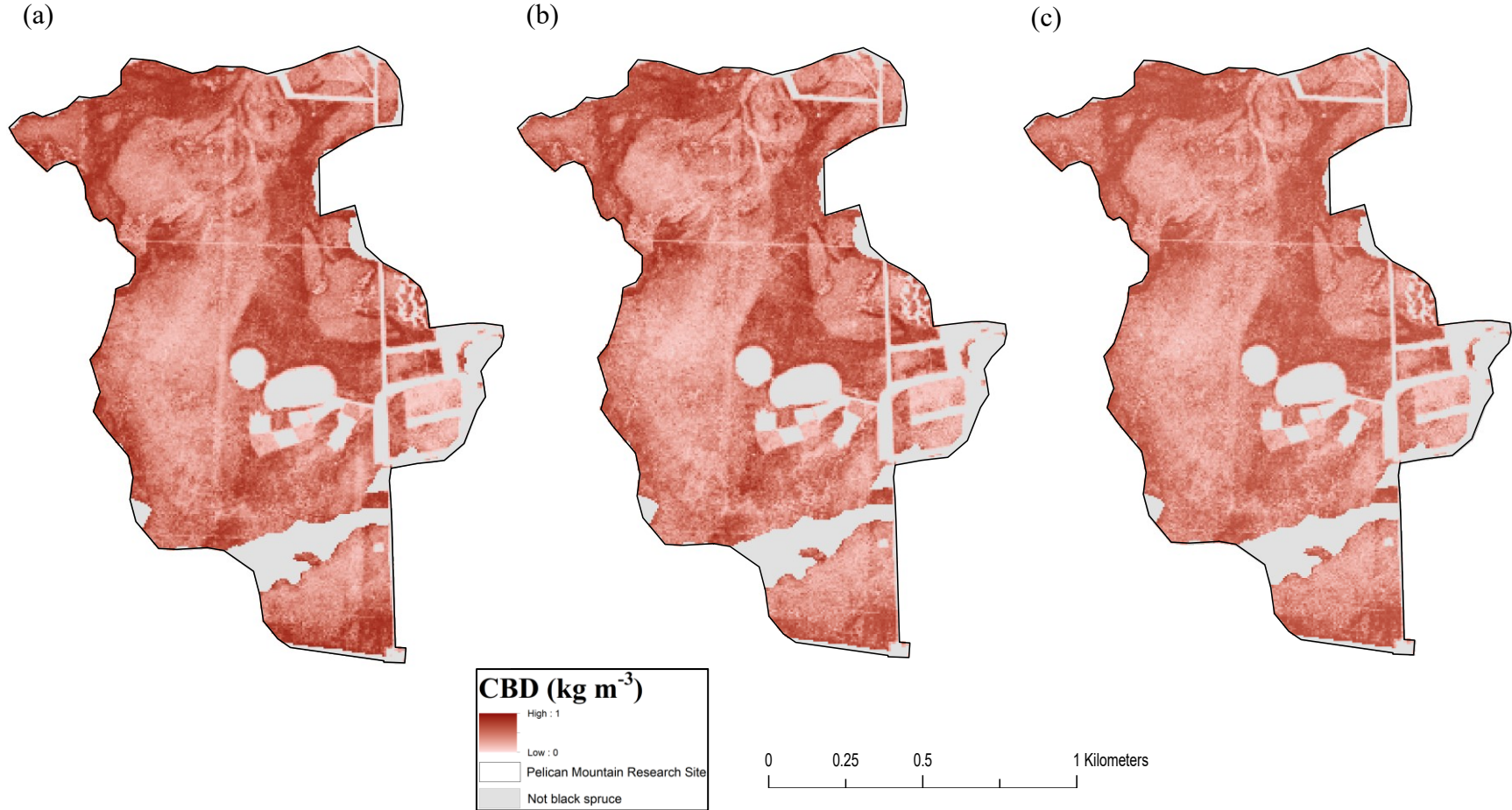
Figure 3.2 Canopy bulk density (CBD) predicted for black spruce stands within the Pelican Mountain Research Site using statistical models developed with three different ALS pulse densities: (a) dense, (b) intermediate, and (c) thin. Note that predicted values from the ALS models were back transformed into original CBD units.
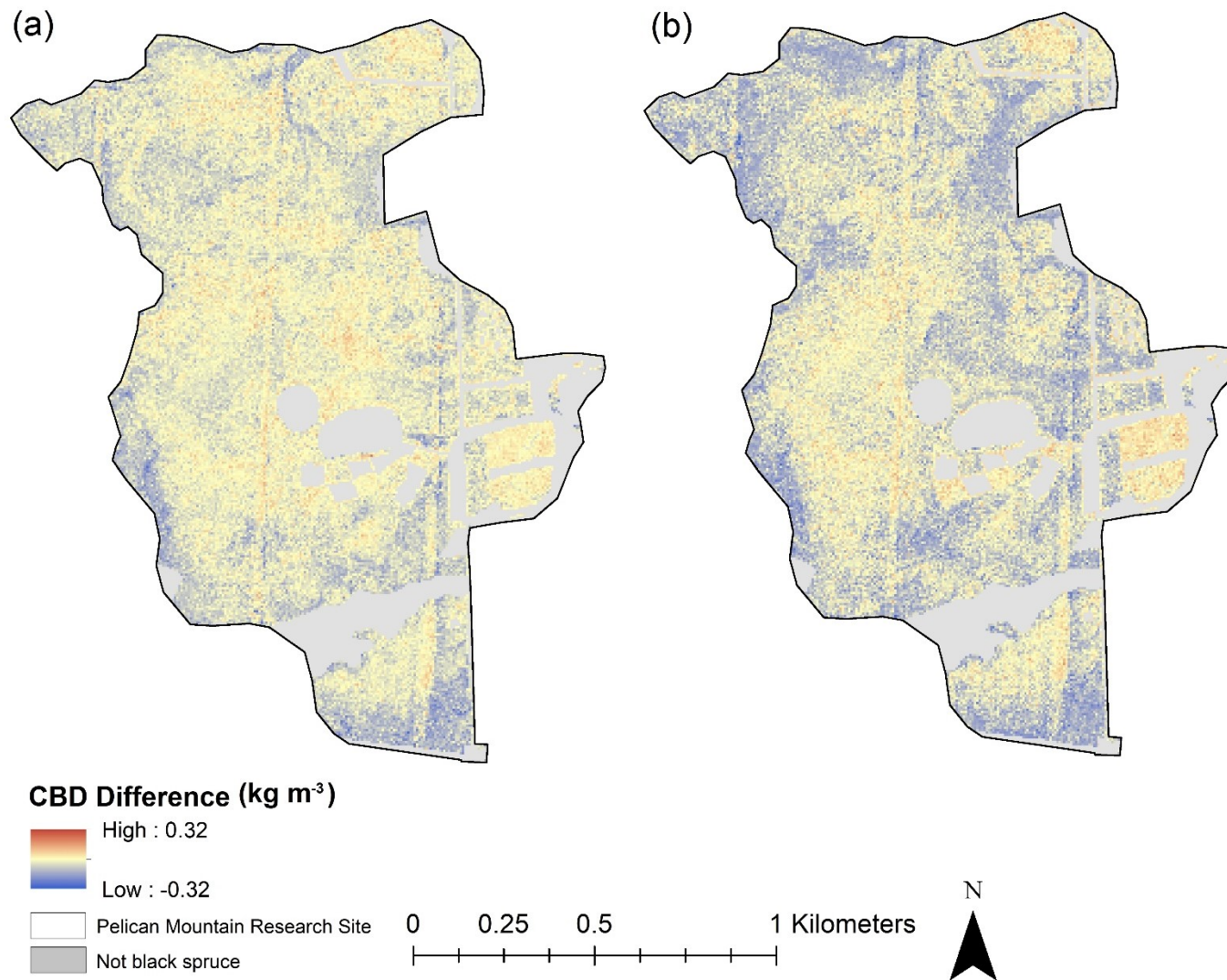
Figure 3.3 The difference between canopy bulk density (CBD) values predicted using (a) models developed with intermediate and dense ALS pulse density datasets and (b) models developed with thin and dense ALS pulse density datasets. Pixels in blue indicate areas where the intermediate/thin model underpredicted CBD in comparison to the dense ALS model. Pixels in red indicate areas where the intermediate/thin model overpredicted CBD in comparison to the dense ALS model.
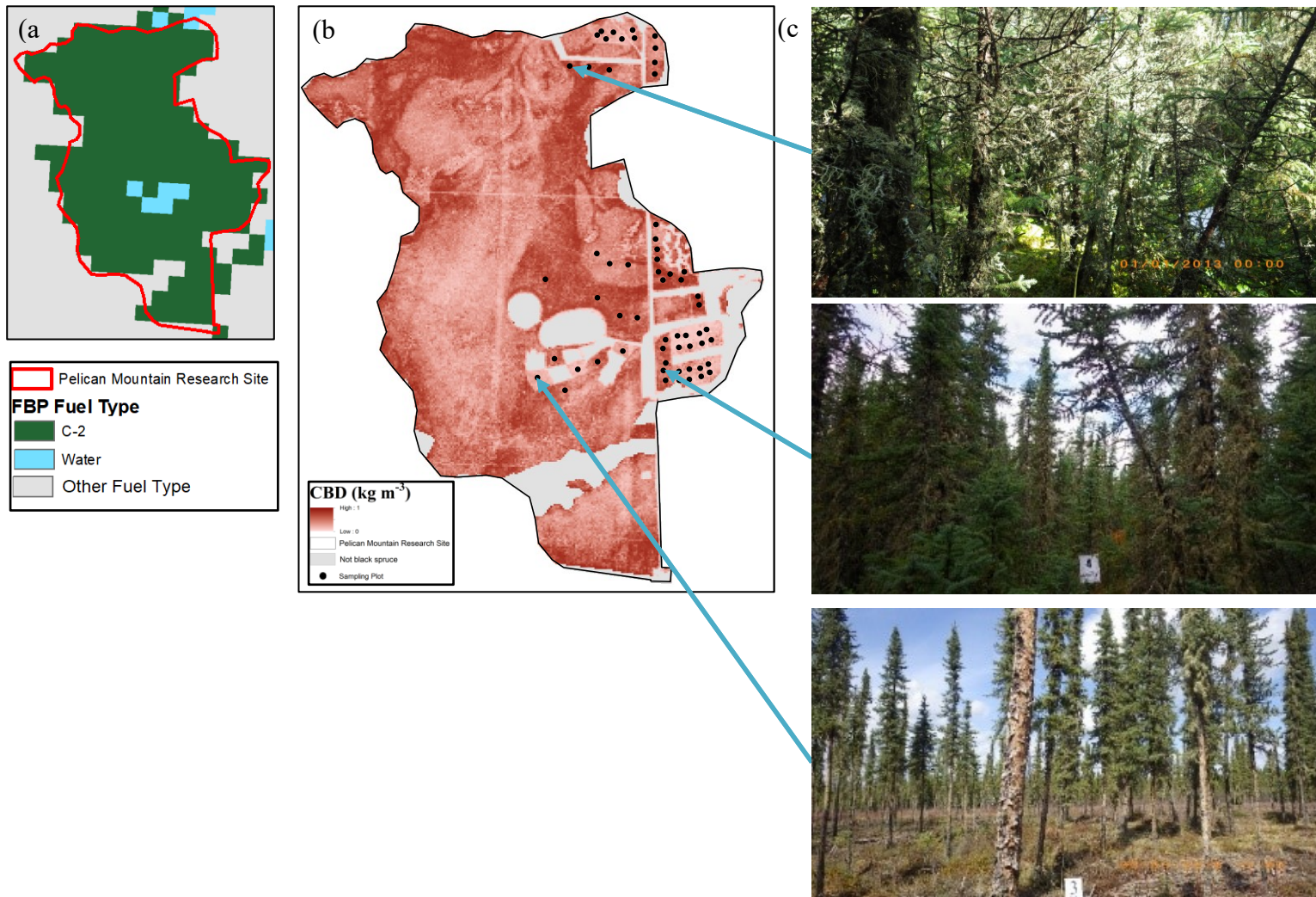
Figure 3.4 (a) The Fire Behaviour Prediction (FBP) fuel type map shows that Pelican Mountain is almost entirely covered by the C-2 Boreal Spruce Fuel Type. Within-stand variation in fuel structure is ignored in FBP System fuel classifications. The ALS-derived fuel attributes from the "dense" dataset shows that canopy bulk density can vary substantially within black spruce stands (b) model results also correspond well with field photos that show the model is accurately detecting areas of high (c, top), intermediate (c, middle), and low (c, bottom) canopy bulk density values.

3.2 Canopy Fuel Load

Field-measured canopy fuel load data did not meet the assumptions of linear regression and a square root transformation was therefore applied. The linear models that were developed to predict the square root of CFL (sqrtCFL) using lasso regression for each ALS point density datasets (i.e., dense, intermediate and thin) are presented in Table 3.4. Simple models with only two predictor variables were selected for each pulse density model ($Pc_{1.37}$ and $Prop_{<0.15}$ for the dense model and $Pc_{1.37}$ and Pc_{mean} for the intermediate and thin models). The R^2 values fitted to the training data for the dense, intermediate and thin models were 0.84, 0.86, and 0.80, respectively. The R^2_{test} values were similar to the training data; for the dense, intermediate and thin models R^2_{test} values were 0.85, 0.82 and 0.77, respectively.

The RMSE and $RMSE_{test}$ for the dense, intermediate and thin models were also closely aligned with values of 0.227 and 0.215, 0.232 and 0.234, and 0.255 and 0.265, respectively. For the dense model, the $RMSE_{test}$ is smaller than the RMSE for the training data. One would expect that the RMSE would be less than the $RMSE_{test}$ given that the model was designed to best fit the training dataset. Although this is unusual, given that the values were so similar this was likely due to random chance. The RMSE and $RMSE_{test}$ values for each model were close enough to conclude that the models are suitable for generalized use.

Scatterplots comparing field-measured (observed) square root transformed CFL and predicted values from ALS point cloud datasets can be seen in Figure 3.5. Data points for all models were scattered symmetrically around the perfect 1:1 line; however, all models showed apparent bias towards underpredicting field-measured values in the mid-range and for very high sqrt(CFL)

values. Once again, this bias was exacerbated when the lowest density ALS data is used to fit the model.

Maps displaying predicted CFL in black spruce stands within the Pelican Mountain Research Site boundaries were created for each ALS pulse density model (Figure 3.6). In all cases, CFL was shown in true units, rather than the square root transformation used in model building. The model was only applied to areas identified as black spruce using the AVI datasets and to cells that had at least one canopy return recorded. Differences in CFL values predicted by the dense model compared to the intermediate and thin models can be seen in Figure 3.7. The mean and standard deviation of CFL differences predicted by the intermediate and dense models across the Pelican Mountain Research Site was -0.14 and 0.23 kg m^{-2}, respectively. The mean and standard deviation of CFL differences predicted by the thin and dense models across the Pelican Mountain Research Site was -0.19 and 0.36 kg m^{-2}, respectively.
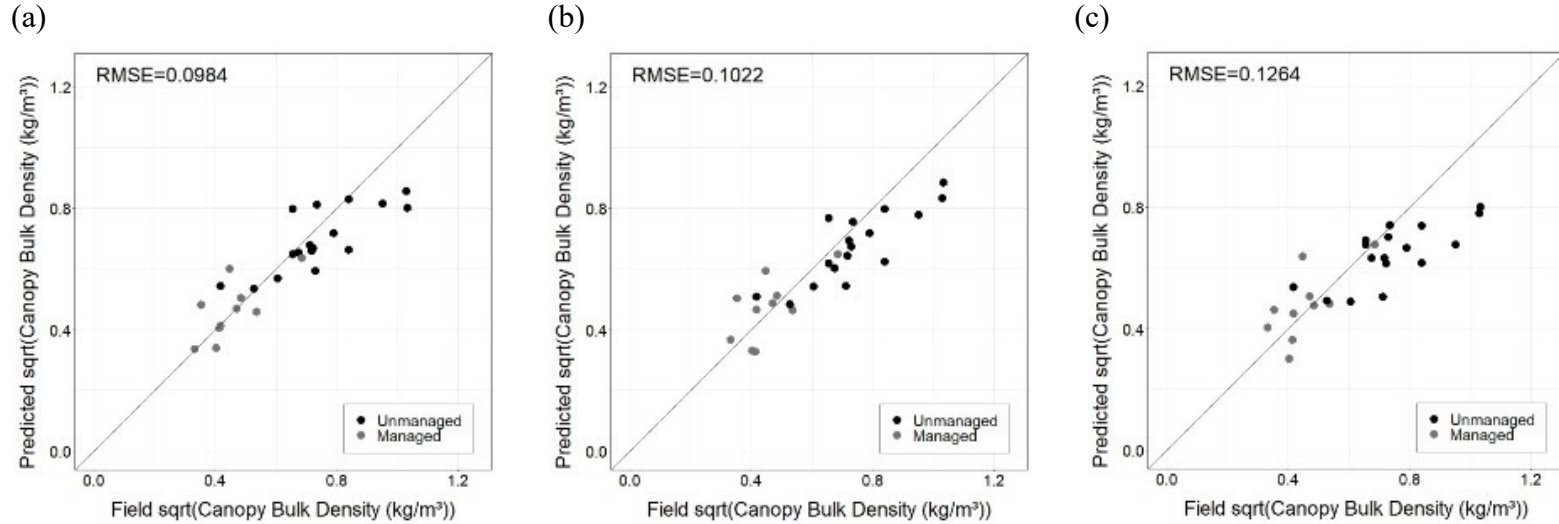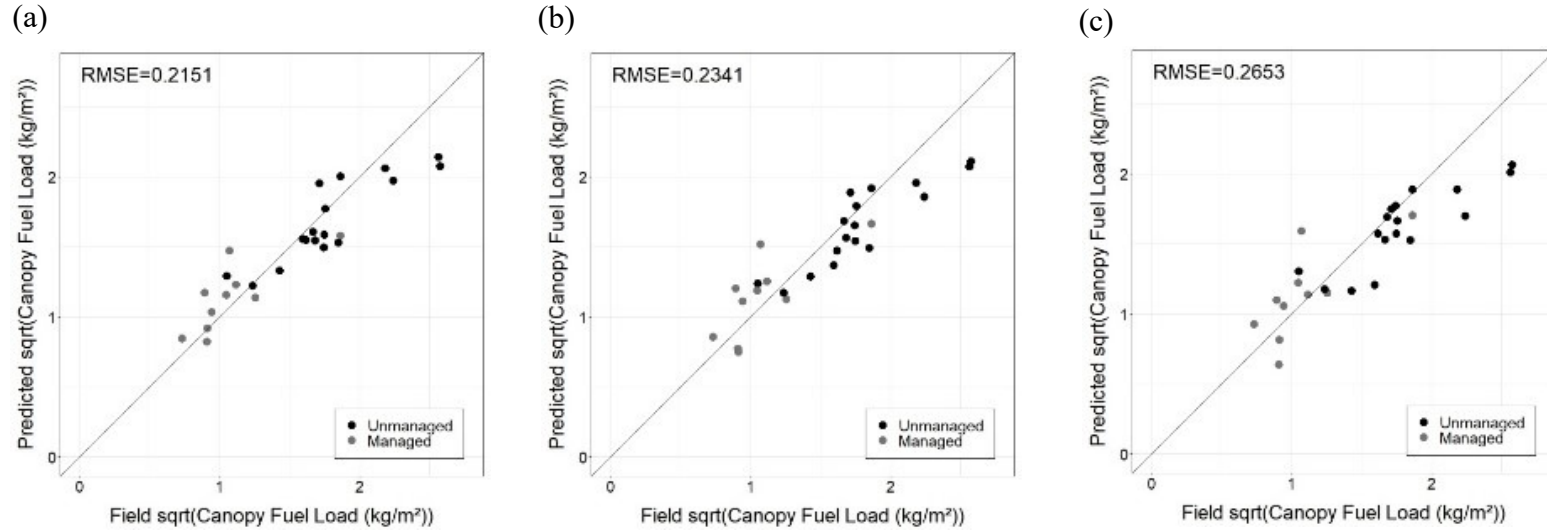
Figure 3.5 Plot-level (square root transformed) canopy fuel load estimated from ALS data for the testing dataset (predicted) versus field-measured values (observed): (a) dense ALS pulse density model, (b) intermediate ALS pulse density model, (c) thin ALS pulse density model. Solid line shows 1:1 relationship denoting perfect model fit.

Table 3.4 Lasso linear regression models and performance metrics predicting the square root of canopy fuel load ($\sqrt{CFL}$) by ALS point cloud density.

| ALS Dataset	Equation	R^2	R^2_{test}	RMSE	$RMSE_{test}$
Dense	$\sqrt{CFL}= 1.11 + (0.012)Pc_{1.37} + (-0.49)Prop_{<0.15}$	0.84	0.85	0.227	0.215
Intermediate	$\sqrt{CFL}= 0.57 + (0.016)Pc_{1.37} + (0.000071)Pc_{mean}$	0.86	0.82	0.232	0.234
Thin	$\sqrt{CFL}= 0.64 + (0.014)Pc_{1.37} + (0.00088)Pc_{mean}$	0.80	0.77	0.255	0.265
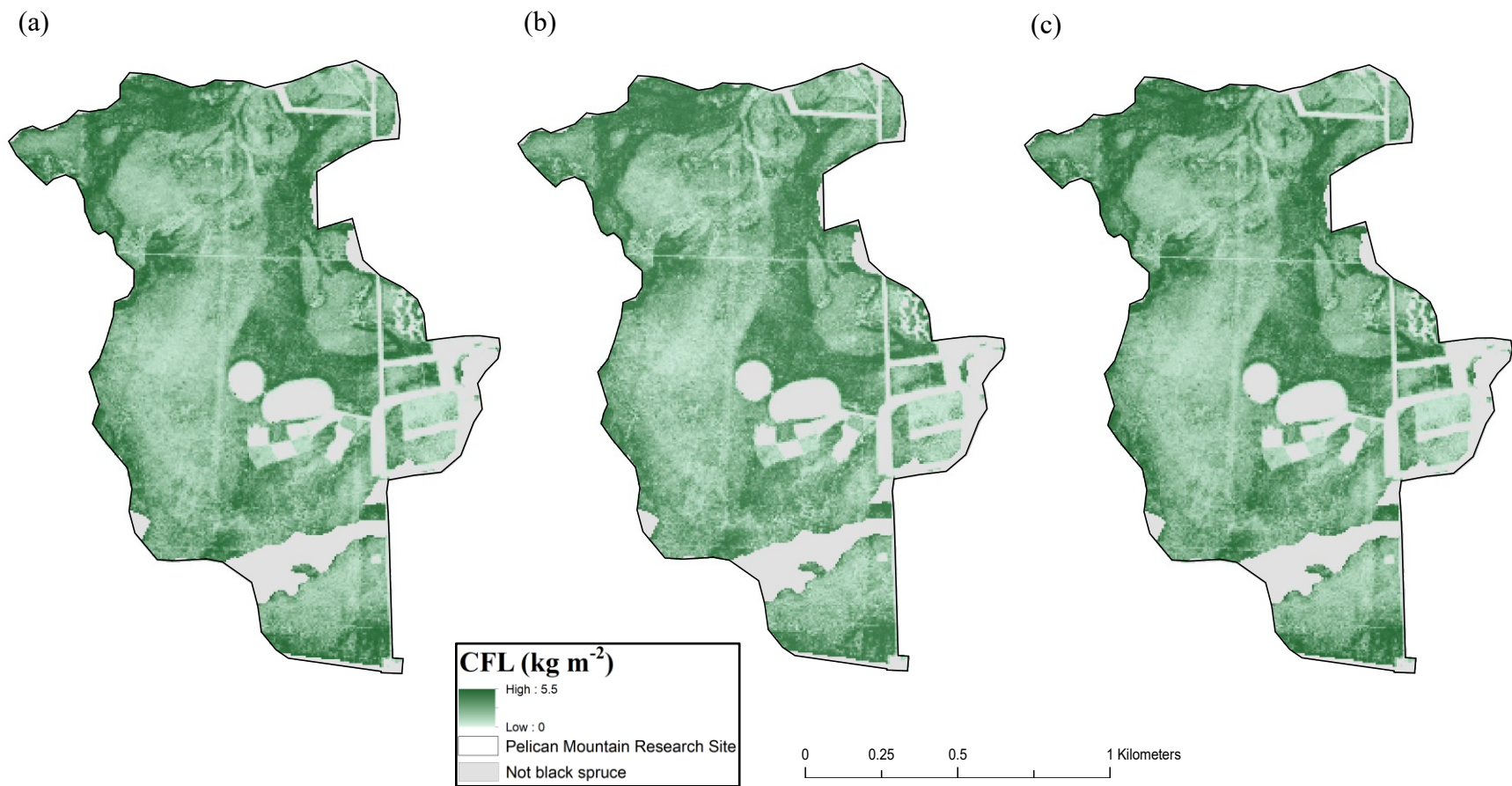
Figure 3.6 Canopy fuel load (CFL) predicted for black spruce stands within the Pelican Mountain Research Site using statistical models developed with three different ALS pulse densities: (a) dense, (b) intermediate, and (c) thin. Note that predicted values from the ALS models were back transformed into original CFL units.

(a)

(b)

CFL Difference (kg m⁻²)

High : 3.1

Low : -3.1

Pelican Mountain Research Site

Not black spruce

0   0.25   0.5   1 Kilometers

N
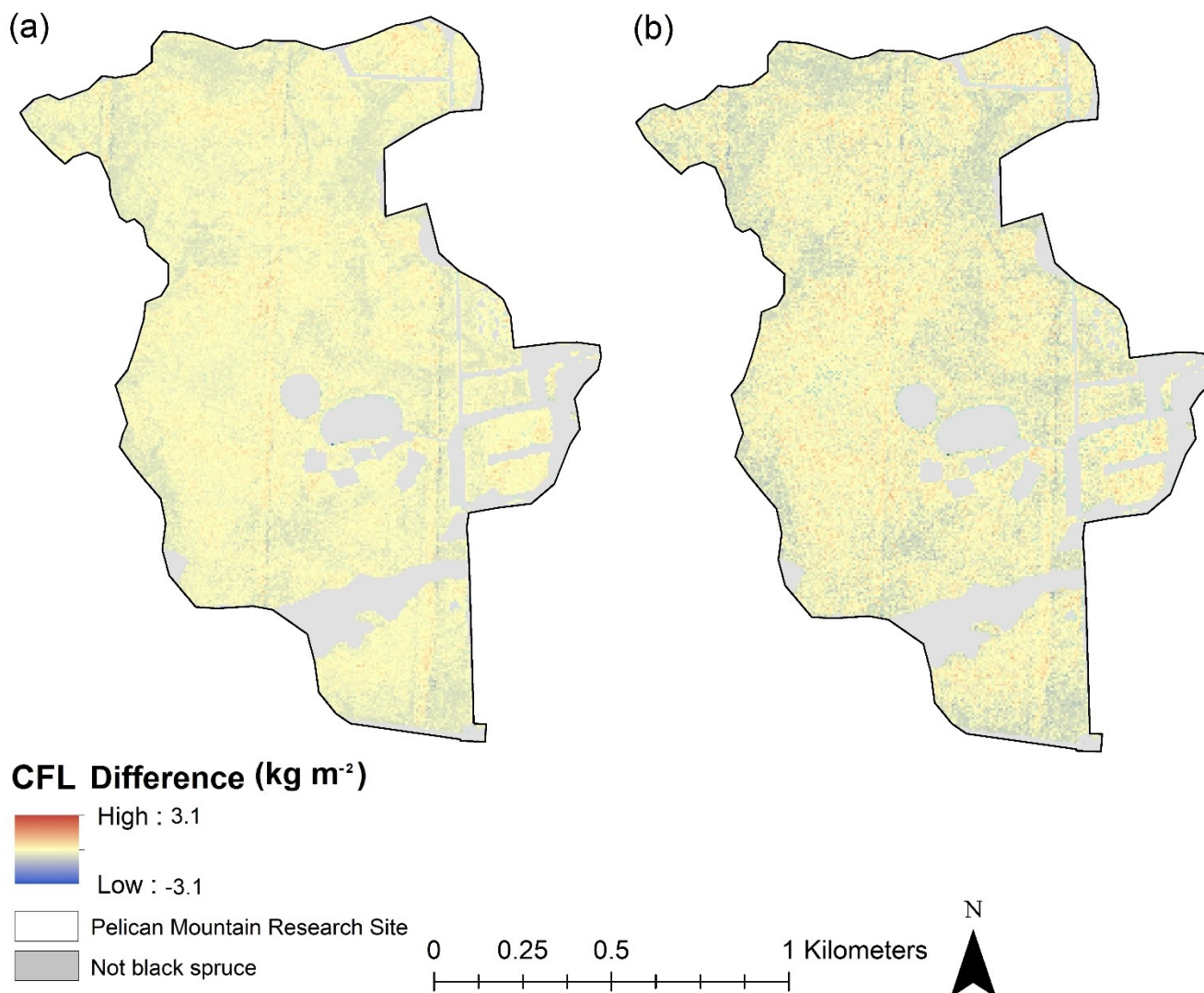
Figure 3.7 The difference between canopy fuel load (CFL) values predicted using (a) models developed with intermediate and dense ALS pulse density datasets and (b) models developed with thin and dense ALS pulse density datasets. Pixels in blue indicate areas where the intermediate/thin model underpredicted CFL in comparison to the dense ALS model. Pixels in red indicate areas where the intermediate/thin model overpredicted CFL in comparison to the dense ALS model.

59

3.3 Stem Density

A square root transformation was applied to stem density measurements to account for nonlinearity and variance observed in the diagnostic plots of all three ALS point resolution models. The linear models that were developed to predict the square root of stem density using lasso regression for each ALS point cloud dataset are presented in Table 3.5. In the dense pulse density ALS model, 5 predictor variables were selected (h_{mean}, h_{CV}, $Pc_{1.37}$, $Prop_{<0.15}$ and $Prop_{1.37to5.00}$). Three predictor variables were selected for the intermediate pulse density ALS model ($Pc_{1.37}$, $Prop_{<0.15}$, $Prop_{1.37to5.00}$) and 4 were selected for the thin pulse density ALS model (h_{mean}, $Pc_{1.37}$, $Prop_{<0.15}$, $Prop_{1.37to5.00}$). The R^2 values for the dense, intermediate and thin models were 0.89, 0.80 and 0.78, respectively. When the models were applied to the testing data the R^2_{test} values were 0.81, 0.74 and 0.71 for the dense, intermediate and thin models, respectively.

The RMSE and $RMSE_{test}$ for the dense, intermediate and thin models were 15.24 and 23.24, 19.30 and 29.62, and 20.71 and 30.04, respectively. Scatterplots comparing field-measured and predicted values from ALS point cloud datasets can be seen in Figure 3.8. All models showed apparent bias towards underpredicting field-measured values for high square root stem density values. Bias was exacerbated as point resolution of the ALS data decreased.

Maps displaying predicted stem density within the Pelican Mountain Research Site boundaries were created for each ALS pulse density model (Figure 3.9). In all cases, stem density was shown in true units. The model was only applied to areas identified as black spruce using the AVI datasets and cells that had at least one canopy return recorded. Differences in stem density values predicted by the dense model compared to the intermediate and thin models can be seen in

Figure 3.10. The mean and standard deviation of stem density differences predicted by the intermediate and dense models across the Pelican Mountain Research Site was -1514 and 2039 stems ha^{-1}, respectively. The mean and standard deviation of stem density differences predicted by the thin and dense models across the Pelican Mountain Research Site was -1220 and 2335 stems ha^{-1}, respectively.
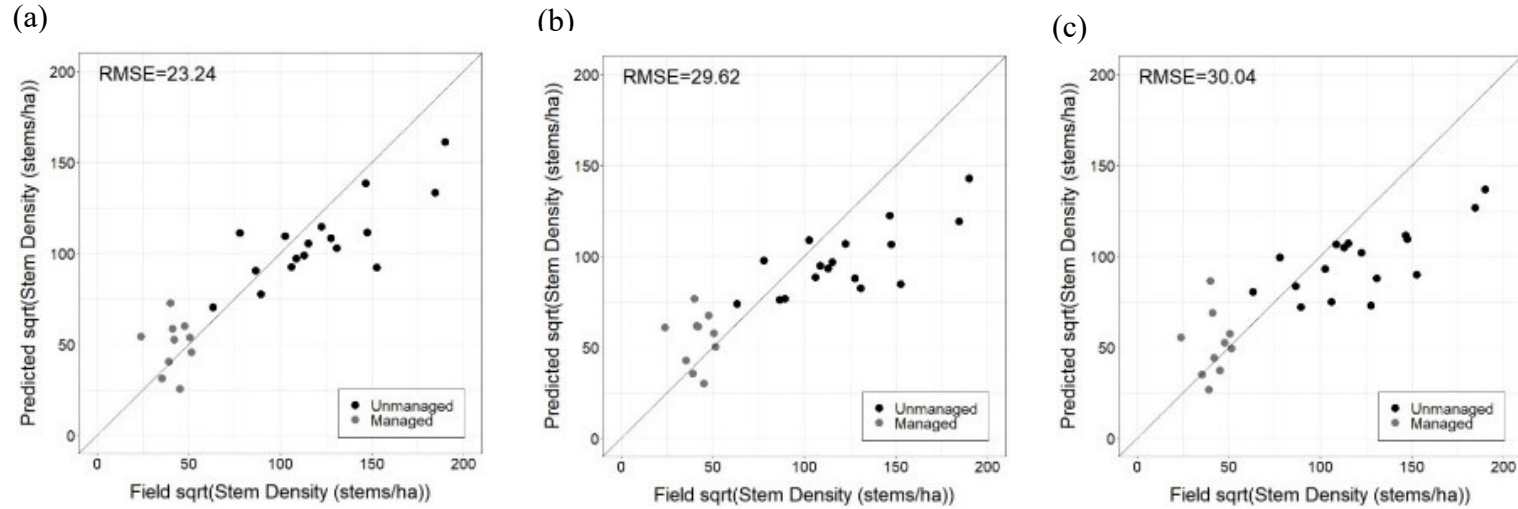
Figure 3.8 Plot-level (square root transformed) stem density estimated from ALS data for the testing dataset (predicted) versus field-measured values (observed): (a) dense ALS pulse density model, (b) intermediate ALS pulse density model, (c) thin ALS pulse density model. Solid line shows 1:1 relationship denoting perfect model fit.

Table 3.5 Lasso linear regression models and performance metrics predicting the square root of stem density ($\sqrt{stem\ density}$) by ALS point cloud density.

ALS Dataset	Equation	R^2	R^2_{test}	RMSE	$RMSE_{test}$
Dense	$\sqrt{stem\ density}$= 57.96 + (-3.27)h_{mean} + (-3.28)h_{CV} + (0.61)$Pc_{1.37}$ + (-23.22)$Prop_{<0.15}$ + (123.99)$Prop_{1.37to5.00}$	0.89	0.81	15.24	23.24
Intermediate	$\sqrt{stem\ density}$= 29.16 + (0.28)$Pc_{1.37}$ + (-16.41)$Prop_{<0.15}$ + (154.02)$Prop_{1.37to5.00}$	0.80	0.74	19.30	29.62
Thin	$\sqrt{stem\ density}$= 42.04 + (-1.49)h_{mean} + (0.46)$Pc_{1.37}$ + (-34.95)$Prop_{<0.15}$ + (122.62)$Prop_{1.37to5.00}$	0.78	0.71	20.71	30.04

(a)　　　　　　　　　　(b)　　　　　　　　　　(c)

Stem Density (Stems ha⁻¹)

High : 40000

Low : 0

Pelican Mountain Research Site

Not black spruce

0   0.25   0.5   1 Kilometers
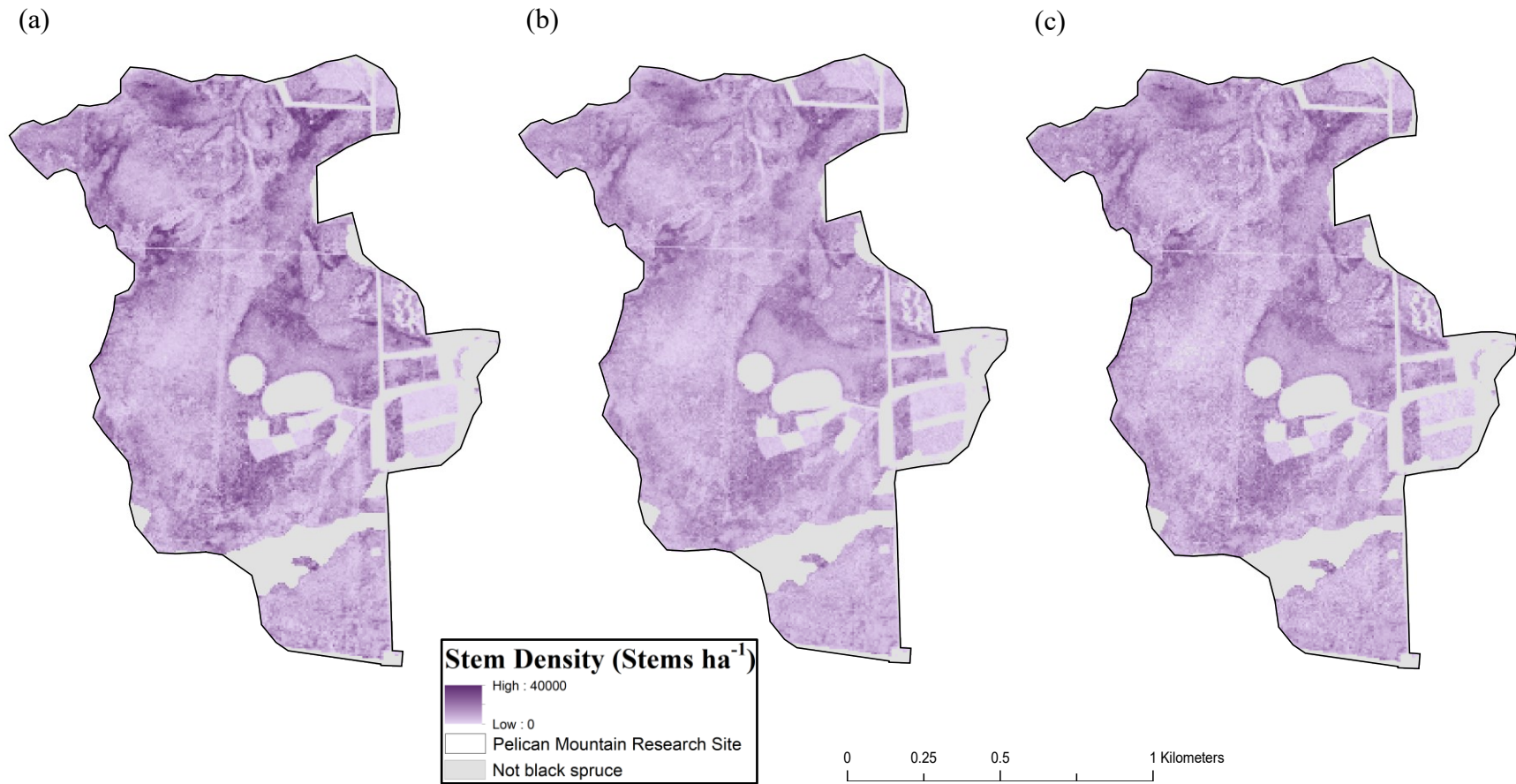
Figure 3.9 Stem density predicted for black spruce stands within the Pelican Mountain Research Site using statistical models developed with three different ALS pulse densities: (a) dense, (b) intermediate, and (c) thin. Note that predicted values from the ALS models were back transformed into original stem density units.
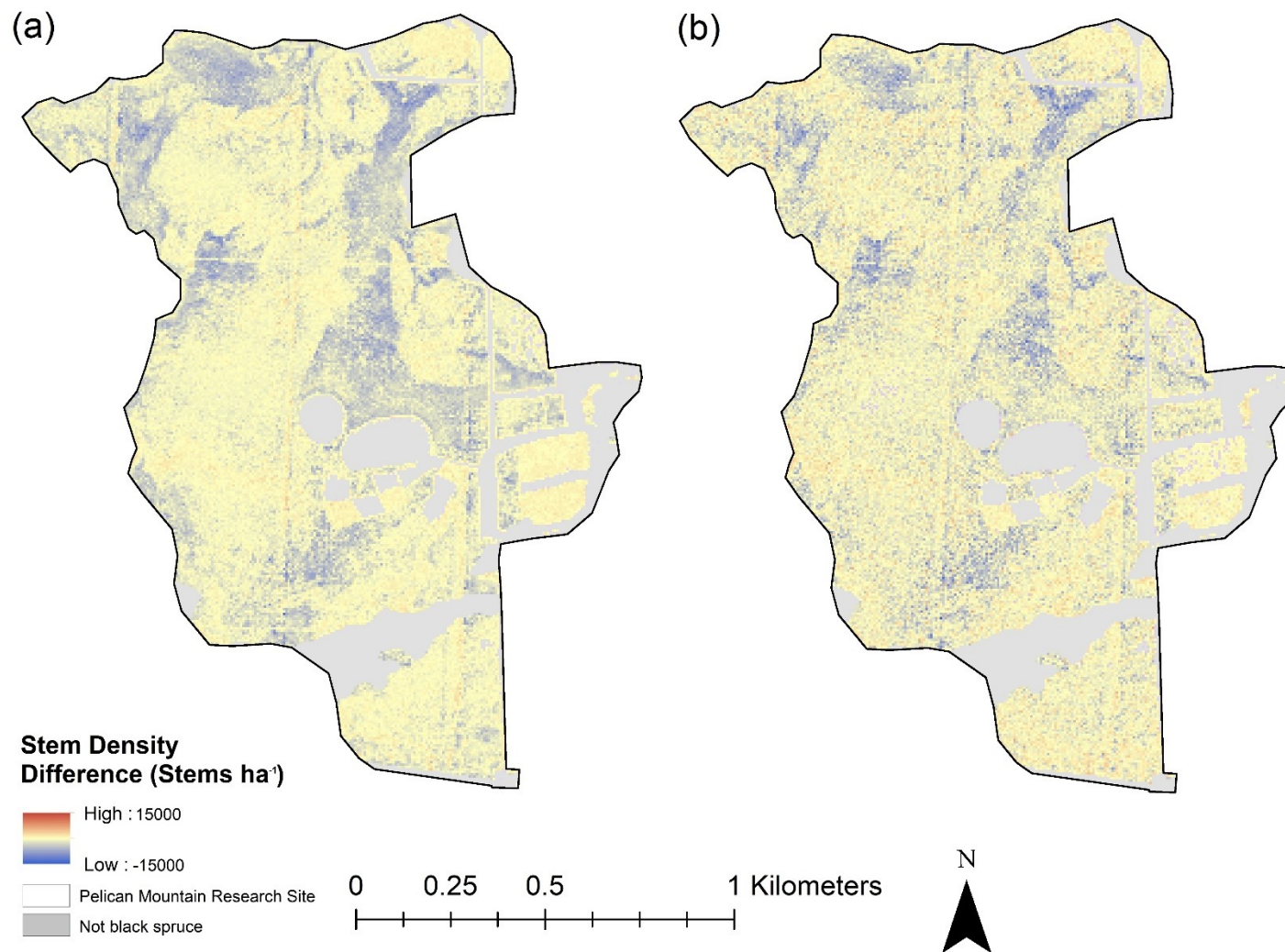
Figure 3.10 The difference between stem density values predicted using (a) models developed with intermediate and dense ALS pulse density datasets and (b) models developed with thin and dense ALS pulse density datasets. Pixels in blue indicate areas where the intermediate/thin model underpredicted stem density in comparison to the dense ALS model. Pixels in red indicate areas where the intermediate/thin model overpredicted stem density in comparison to the dense ALS model.

3.4 Canopy Height

Field-measured canopy height measurements satisfied the requirements of linear regression for all three ALS pulse density models. The linear models that were developed to predict canopy height using lasso regression for each ALS point density dataset are presented in Table 3.6. The dense ALS dataset produced a simple model with only one predictor variable (h_{max}). The intermediate and thin models both had three predictor variables (h_{max}, h_{99} and $Pc_{1.37}$ for the intermediate model and h_{max}, h_{CV} and h_{P90} for the thin model). Although the h_{max} and h_{99} variables that were selected using lasso were highly correlated, the lasso models were not adjusted. This was because the intent of the model was to make predictions and multicollinearity is not an issue for this purpose if the training and testing sets have the same covariance structure (Belsley, 1984). The R^2 values fitted to the training data for the dense, intermediate and thin models were 0.81, 0.79, and 0.69, respectively. When the dense model was applied to the testing data, the R^2_{test} value (0.84) exceeded the R^2 value. The R^2_{test} values for the intermediate and thin testing datasets were 0.73 and 0.66, respectively.

Comparison of RMSE and $RMSE_{test}$ values for dense (1.29, 0.96), intermediate (1.32, 1.21) and thin (1.63, 1.37) models indicated $RMSE_{test}$ was less than the RMSE in all cases, which means the model exhibited a better fit to the independent testing data even though it was derived from the training data.

Scatterplots comparing field-measured canopy height and predicted values from ALS point cloud datasets can be seen in Figure 3.11. Data points for all models strongly follow the 1:1 line; however, there is a slight bias towards overprediction of canopy height when field-measured

values are small. The degree of overprediction appears to increase as the ALS pulse resolution decreases. Maps displaying predicted canopy height in black spruce stands within the Pelican Mountain Research boundaries were created for each ALS pulse density model (Figure 3.12). Differences in canopy height values predicted by the dense model compared to the intermediate and thin models can be seen in Figure 3.13. The mean and standard deviation of stem density differences predicted by the intermediate and dense models across the Pelican Mountain Research Site was 0.13 m and 0.40 m, respectively. The mean and standard deviation of stem density differences predicted by the thin and dense models across the Pelican Mountain Research Site was 0.34 m and 0.72 m, respectively.
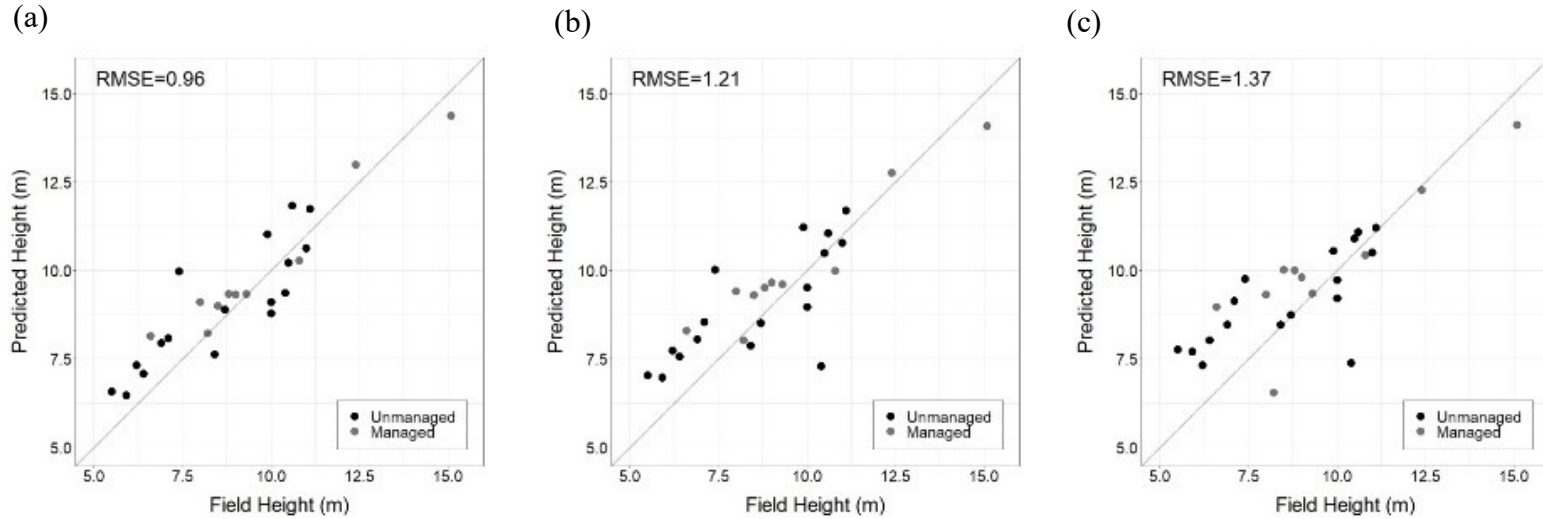
Figure 3.11 Plot-level canopy height estimated from ALS data for the testing dataset (predicted) versus field-measured values (observed): (a) dense ALS pulse density model, (b) intermediate ALS pulse density model, (c) thin ALS pulse density model. Solid line shows 1:1 relationship denoting perfect model fit.

Table 3.6 Lasso linear regression models and performance metrics predicting the canopy height by ALS point cloud density.

ALS Dataset	Equation	R^2	R^2_{test}	RMSE	RMSE$_{test}$
Dense	Height $= 2.71 + (0.79)h_{max}$	0.81	0.84	1.29	0.96
Intermediate	Height $= 3.42 + (0.48)h_{max} + (0.27)h_{99} + (0.0012)Pc_{1.37}$	0.79	0.73	1.32	1.21
Thin	Height $= 4.19 + (0.69)h_{max} + (0.43)h_{CV} + (0.021)h_{90}$	0.69	0.66	1.63	1.37
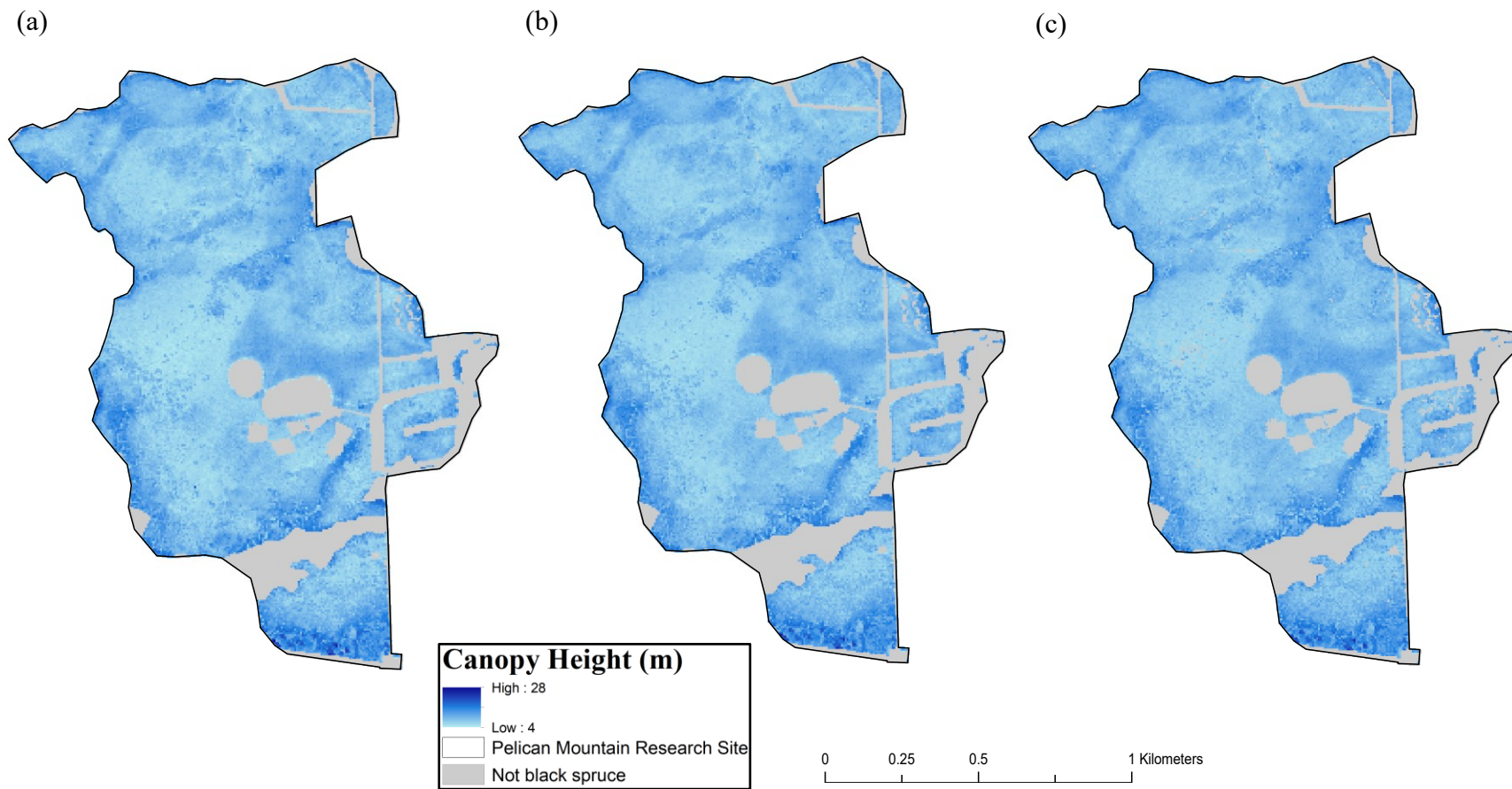
Figure 3.12 Canopy height predicted for black spruce stands within the Pelican Mountain Research Site using statistical models developed with three different ALS pulse densities: (a) dense, (b) intermediate, and (c) thin.
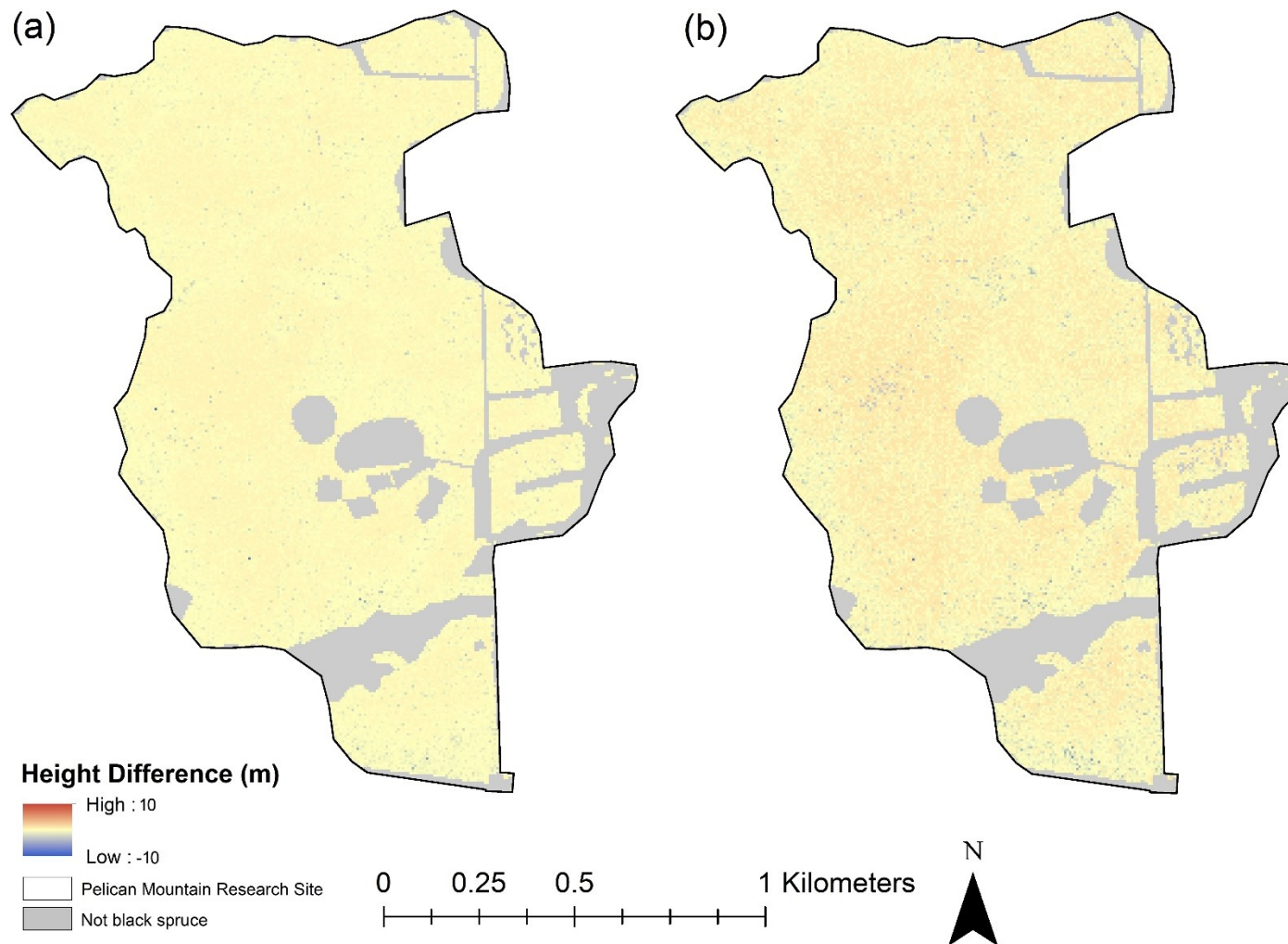
Figure 3.13 The difference between canopy height values predicted using (a) models developed with intermediate and dense ALS pulse density datasets and (b) models developed with thin and dense ALS pulse density datasets. Pixels in blue indicate areas where the intermediate/thin model underpredicted canopy height in comparison to the dense ALS model. Pixels in red indicate areas where the intermediate/thin model overpredicted canopy height in comparison to the dense ALS model.

3.5 Canopy Base Height

A square root transformation was applied to CBH measurements to satisfy the requirements for linear regression based on the diagnostic plots. The linear models that were developed to predict the square root of CBH using lasso regression for each ALS point cloud dataset are presented in Table 3.7. The regression models for the dense and intermediate datasets were almost identical and both utilized only one predictor variable (h_{25}); however, six variables were selected for the thin model (h_{mean}, h_{CV}, $Pc_{1.37}$, Pc_{mean}, $Prop_{<0.15}$ and $Prop_{10to20}$).

The R^2 values fitted to the training data for the dense, intermediate and thin models were 0.63, 0.71 and 0.80, respectively. When the models were applied to the testing data there R^2_{test} values were 0.51, 0.51 and 0.59 for dense, intermediate and thin models. Despite relatively large differences between the R^2 and R^2_{test} values, the RMSE and RMSE$_{test}$ were in close alignment. The RMSE and RMSE$_{test}$ values for dense, intermediate and thin models were 0.2347 and 0.1999, 0.2094 and 0.2001, and 0.2137 and 0.2088. For the thin model, the RMSE of the training data was slightly higher than the RMSE$_{test}$ value.

Scatterplots comparing field-measured square root transformed CBH values and predicted values from ALS point cloud datasets can be seen in Figure 3.14. Significantly more scatter is evident around the 1:1 line for the sqrt(CBH) models compared with all other models developed in this study. This may indicate that this forestry metric may be more challenging to predict compared with canopy bulk density, canopy fuel load, stem density and canopy height values for black spruce stands.

Maps displaying predicted CBH in black spruce within the Pelican Mountain Research Site boundaries were created for each ALS pulse density model (Figure 3.15). All maps look quite similar despite the thin model having more predictor variables than the dense or intermediate models. The scale of CBH measurements for the maps indicates that some CBH values were predicted to be up to 18 m high. These values are inflated in comparison with those measured in the field where all CBH measurements were under 5.5 m. Maps displaying predicted canopy height in black spruce stands within the Pelican Mountain Research boundaries were created for each ALS pulse density model (Figure 3.12). The differences in CBH values predicted by the dense model compared to the intermediate and thin models can be seen in Figure 3.16. The mean and standard deviation of CBH differences predicted by the intermediate and dense models across the Pelican Mountain Research Site was 0.002 m and 0.149 m, respectively. The mean and standard deviation of stem density differences predicted by the thin and dense models across the Pelican Mountain Research Site was -0.25 m and 0.5 m, respectively.
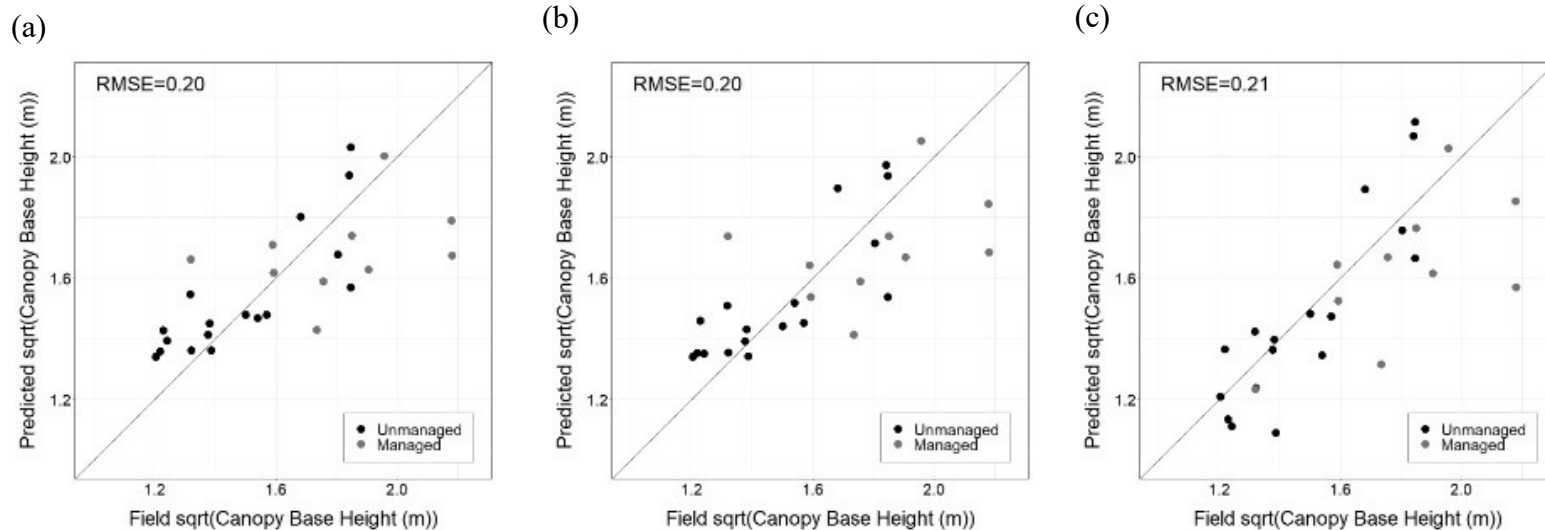
Figure 3.14 Plot-level (square root transformed) canopy base height estimated from ALS data for the testing dataset (predicted) versus field-measured values (observed): (a) dense ALS pulse density model, (b) intermediate ALS pulse density model, (c) thin ALS pulse density model. Solid line shows 1:1 relationship denoting perfect model fit.

Table 3.7 Lasso linear regression models and performance metrics predicting the square root of canopy base height ($\sqrt{CBH}$) by ALS point cloud density.

ALS Dataset	Equation	R^2	R^2_{test}	RMSE	RMSE$_{test}$
Dense	$\sqrt{CBH} = 1.02 + (0.19)h_{25}$	0.63	0.51	0.235	0.200
Intermediate	$\sqrt{CBH} = 1.02 + (0.19)h_{25}$	0.71	0.51	0.209	0.200
Thin	$\sqrt{CBH} = 0.69 + (0.19)h_{mean} + (-1.34)h_{CV} + (0.0049)Pc_{1.37} + (0.00022)Pc_{mean7} + (0.78)Prop_{<0.15} + (-1.67)Prop_{10to20}$	0.80	0.59	0.214	0.209
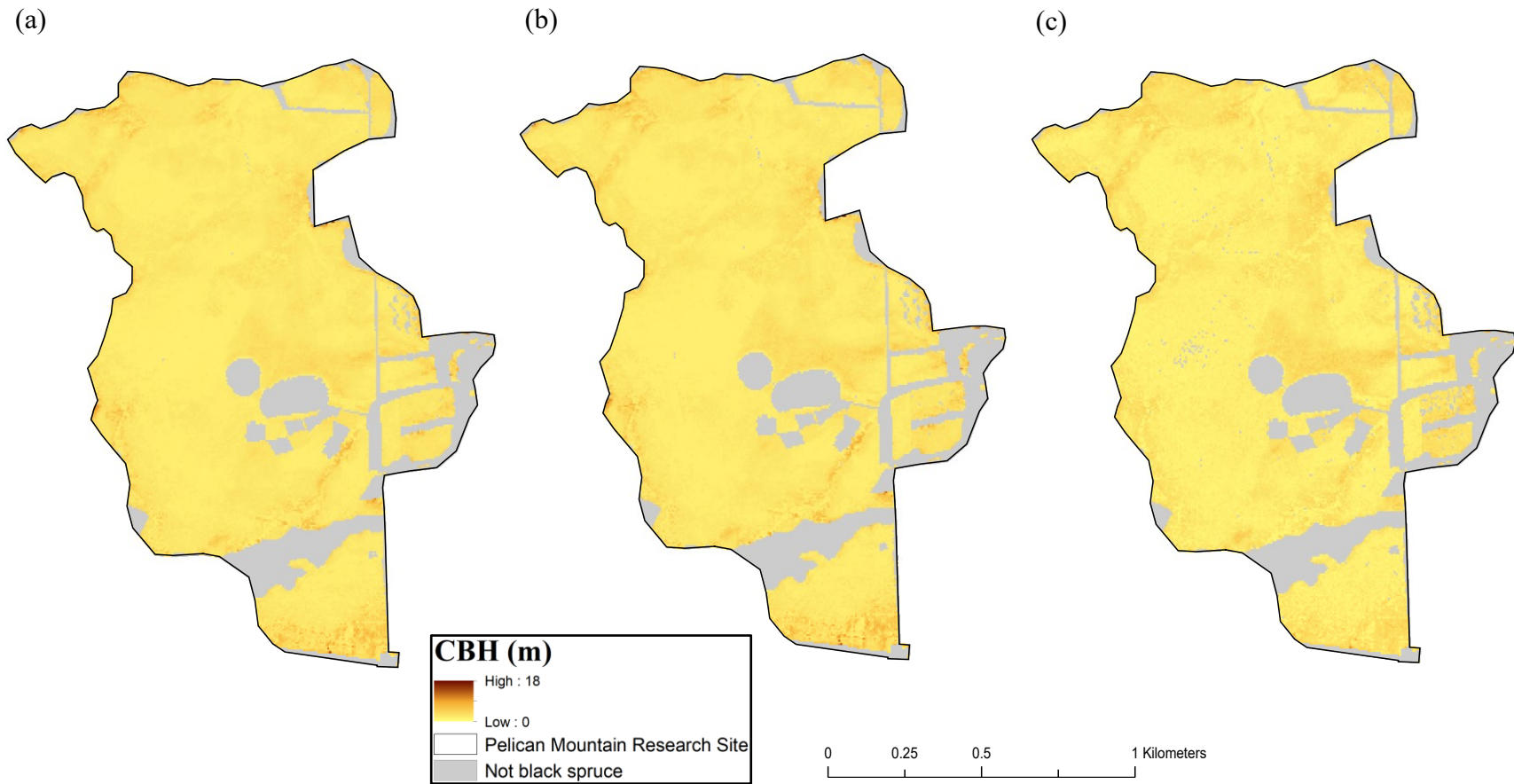
Figure 3.15 Canopy base height (CBH) predicted for black spruce stands within the Pelican Mountain Research Site using statistical models developed with three different ALS pulse densities: (a) dense, (b) intermediate, and (c) thin. Note that predicted values from the ALS models were back transformed into original CBH units.
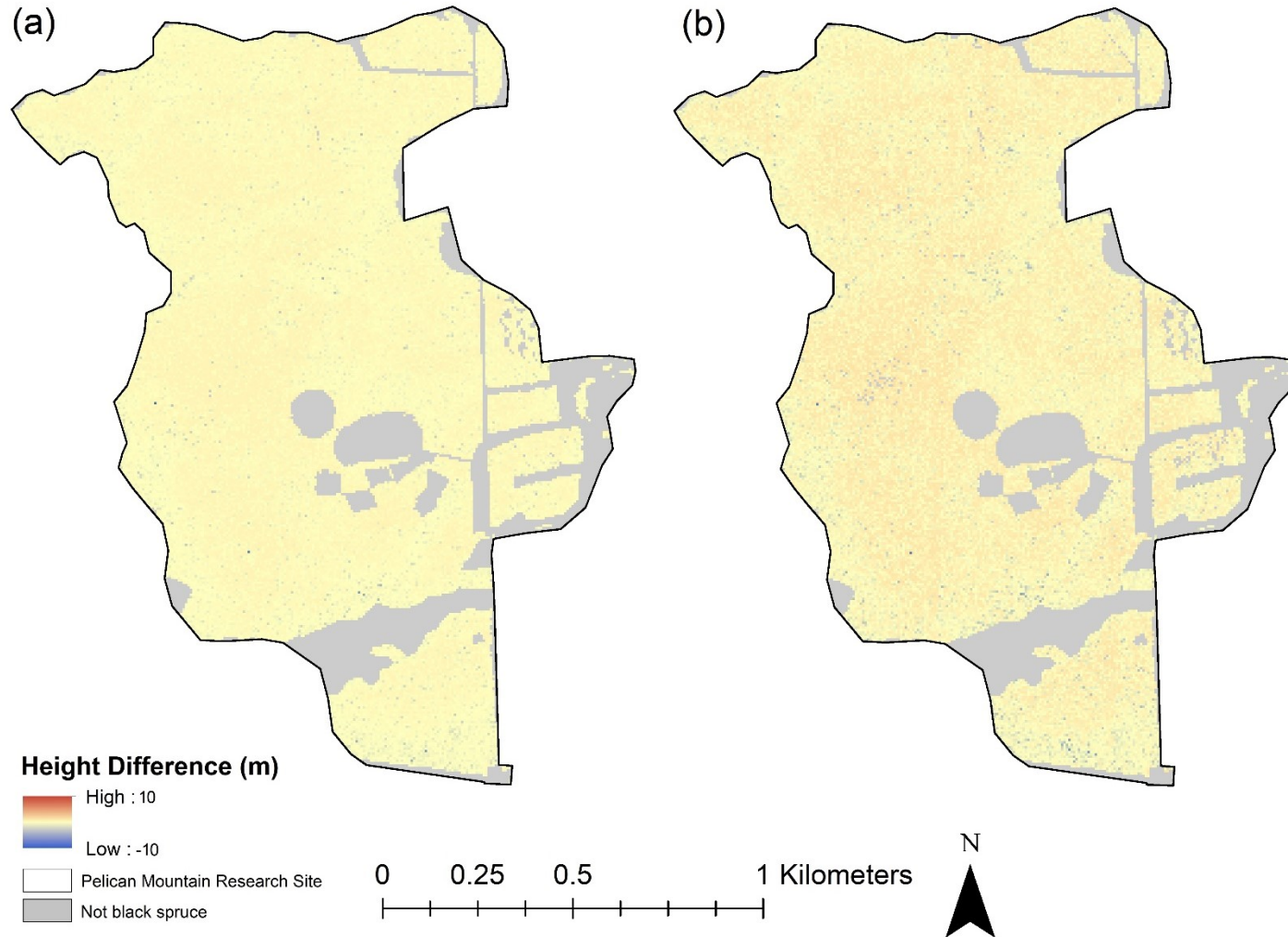
Figure 3.16 The difference between canopy base height (CBH) values predicted using (a) models developed with intermediate and dense ALS pulse density datasets and (b) models developed with thin and dense ALS pulse density datasets. Pixels in blue indicate areas where the intermediate/thin model underpredicted CBH in comparison to the dense ALS model. Pixels in red indicate areas where the intermediate/thin model overpredicted CBH in comparison to the dense ALS model.

Chapter 4 Discussion

Results of this study indicate that Airborne Laser Scanning (ALS) data are a viable resource for predicting forest structural characteristics important to wildfire behaviour in black spruce stands. Similar studies completed for other forest types have reported varying degrees of success when comparing field-based measurements of forest characteristics important to wildfire with ALS data (Table 4.1); however, all of these forest types were quite distinct compared with the black spruce stands analyzed in this study. Black spruce stands typically have shorter canopy height and canopy base height (CBH) values and larger canopy bulk density (CBD), canopy fuel load (CFL) and stem density values compared with other studies. In this chapter, the predictive power of using ALS data to estimate CBD, CFL, stem density, canopy height and CBH in black spruce stands is examined in detail. The influence of ALS pulse density on developing fine scale fuel models in black spruce stands is also evaluated. Possible sources of error and suggestions for future research are discussed. Finally, management implications of this research are reviewed.

4.1 Evaluation of Model Performance

Model performance for predicting sqrt(CBD) and sqrt(CFL) in black spruce stands declined as pulse density of the ALS data decreased. As pulse density decreased, $RMSE_{test}$ values increased and the degree of underprediction increased for the high-end range of field-measured values of CBD and CFL. The $RMSE_{test}$ values for sqrt(CBD) indicate very similar predictive power between models developed using dense and intermediate ALS datasets. In contrast, model performance declined when the least dense ALS dataset was utilized for model building. The $RMSE_{test}$ values for the sqrt(CBD) models developed from dense and intermediate ALS datasets

differed by just 4% whereas there was a 24% increase in $RMSE_{test}$ values between the models derived with the thin and intermediate ALS models, respectively.

For the sqrt(CFL) predictive models, $RMSE_{test}$ values increased by 9% when comparing model results for the intermediate ALS dataset to those estimated from the dense dataset. When comparing model results for the thin ALS dataset to the intermediate dataset, the $RMSE_{test}$ increased by 13%. Although the predictive error increased as ALS pulse density of the data decreased, the thin models still performed reasonably well. The produced fuel maps using the thin ALS dataset for the Pelican Mountain Research Site exhibited spatial variation that was consistent with maps generated using the models derived from dense and intermediate ALS datasets.

These results are consistent with the findings of Jakubowski et al. (2013b) who reported that performance of ALS models for predicting common forestry metrics was largely insensitive to pulse density until it dropped below 1 pulse m^{-2}. The effect of ALS pulse density on predictions of forest variables required in forest resource inventories for black spruce stands in Ontario, Canada was also evaluated by Treitz et al. (2012). In that study, three ALS datasets with varying pulse densities were analyzed (i.e., 3.2, 1.6 and 0.5 pulses m^{-2} resolutions). They found no reduction in model predictive ability as ALS pulse density was reduced. It is important to note that neither of these studies involved predicting either CBD or CFL metrics specifically. Much larger plot sizes of 500 m^2 and 400 m^2 were also used in the Jokubowski et al. (2013) and Treitz et al. (2012) studies, respectively. The sampling area of the majority of plots used in this study was 40 m^2. Use of fine- scale measurements may necessitate higher pulse densities to adequately

describe forest structure, which could potentially explain why results reported in this study were slightly more sensitive to pulse density compared with prior investigations.

To compare the results from this study to other studies, the coefficient of determination (R^2) for the testing data was used (Table 4.1). This is because $RMSE_{test}$ values reflect the range in field measured variables which will change depending on forest type and structure, whereas R^2 is a common statistic reported in similar studies. Nonetheless, comparisons of R^2 values across studies should be approached with caution given differences in forest types, response variables and transformations imposed on dependent variables can all affect results. The coefficient of determination for the sqrt(CBD) estimation models were 0.84, 0.84 and 0.75 for dense, intermediate and thin models respectively, which is higher than the R^2 values reported by Hermosilla et al. (2014), Bright et al. (2017) and Engelstad et al. (2019) and comparable to the R^2 values reported by Andersen et al. (2005), Erdody and Moskal (2010) and Skowronski et al. (2011). The coefficient of determination values for the sqrt(CFL) models (0.84, 0.86 and 0.80 for the dense, intermediate and thin models, respectively) were also comparable to those reported by Andersen et al. (2005), Erdody et al (2010), Skowronski et al. (2011) and Hermosilla et al. (2014) and were significantly higher than reported by Bright et al. (2017).

Table 4.1 Previous studies that utilized Airborne Laser Scanning (ALS) data to predict forest characteristics important to wildfire behaviour. Coefficient of Determination values (R^2) are listed if the study modelled canopy bulk density (CBD), canopy fuel load (CFL), stem density, canopy height and canopy base height (CBH) values. For comparison, R^2 values using the testing data for models derived in this study are also shown.

Author	Study Site Description	Coefficient of Determination (R^2)				
		CBD	CFL	Stem Density	Canopy Height	CBH
Andersen et al. (2005)	Capital State Forest in western Washington State	0.84**	0.86*	n/a	0.98	0.77
Erdody and Moskal (2010)	Ponderosa pine stands in eastern Washington State	0.83**	0.88**	n/a	0.94	0.78*
Skowronski et al. (2011)	Pinelands National Reserve of southern New Jersey	0.83	0.71	n/a	n/a	n/a
González-Olabarria et al. (2012)	Forested areas in the Mediterranean	n/a	n/a	0.64	0.91	0.56
Hermosilla et al. (2014)	Mixedwood forest in north-west Oregon	0.67	0.79	n/a	0.79	0.78
Bright et al. (2017)	Mountain pine beetle affected stands in a coniferous montane forest in Colorado	0.46	0.56	n/a	0.66	0.28
Engelstad et al. (2019)	Boundary Waters Canoe Area in northern Minnesota	0.48	n/a	n/a	n/a	0.7
Results from Present Study						
Models derived using the dense ALS point cloud dataset		0.78*	0.85*	0.81*	0.84	0.51*
Models derived using the intermediate ALS point cloud dataset		0.78*	0.82*	0.74*	0.73	0.51*
Models derived using the thin ALS point cloud dataset		0.69*	0.77*	0.71*	0.66	0.59*

Note: * indicates a square root transformation was used and ** indicates natural log transformation was used in derived model.

Although the CBD and CFL models developed in this study appear to have strong predictive power and similar results compared with other studies, some model shortcomings were evident. Firstly, plots of predicted versus observed (transformed) CBD and CFL values indicated that all models under-predicted at the high end of the range of values. Hermosilla et al. (2014) reported similar findings when developing a model for CBD and suggested the under prediction was caused by outliers. Although not mentioned explicitly, predicted versus observed CBD plots reported by Erdody and Moskal (2010) and Andersen et al. (2005) indicated that CBD values at the high end of the range were also under predicted by their models. These discrepancies may be due to the nature of the forest and ALS data itself. In very dense stands, which would be associated with high CFL and CBD values, the ALS laser pulse may not sufficiently penetrate the canopy. This could lead to occlusion at lower elevations and affect ALS metrics (Vauhkonen et al., 2011; Kandare et al., 2016). Due to the limited number of sampling plots used in this study it is difficult to conclude whether occlusion is causing the slight underprediction of high sqrt(CBD) and sqrt(CFL) values. Further studies of how stand density impacts occlusion in black spruce stands is recommended, as it may be possible to correct the bias through data transformation (e.g., Lefsky et al., 2002).

Underpredicted high sqrt(CBD) and sqrt(CFL) values could also be due to the fixed interval height metrics used. For example, if dense stands happen to be stunted, then ALS metrics, such as the percent of first returns above 1.37 m ($Pc_{1.37}$), may be smaller in value compared with taller stands. This would be because the ALS laser pulse has to travel a shorter distance through the canopy to reach this height value. When comparing the predicted stem density and canopy height maps for the Pelican Mountain Research Site, it does appear that areas of high predicted stem

density often have lower relative canopy heights (elevations). Given the volume of ALS models that have been developed using height strata values (e.g., Andersen et al., 2005; Erdody and Moskal, 2010; Bright et al., 2017; Engelstad et al., 2019), more studies should be conducted to determine how these fixed height variables may affect model results.

In addition to underpredicting high-end values for field-measured sqrt(CFL), the predicted versus observed scatterplots suggest the models also underpredicted field-measured values in the mid-range for sqrt(CFL) values. This resulted in the scatterplots having a slight "step" in appearance in relation to the linear 1:1 line. This may indicate that the square root transformation used to fit the training data was not the best fit for the testing data. The effects of this appear to be very minor given the small $RMSE_{test}$ and high R^2 values for all models. However, if more field data were collected it may help strengthen confidence in the transformations needed to fit a linear model.

The degree of under-prediction for CBD and CFL were minimal for the dense and intermediate models, but more pronounced in the thin models which relied on lower pulse density ALS data. As a result, the range in predicted values were smaller for the thin models when compared with the intermediate and dense models. The effect of this was evident when predicted CBD and CFL values were mapped across the Pelican Mountain Research Site for each ALS pulse density model. Maps produced from models that used intermediate and dense point clouds looked almost identical whereas the maps based on the thin models were slightly muted in colour, indicating that the range of true values was not being detected. This may limit the potential for using CBD and CFL maps from thin ALS point clouds in fire behaviour models. The maps generated with

the thin models were still similar to those generated with the intermediate and dense models and still clearly delineate the same overall trends evident across the research site. Comparison of model results with a field-verified site map that delineated stand conditions demonstrated that all three ALS pulse density models were able to identify the variability of stand structure at the site. For example, patches of managed forests that were thinned appear as lighter areas on the ALS-derived map, indicating lower CBD and CFL values. Stands that were unmanaged and naturally dense appear as dark areas on the map, indicating higher CBD and CFL predictions. Although the model developed using the lowest density ALS point cloud had lower predictive ability in comparison with intermediate or dense models, it may still be suitable for informing land management decisions that do not require highly precise stand structure information and would be more easily applied across larger landscapes where thin density point clouds are widely available.

Use of ALS data to predict stem density is widely recognized as an unresolved challenge, especially in the case of ALS data with lower point cloud density (Kandare et al., 2016). Results of this study confirmed that ALS data currently has limited potential for predicting stem density in black spruce forests, especially as point cloud resolution used for model building decreases. Relatively large differences between the RMSE and RMSE$_{test}$ values for each model indicated that there was overfitting of the training dataset. In addition, the field-measured versus predicted square root stem density scatterplots indicate that all ALS models underpredicted high field-measured stem density values. Under prediction for high stem density values became more pronounced as the ALS pulse density decreased. The increased difficulty with fitting a model in very dense stands is logical. As a stand density increases, the ability for the ALS laser pulse to

penetrate the bottom of the forest floor decreases, which can lead to occlusion and therefore skewed ALS metrics (Vauhkonen et al., 2011; Kandare et al., 2016). Despite these issues, the stem density models have R^2 values of 0.89, 0.80, 0.78 for the dense, intermediate and thin models respectively, which were similar or better than those reported by Treitz et al. (2012), Luther et al. (2013) and Shang et al. (2019).

The studies by Treitz et al. (2012) and Luther et al. (2013) both related ALS data to black spruce forest characteristics in eastern Canada and are the most similar in stand types to this study. In both studies, variables important to the forest industry were examined, such as canopy height and stem density, which has some overlap with the variables analyzed in this study. Treitz et al. (2012) reported R^2 values ranging from 0.79 to 0.89 for models comparing field measured density to ALS data, while Luther et al. (2013) reported an adjusted R^2 value of only 0.55. Both studies only used trees with larger DBH measurements to count towards their density measurements ($\geq$10.0 cm threshold for Treitz et al. (2012) and $\geq$9.0 cm threshold for Luther et al. (2013)). In this study, all trees over 1.37 m in height were counted. As such, mean stem density values were very different. The mean stem densities for this study, Treitz et al.'s (2012) study and Luther et al.'s (2013) study were 8206 stems ha^{-1}, 1643 stems ha^{-1} and 1725 stems ha^{-1}, respectively. Similar to this study, Treitz et al. (2012) required a large number of ALS predictor variables to derive a measure of stem density, which can inflate R^2 values. Luther et al. (2013) only had three ALS predictive variables used in their models.

The canopy height models estimated in this study performed poorly in comparison with prior studies. Canopy height models had R^2 values of 0.81, 0.79 and 0.69 for dense, intermediate and

thin models respectively, which were comparable Hermosilla et al. (2014), but lower than R^2 values reported in several other studies (e.g., Andersen et al., 2005; Erdody and Moskal, 2010; Treitz et al., 2012; Luther et al., 2013). This may reflect the shorter canopy heights of the black spruce stands in this study compared with the forest types investigated in other studies. Even in Treitz et al.'s (2012; R^2 of 0.92) and Luther et al.'s (2013; R^2 of 0.90) studies that were specific to black spruce stands, average stand height was significantly higher at 16.7 m and 11.9 m respectively. In the present study, average stand height was only 9.3 m. Predictor variables chosen to model dominant height by Treitz et al. (2012) using multiple stepwise regression aligned closely with variables chosen with lasso regression in this study. In their study the maximum LiDAR return height and the 90th percentile return height were selected as predictor variables for all three models. In this study, the maximum LiDAR return height was consistently selected, in addition to the 99th percentile return height and percent of first returns above 1.37 m for the intermediate model and coefficient of variation in LiDAR return height and 90th percentile return height for the thin model. In Luther et al.'s (2013) study, dominant stand height (considered analogous to canopy height for comparison) was modeled with the 99th percentile return height, as well as two terrain metrics that were selected using best-subsets regression.

The performance of the canopy height models are more impressive when RMSE errors are compared with other studies rather than R^2 values. The RMSE errors for estimating canopy height using ALS data were 1.5 m for Andersen et al.'s (2005) model, 1.9 m for Erdody and Moskal's (2010) model, between 0.7-0.8 for Treitz et al.'s (2012) models, 1.0 for Luther et al.'s (2013) model and 4.0 m for Hermosilla et al.'s (2014) model. For this study, the $RMSE_{test}$ for the dense, intermediate and thin models were 1.0 m, 1.2 m and 1.4 m respectively. Although the

RMSE$_{test}$ for canopy height models developed in this study are relatively small or comparable to previous studies, the canopy heights for black spruce stands are much shorter so the relative error is larger (hence the lower R^2 values). It is also noteworthy that the scatterplots of predicted versus observed values for canopy height models indicate that all models developed in this study over predicted canopy heights at the lower-end of the range of values, where canopy height was less than 8.0 m. Once again, this bias became more pronounced as the point resolution of the ALS model decreased. Gopalakrishnan et al. (2015) also found that their ALS models over-predicted height for short stands. They suggest that a piecewise linear model may improve predictive ability.

Several prior studies reported success using ALS data to predict the height of the base of the canopy for a variety of different forest stand types (e.g., Andersen et al., 2005; Erdody and Moskal, 2010; Hermosilla et al., 2014; Engelstad et al., 2019); however, when the understory vegetation is close to the base of the canopy it can be difficult to define CBH using ALS models (Popescu and Zhao, 2008). Black spruce trees tend to have crowns that extend to the forest floor with a buildup of dead branches and lichen. The relatively poor CBH models generated with the three different ALS point cloud density datasets support that ALS data is not well suited for measuring the distance between the ground and the base of the canopy in stands where tree morphology includes crown vegetation that extends continuously from the top of the tree to the forest floor.

It is also noteworthy that all canopy height models, all canopy base height models and the dense CFL model, had smaller RMSE$_{test}$ values compared with RMSE values. Although the differences

were small, this was unusual given that the model was designed fit the training data best, rather than the testing data. The higher training errors may indicate that the models were generalizing well and were able to properly adapt to new data. It could also reflect the relatively small size of the testing data and random chance. If the testing error was much larger than the training error, it could indicate that the training and testing groups were not randomly selected. Given that the errors were similar in value, this was likely not the case for the models developed in this study and it can be assumed that the low testing errors are due to random chance. Had a larger training data sample size been used for this study the chance of the model fitting the testing data better than the training data would have been reduced.

4.2 Sources of Error

There are a number of sources of possible error in this study. Firstly, plot summaries of field measurements involved many assumptions. Given the time and logistics involved with destructive sampling, canopy fuel load was calculated from DBH measurements using allometric equations. It is common practice to use allometric equations to infer CFL values (e.g., Andersen et al., 2005; Erdody and Moskal, 2010; Engelstad et al., 2019); however, by doing so can introduce sources of error as trees will naturally have different physical attributes and structure based on location and growing conditions. If the allometric equations used to calculate field-measured CFL values do not adequately represent the trees within the study area then the CFL values may be incorrect. Further, the crown fuel load for each tree was assumed to be distributed evenly across the plot and throughout the crown of the tree. Heterogeneity of stand structure within the sampling plot was therefore ignored, which could affect field-measured CFL values

and subsequently CBD and CBH values used in this study. This error would be propagated into the ALS derived models and could result in inaccurate predictions.

Field measurements in this study were conducted at a relatively fine resolution to minimize the effects of horizontal heterogeneity common in natural black spruce stands; however, these finer-resolution data introduced potential sources of error. White et al. (2013) emphasizes the importance of keeping plot size and grid resolution equivalent when using the area-based approach, which was utilized in this study. Although necessary for generating high resolution maps, smaller plot sizes have increased potential for edge effects. Edge effects occur when tree crowns found along the perimeter of the plot boundary are included in analysis when they are actually located (fully or partially) outside the plot boundary or excluded in analysis when they are actually located (fully or partially) inside the plot boundary (White et al., 2013). Borderline trees are an issue because the ALS point cloud clipped to the boundary of the plot may not reflect exactly what was measured on the ground. Edge effects will increase as the plot area decreases because the perimeter to sampling area ratio increases. In this study, it was assumed that edge effects were offsetting, such that partial crowns of trees in and out of the plot effectively cancelled each other out. Edge effects likely had the most influence on the canopy height models as they all depended on the maximum return height. This value was calculated from a single LiDAR return pulse, rather than the other ALS metrics that were statistical calculations representing the distribution of LiDAR returns. Therefore, the edge effects for this parameter would not cancel out at the plot level and may explain why the canopy height models had relatively poor performance compared to other studies.

Human error during field measurements are another potential source of error. Canopy base height measurements are somewhat subjective in nature, owing to inconsistent tree crown morphology. Accuracy of tree height measurements can be compromised in dense stands where nearby trees obstruct the clear line-of-site required for Vertex Hypsometer readings. Georeferencing errors can also cause discrepancies between ALS data and field data. The center of the ground plot must be determined with a high degree of horizontal accuracy, otherwise the ALS point cloud that is trimmed to the boundary of the plot may not completely align with the ground plot. Small plots are also more prone to the effects of georeferencing errors as there would be less spatial overlap between ground plot and ALS areas given the same degree of error for a larger plot. In this study, plot coordinates were determined with a high horizontal accuracy of 0.39 m using a Trimble® Geo7X global navigation satellite system device with a Trimble® Tempest Antenna (Sunnyvale, CA).

Time elapsed between field measurements and ALS data collection could cause discrepancies between field-measured and ALS data. In this study, field measurements were conducted within 15 months of ALS data collection. It is possible that small changes within the plot could have occurred during this time period; however, black spruce is a slow growing tree (Gamache and Payette, 2004) and minimal impacts on results are expected. Field plots were monitored with frequent on-site visits and no significant disruptions occurred at any of the plots between field measurements and ALS data collection. One thing to note is that in the managed stands trees were occasionally not perpendicular to the ground because they had been affected by higher winds. This angle of the canopy relative to the ground may have affected ALS metrics. It is

assumed that naturally less dense stands would be equally affected by high wind speeds and would have a similar canopy structure.

Different laser wavelengths were used for the dense ALS dataset which may cause inconsistencies when comparing the ALS derived models. The dense ALS dataset used in this study consisted of three multispectral point clouds merged into one. The intermediate and thin ALS datasets only consisted of returns from the 1064 nm laser. There is potential for error when comparing dense ALS point cloud models to intermediate and thin models because different wavelengths were used for the remaining two channels (1550 and 531 nm) and these may be better or worse at detecting various structural attributes. Given that models developed using dense and intermediate ALS datasets had similar performance, the impact of differing wavelengths is expected to be minimal.

4.3 Management Implications

Timely and cost-effective mapping of canopy fuel characteristics across large landscape areas could have a profound impact on fire management practices and decisions and the underlying fire research and decision support tools that guide them. This research shows the potential to utilize ALS data to map canopy fuels at higher resolution than ever before. Airborne laser scanning data has been used extensively to map canopy fuels for a variety of stand types and at a variety of pulse densities (e.g., Andersen et al., 2005; Erdody and Moskal, 2010; Skowronski et al., 2011; Gonzalez-Olabarria et al., 2012; Hermosilla et al., 2014; Bright et al., 2017; Engelstad et al., 2019). The highest resolution canopy fuel maps produced with ALS data to date have resolutions as fine as 100 m^2 (e.g. Bright et al., 2019). In this study, 40 m^2 resolution maps were

generated. This level of detail opens the door to further developing empirical models that can be used for fire behaviour modelling, fire occurrence prediction or strategic planning. In addition, this study shows that expensive, high resolution ALS datasets may not be necessary to adequately describe canopy fuels as lower point cloud densities had reasonable predictive accuracy.

Modeling canopy fuel parameters with low density, 1 pulse m^{-2} ALS data would have immediate applications. In Alberta, low density ALS data is currently available for most of the provincial forest area. The majority of these data were collected between 2007 and 2008. With new ALS data, temporal comparisons between forest structures could be made. Utilizing the provincial ALS dataset could also be used for space-for-time substitution studies. For example, following Beverly's (2017) approach, the age of black spruce stands could be determined using fire perimeter shapefiles obtained from the Government of Alberta. Analysis of how black spruce forest structure changes over time could then be conducted. Forest structure differences could also be compared between time since fire black spruce stands and time since logging black spruce stands to understand how human activities affect stand structure during regeneration. Analysis could also be conducted with forest structure attributes from the ALS data to determine why observed wildfires behaved the way they did. This information could be used to calibrate fire models, especially if rate of spread information were available.

One of the largest unknowns that affects fire management decisions is how black spruce managed stands affect wildfire behaviour (Flat Top Complex Wildfire Review Committee, 2012). The FBP system, currently used by most wildfire operations in Canada to predict wildfire

behaviour, does not account for managed stands. This research not only focused on identifying

forest structure attributes important to wildfire behaviour in natural black spruce stands, but also

stands that have undergone fuel reduction treatments in an effort to reduce potential wildfire

behaviour. By developing a model that works for both natural and managed stands, wildfire

managers can begin to understand what effect these fuel treatments may have on the landscape.

In addition, ALS data could be collected before and after fuel reduction treatments to standardize

fuel treatment design, confirm whether objectives have been met and to justify costs. Collecting

further ALS data overtime could be used to monitor how managed stands change over time and

how often they need to be treated. Finally, ALS data could be used to identify areas where fuel

treatments may be the most effectively placed to protect communities (e.g. Beverly et al., 2010).

The significance of this research extends much further than simply identifying canopy structural

attributes for black spruce stands. Any model attempting to understand the effects of wildfire

depend on fuel information. Whether modeling the impacts of climate change on wildfire

behaviour (e.g., Fried et al., 2004; Flannigan et al., 2005), trying to predict where fire may occur

on the landscape (e.g., Martell et al., 1987; Wotton et al., 2003) or trying to predict how a

wildfire might behave (e.g., Forest Fire Danger Group, 1992; Linn et al., 2002; Reinhardt and

Crookston, 2003; Rebain et al., 2010), fuel information will be either a direct or indirect input. In

addition, there are endless other research applications that mapping fuel structure could inform.

For example, being able to better describe fuels could be used for ecological studies (e.g.,

Rhodes and Baker, 2008; McArthur and Cheney, 2015), habitat suitability (e.g., Southgate et al.,

2007; Brown et al., 2009) and for monitoring changes/recovery after a disturbance (e.g., Bater et

al., 2010; Bright et al., 2012; McCarley et al., 2017). By offering higher resolution data, increased performance and reliability could be expected for any of these research pursuits.

Although results of this study are promising, they should be used with caution and consideration of data and methodological weaknesses and limitations. If using fuel maps produced from ALS as inputs into other models it is important to understand how the error and variability in predictions may be propagated. It is also important to recognize that the models developed in this study are only suitable for mapping stand attributes in black spruce forests with structural characteristics that fall within the range of variability observed in the model source data. Stand structural characteristics present at the Pelican Mountain and Conklin study sites used in this study are unlikely to represent the full range of variability in black spruce stands in Alberta. To improve the robustness of the models, additional plots could be collected for black spruce stands with a wider range of structural variability. A larger sample size of field measurements would also be expected to reduce bias observed in some of the predictive models. Finally, it is important to note that these models were only designed for black spruce stands and are not intended to summarize forest attributes of any other stand type. Future work could focus on using the multispectral ALS data to distinguish different tree species automatically, creating models for other stand types and studying the effects that plot size has on the predictive models.

Chapter 5 Conclusion

Fuel flammability and observed wildfire behaviour both depend on the structure of the fuel complex. In a forested stand, the structure and attributes of the canopy fuels can affect how efficiently a surface fire can transition into a crown fire, how intense the crown fire may be and how fast the wildfire is able to move. Fuel type maps were created to provide fire managers a very general description of the vegetation to be expected across a landscape; however, no within stand variation is accounted for within these broad categories despite its influence on fire behaviour. With present day technology, fuels can be accurately mapped at high resolutions. This provides an opportunity for models that use fuel information to evolve and perhaps produce more accurate predictions with the higher quality data. Even on their own, fuel maps have the ability to help fire management personnel develop prevention and management strategies.

This study evaluated whether airborne laser scanning (ALS) data is a viable tool for predicting forest structure characteristics important to wildfire behaviour on a fine scale (40 m^2 resolution) in black spruce stands. We also analyzed the influence of ALS pulse density on model form and performance. To achieve these objectives, 79 field plots were established in black spruce stands across two study sites in Alberta. Airborne laser scanning data were collected over the study sites and processed into three different pulse density datasets (with pulse densities of approximately 10.7, 4.5 and 1 pulse m^{-2}). Field data were randomly divided into training (52 plots) and testing (27 plots) datasets. Least absolute shrinkage and selection operator (lasso) regression was used for variable selection and fitting a linear model between the training data and ALS data. Model performance was evaluated on the testing dataset using root mean square error (RMSE) and

coefficient of determination (R^2) statistics. Models were also applied across the Pelican Mountain study area to visually assess model performance.

Results indicate that ALS data are suitable for accurately estimating forest structure characteristics important to wildfire behaviour within pure black spruce stands in Alberta, Canada. Maps generated with the ALS data provided much greater detail over larger areas than would otherwise be possible using limited plot-based information. Model performance was strong for all point density datasets analyzed in this study; however, predictive power did decrease for all canopy fuel parameters analyzed as point resolution decreased. Although performance of the 1 pulse m^{-2} dataset was weaker than the higher resolution datasets, ALS data at this low-density is currently available for much of Alberta's forests. This data availability offers endless opportunities for future studies to evaluate how canopy fuel structure changes over time, how it may affect wildfire behaviour or occurrence and how we can better manage fuel on the landscape. In addition, it can be used towards numerous other studies that may indirectly use canopy fuel information, such as determining habitat suitability, ecological impacts of disturbances or analyzing post-harvest forest structures.

Results of the lasso regression technique used in this study exhibited similar performance to prior studies that used stepwise regression to relate ALS and field data; however, the lasso method is less prone to overfitting data and is therefore recommended for future studies of this nature. Recommended future work includes collection of field data to enable development of more robust models. New sampling plots could be established at different study sites in an effort to capture a broader range of black spruce characteristics.

References

Agee, J. K., Wright, C. S., Williamson, N., & Huff, M. H. (2002). Foliar moisture content of pacific northwest vegetation and its relation to wildland fire behavior. *Forest Ecology and Management, 167*(1-3), 57-66.

Alberta Agriculture and Forestry. (2017). *Alberta's Community FireSmart Funding 2011-2017.* Internal Alberta Wildfire Report: Unpublished.

Alberta Wildfire. (2019). Wildfire Management 2019 Policy, Standard Operating Procedures, and Business Rules. Unpublished internal document, Alberta Agriculture and Forestry.

Alexander, M. E. (1982). Calculating and interpreting forest fire intensities. *Canadian Journal of Botany*, *60*(4), 349-357.

Alexander, M.E., Stefner, C.N., Mason, J.A., Stocks, B.J., Hartley, G.R., Maffey, M.E., Wotton, B.M., Taylor, S.W., Lavoie, N., and Dalrymple, G.N. 2004. Characterizing the jack pine– black spruce fuel complex of the International Crown Fire Modelling Experiment (ICFME). Can. For. Serv. Inf. Rep. NOR-X-393.

Anderson, H. E. (1981). *Aids to determining fuel models for estimating fire behavior* (Vol. 122). US Department of Agriculture, Forest Service, Intermountain Forest and Range Experiment Station.

Anderson, H.E., Brackebusch, A.P., Mutch R.W & Rothermel, R.C. (1966). *Mechanisms of fire spread research progress report No. 2* (INT-28). U.S.D.A Department of Agriculture, Forest Service, Intermountain Forest and Range Experiment Station. Retrieved from: https://www.fs.fed.us/rm/pubs_exp_for/priest_river/exp_for_priest_river_1966_anderson.pdf

Andersen, H., McGaughey, R. J., & Reutebuch, S. E. (2005). Estimating forest canopy fuel parameters using LIDAR data. *Remote Sensing of Environment, 94*(4), 441-449.

Andrews, P. L., Bevins, C. D., & Seli, R. C. (2005). BehavePlus fire modeling system, version 4.0: User's guide. *Gen.Tech.Rep.RMRS-GTR-106 Revised.Ogden, UT: Department of Agriculture, Forest Service, Rocky Mountain Research Station.132p., 106*

Andrews, P., & Queen, L. (2001). Fire Modeling And Information System Technology. Collingwood, Victoria, Australia: CSIRO Pub.

Arroyo, L. A., Pascual, C., & Manzanera, J. A. (2008). Fire models and methods to map fuel types: The role of remote sensing. *Forest Ecology and Management, 256*(6), 1239-1252.

Babyak, M. A. (2004). What you see may not be what you get: A brief, nontechnical introduction to overfitting in regression-type models. *Psychosomatic Medicine, 66*(3), 411-421.

Barker, J. S., Fried, J. S., & Gray, A. N. (2019). Evaluating Model Predictions of Fire Induced Tree Mortality Using Wildfire-Affected Forest Inventory Measurements. *Forests*, *10*(11), 958.

Bater, C. W., Wulder, M. A., White, J. C., & Coops, N. C. (2010). Integration of LIDAR and Digital Aerial Imagery for Detailed Estimates of Lodgepole Pine (Pinus contorta) Volume Killed by Mountain Pine Beetle (Dendroctonus ponderosae). *Journal of Forestry*, *108*(3).

Belsley, D. A. (1984). Collinearity and forecasting. *Journal of Forecasting*, *3*(2), 183-196.

Beverly, J. L. (2017). Time since prior wildfire affects subsequent fire containment in black spruce. *International Journal of Wildland Fire, 26*(11), 919. doi:10.1071/WF17051

Beverly, J.L., Bothwell, P., Conner, J.C.R., & Herd, E.P.K. (2010) Assessing the exposure of the built environment to potential ignition sources generated from vegetative fuel. *International Journal of Wildland Fire*, 19(3), 299-313.

Beverly, J. L., & Wotton, B. M. (2007). Modelling the probability of sustained flaming: predictive value of fire weather index components compared with observations of site weather and fuel moisture conditions. *International Journal of Wildland Fire*, *16*(2), 161-173.

Bivand, R., Keitt, T., & Rowlingson, B. (2019). Rgdal: Bindings for the 'Geospatial' Data Abstraction Library. R package version 1.4-4. http://CRAN.R-project.org/package=rgdal

Bonan, G. B., & Shugart, H. H. (1989). Environmental factors and ecological processes in boreal forests. *Annual review of ecology and systematics*, *20*(1), 1-28.

Botequim, B., Fernandes, P. M., Borges, J. G., González-Ferreiro, E., & Guerra-Hernández, J. (2019). Improving silvicultural practices for mediterranean forests through fire behaviour modelling using LiDAR-derived canopy fuel characteristics. *International Journal of Wildland Fire, 28, 823–839*

Bouvier, M., Durrieu, S., Fournier, R. A., & Renaud, J. P. (2015). Generalizing predictive models of forest inventory attributes using an area-based approach with airborne LiDAR data. *Remote Sensing of Environment*, *156*, 322-334.

Breidenbach, J., Næsset, E., Lien, V., Gobakken, T., & Solberg, S. (2010). Prediction of species specific forest inventory attributes using a nonparametric semi-individual tree crown approach based on fused airborne laser scanning and multispectral data. *Remote Sensing of Environment, 114*(4), 911-924.

Bright, B. C., Hicke, J. A., & Hudak, A. T. (2012). Estimating aboveground carbon stocks of a forest affected by mountain pine beetle in Idaho using lidar and multispectral imagery. *Remote Sensing of Environment*, *124*, 270-281.

Bright, B.C, Hudak, A.T., Meddens, A.J.H., Hawbaker, T.J., Briggs, J.S., & Kennedy, R.E. (2017). Prediction of forest canopy and surface fuels from lidar and satellite time series data in a bark beetle-affected forest. *Forests, 8*(9), 322. doi:10.3390/f8090322

Brown, S., Clarke, M., & Clarke, R. (2009). Fire is a key element in the landscape-scale habitat requirements and global population status of a threatened bird: the Mallee Emu-wren (Stipiturus mallee). *Biological Conservation*, *142*(2), 432-445.

Butler, B. W., Ottmar, R. D., Rupp, T. S., Jandt, R., Miller, E., Howard, K., ... & Jimenez, D. (2013). Quantifying the effect of fuel reduction treatments on fire behavior in boreal forests. *Canadian journal of forest research*, *43*(1), 97-102.

Chuvieco, E., Riaño, D., Van Wagtendok, J., & Morsdof, F. (2003). Fuel loads and fuel type mapping. *Wildland fire danger estimation and mapping: The role of remote sensing data* (pp. 119-142) World Scientific.

CIFFC. 2018. Canada Report 2018. https://www.ciffc.ca/sites/default/files/2019-06/2018%20Canada%20Report%202019_05_28%20R1.pdf: Canadian Interagency Forest Fire Center Inc.

CIFFC. 2017. Canadian Wildland Fire Management Glossary. https://www.ciffc.ca/sites/default/files/2019-03/CIFFC_Canadian_Wildland_Fire_Mgmt_Glossary_2017_10_24.pdf. Canadian Interagency Forest Fire Center Inc.

Cruz, M. G., & Alexander, M. E. (2010). Assessing crown fire potential in coniferous forests of western North America: a critique of current approaches and recent simulation studies. *International Journal of Wildland Fire*, *19*(4), 377-398.

Cruz, M. G., Alexander, M. E., & Wakimoto, R. H. (2003). Assessing canopy fuel stratum characteristics in crown fire prone fuel types of western north america. *International Journal of Wildland Fire, 12*(1), 39-50.

Domingo, D., Lamelas, M., Montealegre, A., García-Martín, A., & De la Riva, J. (2018). Estimation of total biomass in aleppo pine forest stands applying parametric and nonparametric methods to low-density airborne laser scanning data. *Forests, 9*(4), 158.

Dubayah, R. O., & Drake, J. B. (2000). Lidar remote sensing for forestry. *Journal of Forestry, 98*(6), 44-46.

Engelstad, P. S., Falkowski, M., Wolter, P., Poznanovic, A., & Johnson, P. (2019). Estimating canopy fuel attributes from low-density LiDAR. *Fire, 2*(3), 38.

Erdody, T. L., & Moskal, L. M. (2010). Fusion of LiDAR and imagery for estimating forest canopy fuels. *Remote Sensing of Environment, 114*(4), 725-737.

ESRI (2017). ArcGIS Desktop: Release 10. *Redlands, CA: Environmental Systems Research Institute.*

Estornell, J., Ruiz, L. A., Velázquez-Martí, B., & Fernández-Sarría, A. (2011). Estimation of shrub biomass by airborne LiDAR data in small forest stands. *Forest Ecology and Management, 262*(9), 1697-1703. doi:10.1016/j.foreco.2011.07.026

Ex, S. A., Smith, F. W., Keyser, T. L., & Rebain, S. A. (2016). Estimating canopy bulk density and canopy base height for interior western US conifer stands. *Forest Science*, *62*(6), 690-697.

Finney, M. A. (1998). *FARSITE, Fire Area Simulator--model development and evaluation* (No. 4). US Department of Agriculture, Forest Service, Rocky Mountain Research Station.

Flannigan, M. D., Krawchuk, M. A., de Groot, W. J., Wotton, B. M., & Gowman, L. M. (2009). Implications of changing climate for global wildland fire. *International Journal of Wildland Fire, 18*(5), 483-507.

Flannigan, M. D., Logan, K. A., Amiro, B. D., Skinner, W. R., & Stocks, B. J. (2005). Future area burned in Canada. *Climatic change*, *72*(1-2), 1-16.

Flat Top Complex Wildfire Review Committee. (2012). Flat Top Complex: Final Report from the Flat Top Complex Wildfire Review Committee. Alberta Ministry of Environment and Sustainable Resource Development, May 2012, Edmonton, Alberta.

Forestry Fire Danger Group Canada. (1992). *Development and structure of the Canadian Forest Fire Behavior Prediction System* (Information Report ST-X-3). Forestry Canada, Headquarters, Fire Danger Group and Science and Sustainable Development Directorate, Ottawa.

Fosberg, M. A. (1970). Drying rates of heartwood below fiber saturation. *Forest Science*, *16*(1), 57-63.

Frazer, G. W., Magnussen, S., Wulder, M. A., & Niemann, K. O. (2011). Simulated impact of sample plot size and co-registration error on the accuracy and uncertainty of LiDAR-derived estimates of forest stand biomass. *Remote Sensing of Environment, 115*(2), 636-649.

Fried, J. S., Torn, M. S., & Mills, E. (2004). The impact of climate change on wildfire severity: a regional forecast for northern California. *Climatic change*, *64*(1-2), 169-191.

Friedman J, Hastie T, Tibshirani R (2010). "Regularization Paths for Generalized Linear Models via Coordinate Descent." *Journal of Statistical Software*, **33**(1), 1–22. http://www.jstatsoft.org/v33/i01/.

Gamache, I., & Payette, S. (2004). Height growth response of tree line black spruce to recent climate warming across the forest-tundra of eastern canada. *Journal of Ecology, 92*(5), 835-845.

González-Ferreiro, E., Diéguez-Aranda, U., Crecente-Campo, F., Barreiro-Fernández, L., Miranda, D., & Castedo-Dorado, F. (2014). Modelling canopy fuel variables for pinus

radiata D. don in NW spain with low-density LiDAR data. *International Journal of Wildland Fire, 23*(3), 350-362.

González-Olabarria, J., Rodríguez, F., Fernández-Landa, A., & Mola-Yudego, B. (2012). Mapping fire risk in the model forest of urbión (spain) based on airborne LiDAR measurements. *Forest Ecology and Management, 282*, 149-156.

Gopalakrishnan, R., Thomas, V. A., Coulston, J. W., & Wynne, R. H. (2015). Prediction of canopy heights over a large region using heterogeneous lidar datasets: Efficacy and challenges. *Remote Sensing, 7*(9), 11036-11060.

Government of Saskatchewan. (2014). *14LA-lagoon fire: How fuel treatment areas affect wildland urban interface fires.* Retrieved from https://publications.saskatchewan.ca/#/products/79437

Greaves, H. E., Vierling, L. A., Eitel, J. U. H., Boelman, N. T., Magney, T. S., Prager, C. M., & Griffin, K. L. (2016). High-resolution mapping of aboveground shrub biomass in arctic tundra using airborne lidar and imagery. *Remote Sensing of Environment, 184*, 361-373. doi:10.1016/j.rse.2016.07.026

Hall, S. A., Burke, I. C., Box, D. O., Kaufmann, M. R., & Stoker, J. M. (2005). Estimating stand structure using discrete-return lidar: An example from low density, fire prone ponderosa pine forests. *Forest Ecology and Management, 208*(1-3), 189-209.

Hanes, C. C., Wang, X., Jain, P., Parisien, M., Little, J. M., & Flannigan, M. D. (2018). Fire-regime changes in canada over the last half century. *Canadian Journal of Forest Research, 49*(3), 256-269.

Heinselman ML (1981) Fire intensity and frequency as factors in the distribution and structure of northern ecosystems. In 'Fire regimes and Ecosystem Properties – Conference Proceedings', 11–15 December 1978, Honolulu, HI, USA. (Eds HA Mooney, TM Bonnicksen, NL Christensen, JE Lotan, WA Reiners) USDA Forest Service, General Technical Report WO-GRT-26. (Washington, DC, USA).

Hermosilla, T., Ruiz, L. A., Kazakova, A. N., Coops, N. C., & Moskal, L. M. (2014). Estimation of forest structure and canopy fuel parameters from small-footprint full-waveform LiDAR data. *International Journal of Wildland Fire, 23*(2), 224-233.

Hirsch, K. G., Corey, P. N., & Martell, D. L. (1998). Using expert judgment to model initial attack fire crew effectiveness. *Forest Science*, *44*(4), 539-549.

Hyyppä, J., Hyyppä, H., Leckie, D., Gougeon, F., Yu, X., & Maltamo, M. (2008). Review of methods of small-footprint airborne laser scanning for extracting forest inventory data in boreal forests. *International Journal of Remote Sensing*, *29*(5), 1339-1366.

Insurance Bureau of Canada. (2016). Northern Alberta wildfire costliest insured natural disaster in Canadian history. Retrieved from http://www.ibc.ca/bc/resources/media-centre/media-

releases/northern-alberta-wildfire-costliest-insured-natural-disaster-in-canadian-history. Accessed 26 November 2019.

Isenburg, M. (2018). LASzip: Lossless compression of LiDAR data [computer software]. Retrieved from: http://laszip.org

Jakubowksi, M. K., Guo, Q., Collins, B., Stephens, S., & Kelly, M. (2013a). Predicting surface fuel models and fuel metrics using lidar and CIR imagery in a dense, mountainous forest. *Photogrammetric Engineering & Remote Sensing, 79*(1), 37-49.

Jakubowski, M. K., Guo, Q., & Kelly, M. (2013b). Tradeoffs between lidar pulse density and forest measurement accuracy. *Remote Sensing of Environment, 130*, 245-253.

Johnson, A. F., Woodard, P. M., & Titus, S. J. (1990). Lodgepole pine and white spruce crown fuel weights predicted from diameter at breast height. *The Forestry Chronicle*, *66*(6), 596-599.

Johnston, D. C. (2012). *Quantifying the fuel load, fuel structure and fire behaviour of forested bogs and blowdown*

Johnston, D. C., Turetsky, M. R., Benscoter, B. W., & Wotton, B. M. (2015). Fuel load, structure, and potential fire behaviour in black spruce bogs. *Canadian Journal of Forest Research, 45*(7), 888-899.

Kaartinen, H., Hyyppä, J., Yu, X., Vastaranta, M., Hyyppä, H., Kukko, A. Holopainen, M., Heipke, C., Hirschmugl, M., Morsdorf, F., Næsset, E., Pitanen, J., Popescu, S., Solberg, S., Wolf, B.M., & Wu, J. (2012). An international comparison of individual tree detection and extraction using airborne laser scanning. *Remote Sensing*, *4*(4), 950-974.

Kandare, K., Ørka, H. O., Chan, J. C. W., & Dalponte, M. (2016). Effects of forest structure and airborne laser scanning point cloud density on 3D delineation of individual tree crowns. *European Journal of Remote Sensing*, *49*(1), 337-359.

Ke, Y., & Quackenbush, L. J. (2011). A review of methods for automatic individual tree-crown detection and delineation from passive remote sensing. *International Journal of Remote Sensing*, *32*(17), 4725-4747.

Keane, R. E. (2013). Describing wildland surface fuel loading for fire management: A review of approaches, methods and systems. *International Journal of Wildland Fire, 22*(1), 51-62.

Keane, R. E., Burgan, R., & van Wagtendonk, J. (2001). Mapping wildland fuels for fire management across multiple scales: integrating remote sensing, GIS, and biophysical modeling. *International Journal of Wildland Fire*, *10*(4), 301-319.

Keane, R. E., Gray, K., Bacciu, V., & Leirfallom, S. (2012). Spatial scaling of wildland fuels for six forest and rangeland ecosystems of the northern rocky mountains, USA. *Landscape Ecology, 27*(8), 1213-1234.

Knapp, E. E., & Keeley, J. E. (2006). Heterogeneity in fire severity within early season and late season prescribed burns in a mixed-conifer forest. *International Journal of Wildland Fire*, *15*(1), 37-45.

Krezek-Hanes, C., Ahern, F., Cantin, A., & Flannigan, M. (2011). Trends in large fires in Canada, 1957-2007. Canadian Biodiversity: Ecosystem Status and Trends 2010, Technican Thematic Report No. 6. Ottawa, ON 48p http://www.biodivcanada.ca/default.asp?lang=En&n=137E1147-0: Canadian Councils of Resource Ministers., AB: Natural Resources of Canada, Canadian Forest Service, Northern Forestry Centre.

Lavoie, N. (2004). *Variation in flammability of jack pine/black spruce forests with time since fire in the Northwest Territories, Canada.* PhD Thesis, University of Alberta, Edmonton, AB, Canada

Lefsky, M. A., Cohen, W. B., Harding, D. J., Parker, G. G., Acker, S. A., & Gower, S. T. (2002). Lidar remote sensing of above-ground biomass in three biomes. *Global ecology and biogeography*, *11*(5), 393-399.

Li, Y., Andersen, H.E., McGaughey, R., 2008. A comparison of statistical methods for estimating forest biomass from light detection and ranging data. Western Journal of Applied Forestry 23, 223–231.

Lim, K., Treitz, P., Wulder, M., St-Onge, B., & Flood, M. (2003). LiDAR remote sensing of forest structure. *Progress in Physical Geography, 27*(1), 88-106.

Linn, R. (1997). *A transport model for prediction of wildfire behavior* (No. LA-13334-T). Los Alamos National Lab., NM (United States).

Linn, R., Anderson, K., Winterkamp, J., Brooks, A., Wotton, M., Dupuy, J. L., ... & Edminster, C. (2012). Incorporating field wind data into FIRETEC simulations of the International Crown Fire Modeling Experiment (ICFME): preliminary lessons learned. *Canadian Journal of Forest Research*, *42*(5), 879-898.

Linn, R., Reisner, J., Colman, J. J., & Winterkamp, J. (2002). Studying wildfire behavior using FIRETEC. *International journal of wildland fire*, *11*(4), 233-246.

Little, J., Jandt, R., Drury, S., Molina, A., & Lane, B. (2019). Final report evaluating the effectiveness of fuel treatments in alaska JFSP project 14-5-01-27.

Luther, J. E., Skinner, R., Fournier, R. A., van Lier, O. R., Bowers, W. W., Coté, J., . . . Moulton, T. (2013). Predicting wood quantity and quality attributes of balsam fir and black spruce using airborne laser scanner data. *Forestry, 87*(2), 313-326.

Martell, D. (2001). Forest fire management; In E. Johnson, & K. Miyanishi (Eds.), *Forest fires: Behavior and ecological effects* (pp. 527-581). San Diego, California: Academic Press.

Martell, D. L., Otukol, S., & Stocks, B. J. (1987). A logistic model for predicting daily people-caused forest fire occurrence in Ontario. *Canadian Journal of Forest Research*, *17*(5), 394-401.

McArthur, A. G., & Cheney, N. P. (2015). The characterization of fires in relation to ecological studies. *Fire Ecology*, *11*(1), 3-9.

McCarley, T. R., Kolden, C. A., Vaillant, N. M., Hudak, A. T., Smith, A. M., Wing, B. M., ... & Kreitler, J. (2017). Multi-temporal LiDAR and Landsat quantification of fire-induced changes to forest structure. *Remote Sensing of Environment*, *191*, 419-432.

McGaughey, R. J. (2018a). FUSION/LDV: [Computer Software]. Retrieved at: http://forsys.cfr.washington.edu/fusion/fusionlatest.html

McGaughey, R. J. (2018b). FUSION/LDV: Software for LIDAR data analysis and visualization. *US Department of Agriculture, Forest Service, Pacific Northwest Research Station: Seattle, WA, USA*, *123*(2).

McRae, D. J., Duchesne, L. C., Freedman, B., Lynham, T. J., & Woodley, S. (2001). Comparisons between wildfire and forest harvesting and their implications in forest management. *Environmental Reviews*, *9*(4), 223-260.

Merrill, D. F., & Alexander, M. E. (1987). Glossary of forest fire management terms. 4th ed. *Canadian Committee on Forest Fire Management, National Research Council of Canada, Ottawa, ON, Canada*. NRCC No. 26516.

Miller, EA. (2016). Forest thinning reduces crown fire behavior in Interior Alaska. Western Forester 61(1):17-18.

Mohan, M., Silva, C.B., Klauberg, C., Jat, P., Catts, G., Cardil, A., Hudak, A.T., Dia, M. (2017). Individual tree detection from unmanned aerial vehicle (UAV) derived canopy height model in an open canopy mixed conifer forest. *Forests, 8*(9), 340. doi:10.3390/f8090340

Moritz, M. A., Batllori, E., Bradstock, R. A., Gill, A. M., Handmer, J., Hessburg, P. F., Leonard, J., McCaffrey S., Odion, D.C., Schoennagel, T. & Syphard, A. D. (2014). Learning to coexist with wildfire. *Nature*, *515*(7525), 58-66.

Nadeau, L. B., McRae, D. J., & Jin, J. Z. (2005). *Development of a national fuel-type map for Canada using fuzzy logic*. Natural Resources Canada, Canadian Forest Service, Northern Forestry Centre. Information Report NOR-X-406.

Næsset, E. (2014). Area-based inventory in norway–from innovation to an operational reality. In N. Maltamo, E. Næsset & J. Vauhkonen (Eds.), *Forestry applications of airborne laser scanning* (pp. 215-240). New York: Springer.

Næsset, E., Bollandsås, O. M., & Gobakken, T. (2005). Comparing regression methods in estimation of biophysical properties of forest stands from two different inventories using laser scanner data. *Remote Sensing of Environment, 94*(4), 541-553. Natural Regions

Committee. (2006). *Natural regions and subregions of Alberta*. Edmonton, Alberta, Canada: Complied by DJ Downing and WW Pettapoece.

NFI (National Forest Inventory). 2013. Canada's National Forest Inventory, revised 2006 baseline. Natural Resources Canada, Victoria, B.C. Available from https://nfi.nfis.org/en/standardreports [accessed March 2020].

Nguyen-Xuan, T., Bergeron, Y., Simard, D., Fyles, J. W., & Paré, D. (2000). The importance of forest floor disturbance in the early regeneration patterns of the boreal forest of western and central Quebec: a wildfire versus logging comparison. *Canadian Journal of Forest Research*, *30*(9), 1353-1364.

Okhrimenko, M., Coburn, C., & Hopkinson, C. (2019). Multi-spectral lidar: Radiometric calibration, canopy spectral reflectance, and vegetation vertical SVI profiles. *Remote Sensing*, *11*(13), 1556.

Parise, M., & Cannon, S. H. (2012). Wildfire impacts on the processes that generate debris flows in burned watersheds. *Natural Hazards*, *61*(1), 217-227.

Parisien, M. A., Kafka, V. G., Hirsch, K. G., Todd, J. B., Lavoie, S. G., & Maczek, P. D. (2005). Mapping wildfire susceptibility with the BURN-P3 simulation model. Natural Resources Canada, Canadian Forest Service, Northern Forestry Center, Edmonton, Alberta. Information Report NOR-X-405.

Parsons, R. A., Mell, W. E., & McCauley, P. (2011). Linking 3D spatial models of fuels and fire: Effects of spatial heterogeneity on fire behavior. *Ecological Modelling, 222*(3), 679-691.

Penner, M., Pitt, D. G., & Woods, M. E. (2013). Parametric vs. nonparametric LiDAR models for operational forest inventory in boreal Ontario. *Canadian Journal of Remote Sensing*, *39*(5), 426-443.

Perrine, N.. (2016). The effects and use of fuel treatments in the Skilak Loop area during the 2015 Card Street Fire, Alaska. Soldotna, AK: US Fish & Wildlife Service. 21 p.

Pimont, F., Dupuy, J., Caraglio, Y., & Morvan, D. (2009). Effect of vegetation heterogeneity on radiative transfer in forest fires. *International Journal of Wildland Fire, 18*(5), 536-553.

Popescu, S. C., & Zhao, K. (2008). A voxel-based lidar method for estimating crown base height for deciduous and pine trees. *Remote sensing of environment*, *112*(3), 767-781.

Popescu, S. C., Zhao, K., Neuenschwander, A., & Lin, C. (2011). Satellite lidar vs. small footprint airborne lidar: Comparing the accuracy of aboveground biomass estimates and forest structure metrics at footprint level. *Remote Sensing of Environment, 115*(11), 2786-2797.

R Core Team (2018). R: A language and environment for statistical computing. R Foundation for Statistical Computing, Vienna, Austria. URL https://www.R-project.org/.

Rebain, S. A., Reinhardt, E. D., Crookston, N. L., Beukema, S. J., Kurz, W. A., Greenough, J.

A., . . . Lutes, D. C. (2010). The fire and fuels extension to the forest vegetation simulator: Updated model documentation. *US Department of Agriculture, for.Serv.Int.Rep, 408*

Reid, C. E., Brauer, M., Johnston, F. H., Jerrett, M., Balmes, J. R., & Elliott, C. T. (2016). Critical review of health impacts of wildfire smoke exposure. *Environmental health perspectives*, *124*(9), 1334-1343.

Reinhardt, E., & Crookston, N. L. (2003). The fire and fuels extension to the forest vegetation simulator. *Gen.Tech.Rep.RMRS-GTR-116.Ogden, UT: US Department of Agriculture, Forest Service, Rocky Mountain Research Station.209 P., 116*

Reinhardt E, Lutes D, Scott J (2006) FuelCalc: a method for estimating fuel characteristics. In 'Fuels Management – How to Measure Success: Conference Proceedings', 28–30 March 2006, Portland, OR. (Eds PL Andrews, BW Butler) USDA Forest Service, Rocky Mountain Research Station, Proceedings RMRS-P 41, pp. 273–282. (Fort Collins, CO)

Reutebuch, S. E., Andersen, H. E., & McGaughey, R. J. (2005). Light detection and ranging (LIDAR): an emerging tool for multiple resource inventory. *Journal of Forestry*, *103*(6), 286-292.

Rhodes, J. J., & Baker, W. L. (2008). Fire probability, fuel treatment effectiveness and ecological tradeoffs in western US public forests. *The Open Forest Science Journal*, *1*(1).

Rowe, J. S. (1983). Concepts of fire effects on plant individuals and species. *The Role of Fire in Northern Circumpolar Ecosystems, 18*

Saperstein, L, B Fay, J. O'Connor, B. Reed. (2014). Use and Effectiveness of Fuel Treatments During the 2014 Funny River Fire, Alaska. USFWS, Fire Management Report 10/17/2014, Anchorage, AK.

Scott, J. H., & Reinhardt, E. D. (2001). Assessing crown fire potential by linking models of surface and crown fire behavior. *Res.Pap.RMRS-RP-29.Fort Collins, CO: US Department of Agriculture, Forest Service, Rocky Mountain Research Station.59 P., 29*

Shang, C., Treitz, P., Caspersen, J., & Jones, T. (2019). Estimation of forest structural and compositional variables using ALS data and multi-seasonal satellite imagery. *International Journal of Applied Earth Observation and Geoinformation*, *78*, 360-371.

Shakesby, R. A., Coelho, C. D. A., Ferreira, A. D., Terry, J. P., & Walsh, R. P. (1993). Wildfire impacts on soil-erosion and hydrology in wet Mediterranean forest, Portugal. *International Journal of Wildland Fire*, *3*(2), 95-110.

Skowronski, N. S., Clark, K. L., Duveneck, M., & Hom, J. (2011). Three-dimensional canopy fuel loading predicted using upward and downward sensing LiDAR systems. *Remote Sensing of Environment, 115*(2), 703-714.

Skowronski, N., Clark, K., Nelson, R., Hom, J., & Patterson, M. (2007). Remotely sensed measurements of forest structure and fuel loads in the pinelands of new jersey. *Remote Sensing of Environment, 108*(2), 123-129.

Southgate, R., Paltridge, R., Masters, P., & Carthew, S. (2007). Bilby distribution and fire: a test of alternative models of habitat suitability in the Tanami Desert, Australia. *Ecography*, *30*(6), 759-776.

Statistics Canada. (2016). Population and dwelling count highlight tables, 2016 census. Retrieved from https://www12.statcan.gc.ca/census-recensement/2016/dp-pd/hlt-fst/pd-pl/Table.cfm?Lang=Eng&T=1301&SR=1&S=45&O=A&RPP=9999&PR=48&CMA=0#tPopDwell

Stephens, S. L. (1998). Evaluation of the effects of silvicultural and fuels treatments on potential fire behaviour in Sierra Nevada mixed-conifer forests. *Forest Ecology and Management*, *105*(1-3), 21-35.

Stockdale, C., Barber, Q., & Parisien, M. A. (2018). Wildfire Risk to Caribou Conservation Projects in Northeastern Alberta. Natural Resources Canada, Canadian Forest Service, Northern Forestry Center, Edmonton, Alberta.

Stocks, B. J., Alexander, M. E., Wotton, B. M., Stefner, C. N., Flannigan, M. D., Taylor, S. W., ... & Dalrymple, G. N. (2004). Crown fire behaviour in a northern jack pine black spruce forest. *Canadian Journal of Forest Research*, *34*(8), 1548-1560.

Stocks, B. J., Lynham, T. J., Lawson, B. D., Alexander, M. E., Wagner, C. V., McAlpine, R. S., & Dube, D. E. (1989). Canadian forest fire danger rating system: an overview. *The Forestry Chronicle*, *65*(4), 258-265.

Stocks, B. J., Mason, J. A., Todd, J. B., Bosch, E. M., Wotton, B. M., Amiro, B. D., . . . Skinner, W.R. (2002). Large forest fires in canada, 1959–1997. *Journal of Geophysical Research: Atmospheres, 107*(D1), FFR -12.

Sugihara, N. G., Van Wagtendonk, J. W., & Fites-Kaufman, J. (2006). Fire as an ecological process. *Fire in California's ecosystems*, 58-74.

Taylor S.W., Alexander M. E. (2016). *Field guide to the Canadian forest fire behavior prediction (FBP) system* (2nd ed.). Canadian Forest Service, Northern Forestry Centre, Edmonton AB: Natural Resources Canada.

Taylor, S. W., Wotton, B. M., Alexander, M. E., & Dalrymple, G. N. (2004). Variation in wind and crown fire behaviour in a northern jack pine black spruce forest. *Canadian Journal of Forest Research, 34*(8), 1561-1576.

Thompson, B. (1995). Stepwise Regression and Stepwise Discriminant Analysis Need Not Apply here: A Guidelines Editorial. *Educational and Psychological Measurement,* 55(4), 525-534

Tibshirani, R. (1996). Regression shrinkage and selection via the lasso. *Journal of the Royal Statistical Society: Series B (Methodological), 58*(1), 267-288.

Treitz, P., Lim, K., Woods, M., Pitt, D., Nesbitt, D., & Etheridge, D. (2012). LiDAR sampling density for forest resource inventories in ontario, canada. *Remote Sensing, 4*(4), 830-848.

Van Wagner, C. V. (1977). Conditions for the start and spread of crown fire. *Canadian Journal of Forest Research, 7*(1), 23-34.

Van Wagner, C.E. (1993). Prediction of crown fire behavior in two stands of jack pine. *Canadian Journal of Forest Research*, *23*(3), 442-449.

Van Wagner, C.E., & Forest, P. (1987). Development and structure of the canadian forest fire weather index system. In Canadian Forest Service, Technical Report 25, Ottawa, ON

Vastaranta, M., Holopainen, M., Yu, X., Haapanen, R., Melkas, T., Hyyppä, J., & Hyyppä, H. (2011). Individual tree detection and area-based approach in retrieval of forest inventory characteristics from low-pulse airborne laser scanning data. *Photogrammetric Journal of Finland, 22*(2), 1-13.

Vastaranta, M., Kankare, V., Holopainen, M., Yu, X., Hyyppä, J., & Hyyppä, H. (2012). Combination of individual tree detection and area-based approach in imputation of forest variables using airborne laser data. *ISPRS Journal of Photogrammetry and Remote Sensing, 67*, 73-79.

Vauhkonen, J., Ene, L., Gupta, S., Heinzel, J., Holmgren, J., Pitkänen, J., . . . Hauglin, K. M. (2011). Comparative testing of single-tree detection algorithms under different types of forest. *Forestry, 85*(1), 27-40.

Vicars, M., & Luckhurst, J. (1999). Firesmart: protecting your community from wildfire. *Partners in Protection. Edmonton, Alberta*.

Viereck, L. A. (1983). The effects of fire in black spruce ecosystemsof alaska and northern canada. *The Role of Fire in Northern Circumpolar Ecosystems, Wiley, New York, USA,* , 210-220.

Viereck, L. A., & Little, E. L. (1972). *Alaska trees and shrubs* US Forest Service.

Weber, M. G., & Flannigan, M. D. (1997). Canadian boreal forest ecosystem structure and function in a changing climate: impact on fire regimes. *Environmental Reviews*, *5*(3-4), 145-166.

Werth, P. A., Potter, B. E., Alexander, M. E., Clements, C. B., Cruz, M. G., Finney, M. A., ... & McAllister, S. S. (2016). Synthesis of knowledge of extreme fire behavior: volume 2 for fire behavior specialists, researchers, and meteorologists. *Gen. Tech. Rep. PNW-GTR-891. Portland, OR: US Department of Agriculture, Forest Service, Pacific Northwest Research Station. 258 p.*, *891*.

White, J. C., Coops, N. C., Wulder, M. A., Vastaranta, M., Hilker, T., & Tompalski, P. (2016). Remote sensing technologies for enhancing forest inventories: A review. *Canadian Journal of Remote Sensing, 42*(5), 619-641.

White, J., Tompalski, P., Vastaranta, M., Wulder, M. A., Saarinen, N., Stepper, C., . . . Coops, N. C. (2017). *A model development and application guide for generating an enhanced forest inventory using airborne laser scanning data and an area-based approach* Natural Resources Canada= Ressources naturelles Canada.

White, J. C., Wulder, M. A., Varhola, A., Vastaranta, M., Coops, N. C., Cook, B. D., . . . Woods, M. (2013). A best practices guide for generating forest inventory attributes from airborne laser scanning data using an area-based approach. *The Forestry Chronicle, 89*(6), 722-723.

Wilson, B. A., Ow, C. F., Heathcott, M., Milne, D., McCaffrey, T. M., Ghitter, G., & Franklin, S. E. (1994). Landsat MSS classification of fire fuel types in Wood Buffalo National Park, northern Canada. *Global Ecology and Biogeography Letters*, 33-39.

Wotton, B. M., Martell, D. L., & Logan, K. A. (2003). Climate change and people-caused forest fire occurrence in Ontario. *Climatic Change, 60*(3), 275-295.

Wu, B., Yu, B., Wu, Q., Huang, Y., Chen, Z., & Wu, J. (2016). Individual tree crown delineation using localized contour tree method and airborne LiDAR data in coniferous forests. *International Journal of Applied Earth Observation and Geoinformation, 52*, 82-94.

Wulder, M. A., Bater, C. W., Coops, N. C., Hilker, T., & White, J. C. (2008). The role of LiDAR in sustainable forest management. *The Forestry Chronicle, 84*(6), 807-826.

Wulder, M. A., Coops, N. C., Hudak, A. T., Morsdorf, F., Nelson, R., Newnham, G., & Vastaranta, M. (2013). Status and prospects for LiDAR remote sensing of forested ecosystems. *Canadian Journal of Remote Sensing, 39*(sup1), S1-S5.

Wykoff, W. R., Crookston, N. L., & Stage, A. R. (1982). User's guide to the stand prognosis model. *Gen.Tech.Rep.INT-133.Ogden, UT: US Department of Agriculture, Forest Service, Intermountain Forest and Range Experiment Station; 1982.112 P., 133*

Zackrisson, O., Nilsson, M. C., & Wardle, D. A. (1996). Key ecological function of charcoal from wildfire in the Boreal forest. *Oikos*, 10-19.

Zhang, Z., Cao, L., & She, G. (2017). Estimating forest structural parameters using canopy metrics derived from airborne LiDAR data in subtropical forests. *Remote Sensing, 9*(9), 940.

Zhao, K., Popescu, S., & Nelson, R. (2009). Lidar remote sensing of forest biomass: A scale-invariant estimation approach using airborne lasers. *Remote Sensing of Environment, 113*(1), 182-196.

Zhen, Z., Quackenbush, L., & Zhang, L. (2016). Trends in automatic individual tree crown

detection and Delineation—Evolution of LiDAR data. *Remote Sensing, 8*(4), 333. doi:10.3390/rs8040333